

Life Cycle Assessment and Greenhouse Gas Abatement Costs of Hydrogen Production
from Underground Coal Gasification

by

Aman Verma

A thesis submitted in partial fulfillment of the requirements for the degree of

Master of Science

Department of Mechanical Engineering
University of Alberta

© Aman Verma, 2014

Abstract

Large amounts of hydrogen (H_2) are required for the upgrading of bitumen from oil sands to produce synthetic crude oil (SCO). Currently, natural gas is used in the bitumen upgrading industry to produce H_2 through steam methane reforming (SMR). This process has a significant life cycle greenhouse gas (GHG) footprint. Due to rising SCO production from the Canadian oil sands and climate change concerns, there is a growing need to explore more environmentally sustainable pathways for H_2 production that have lower GHG footprint. Western Canada is endowed with considerable reserves of deep unmineable coal that can be converted to syngas through a gasification process called underground coal gasification (UCG). The syngas can be transformed into H_2 through commercially available technologies used in conventional fossil-fuel based H_2 production pathways. Moreover, GHGs (mainly CO_2) from the H_2 plant operation can be captured using a physical solvent like Selexol and sequestered underground or used as a feedstock for enhanced oil recovery (EOR) operations.

A life cycle assessment (LCA) is a useful tool to evaluate the environmental impact of a system. This research presents a model to perform energy balances, estimate H_2 conversion efficiency, and implement LCA to quantify life cycle GHG emissions in different unit operations of H_2 production from UCG-based syngas with and without carbon capture and sequestration (CCS). In addition, a detailed analysis of the impact of key UCG parameters, i.e., H_2O -to- O_2 injection ratio, ground water influx, and steam-to-

carbon ratio in syngas conversion, is completed on the results. Furthermore, seven practical H₂ production scenarios, applicable to western Canada, are considered to assess the GHG abatement costs of implementing UCG vis-à-vis SMR along with the consideration of CCS.

The life cycle GHG emissions are calculated to be 0.91 and 18.0 kg-CO₂-eq/kg-H₂ in a small-scale H₂ production (16.3 tonnes/day) from UCG-based syngas with and without CCS, respectively. The heat exchanger efficiency and the separation efficiency of the pressure swing adsorption (PSA) unit are major parameters affecting these emissions. The emissions increase marginally with a rise in the H₂O-to-O₂ injection ratio and the steam-to-carbon ratio in H₂ production from UCG with CCS. Considering SMR technology without CCS as the base case, the GHG abatement costs of implementing the UCG-CCS technology is calculated to be in the range of C\$41-109 /tonne-CO₂-eq depending on the transportation distance from the UCG-H₂ production plant to the CCS site. On the other hand, the GHG abatement costs for SMR-CCS-based scenarios are higher than for UCG-CCS-based scenarios; they range from C\$87-158 /tonne-CO₂-eq in a similar manner to UCG-CCS. However, there is no GHG abatement for implementing UCG without CCS; the life cycle GHG emissions are higher in UCG than in SMR. The sale of the CO₂ captured in the H₂ production plant (applicable in SMR-CCS and UCG-CCS) to an EOR operator reduces the GHG abatement costs; in fact, a prospect for revenue generation is realized in the UCG-CCS case.

Acknowledgments

First, I would like to thank Dr. Amit Kumar for his ongoing support and guidance starting from my transition to the University of Alberta from Clemson University. During the course of the graduate program, as a supervisor and a mentor, Dr. Kumar provided constructive criticism for my research work. It was a wonderful experience to learn from and contribute to his research group. I have progressed at a personal level working with him. His professional conduct has and will continue to benefit my career development.

I also want to take this opportunity to acknowledge the NSERC/Cenovus/Alberta Innovates Associate Industrial Research Chair Program in Energy and Environmental Systems Engineering and the Cenovus Energy Endowed Chair Program in Environmental Engineering for providing financial support for the research project. In addition, I thank my supervisory committee for reviewing the dissertation and providing useful insights and feedback. I thank Babatunde Olateju for reviewing the research results and the papers. I express my thanks to Astrid Blodgett for providing editorial support for all the journal papers and the thesis.

Our Sustainable Energy Research Laboratory was no less than a home away from home. Intellectual and meaningful discussions among peers were helpful in increasing my curiosity in various aspects of research and life in general. The diversity in the lab helped me to understand the cultures and traditions of different countries. Birthday celebrations,

pizza parties, and potlucks truly made the experience unforgettable. Undoubtedly, the associations made, and the camaraderie I share with some members in the lab, will be memorable and are for a lifetime.

Lastly, I would like pay regards and thank my lovely parents, grandmother, sister-in-law and brother, who from miles away provided unconditional love and mental support. They have been pillars of my success and failures.

Preface

Chapter 2 of this thesis will be submitted to *International Journal of Hydrogen Energy* as Verma A., Olateju B., Kumar A., Gupta R., “Development of a Process Simulation Model for Energy Analysis of Hydrogen Production from Underground Coal Gasification (UCG)”. Chapter 3 of this thesis has been submitted to *Applied Energy* as Verma A., Kumar A., “Life Cycle Assessment (LCA) of Hydrogen Production from Underground Coal Gasification (UCG) with Carbon Capture and Sequestration (CCS)”. Chapter 4 of this thesis has been submitted to *Energy* as Verma A., Olateju B., Kumar A., “Greenhouse Gas Abatement Costs of Hydrogen Production from Underground Coal Gasification (UCG)”. I was responsible for the concept development, data gathering, model development, analysis of the results, and arrangement of the manuscripts. A. Kumar was the supervising author and was involved in the concept development, analysis of the results, and arrangement of the manuscripts. R. Gupta helped in model development and reviewed the overall results specially related to simulation of the UCG process. B. Olateju reviewed the results.

Table of Contents

Abstract.....	ii
Acknowledgments.....	iv
Preface.....	vi
Table of Contents.....	vii
List of Tables.....	xi
List of Figures.....	xiii
Nomenclature.....	xvi
Chapter 1.....	1
Introduction.....	1
1.1. Background.....	1
1.2. Life cycle assessment.....	5
1.3. Research motivation.....	10
1.4. Thesis objectives.....	12
1.5. Organization of thesis.....	13
Chapter 2.....	15
Development of a Process Simulation Model for Energy Analysis of Hydrogen Production from Underground Coal Gasification (UCG).....	15
2.1. Background.....	15
2.2. Methodology.....	16
2.2.1. Plant layout overview: H ₂ production from UCG with and without CCS.....	16

2.2.2. H ₂ production from UCG – An overview of unit operations.....	19
2.2.2.1. Injection	19
2.2.2.2. Underground coal gasification.....	19
2.2.2.3. Hydrogen sulphide (H ₂ S) removal.....	24
2.2.2.4. Syngas to H ₂ conversion	25
2.2.2.5. CO ₂ removal and transportation.....	26
2.2.2.6. H ₂ removal and transportation	29
2.2.2.7. Co-generation plant.....	30
2.3. Results and discussion	32
2.3.1. Power requirement in different unit operations: H ₂ production from UCG with and without CCS.....	32
2.3.2. Effect of the steam-to-carbon ratio on η_h , and η_e	39
2.3.3. The effect of H ₂ O-to-O ₂ injection flow ratio on coal-to-H ₂ conversion efficiency, η_h	43
2.3.4. Electricity production from UCG with and without CCS.....	46
2.3.5. Comparative analysis: H ₂ production from UCG vs. SCG vs. SMR.....	47
2.3.6. Sensitivity analysis.....	50
2.4. Conclusions.....	52
Chapter 3.....	53
Life Cycle Assessment (LCA) of Hydrogen Production from Underground Coal Gasification (UCG) with Carbon Capture and Sequestration (CCS).....	53
3.1. Background	53
3.2. Methodology	54

3.2.1. Goal and Scope	55
3.2.1.1. Functional unit	55
3.2.1.2. System boundaries	56
3.2.2. Life cycle inventory (LCI)	58
3.2.2.1. H ₂ production from UCG	58
3.2.2.2. Drilling	64
3.2.2.3. CO ₂ pipeline design and EOR well characteristics for sequestration	64
3.2.2.4. H ₂ pipeline design	66
3.2.3. Life cycle impact assessment (LCIA)	67
3.3. Results and discussion	69
3.3.1. Life cycle GHG emissions	69
3.3.2. Net energy ratio (NER)	74
3.3.3. The effect of steam-to-carbon ratio on life cycle GHG emissions	77
3.3.4. The effect of the H ₂ O-to-O ₂ injection ratio on life cycle GHG emissions	81
3.3.5. Comparative assessment of life cycle GHG emissions in H ₂ production from UCG with other H ₂ production pathways	84
3.3.6. Sensitivity analysis	88
3.3.6.1 Sensitivity analysis on net life cycle GHG emissions	88
3.3.6.2 Sensitivity analysis on gross life cycle GHG emissions	90
3.4. Conclusions	92
Chapter 4	93
Greenhouse Gas Abatement Costs of Hydrogen Production from Underground Coal Gasification (UCG)	93

4.1. Background	93
4.2. Western Canadian H ₂ production scenarios.....	95
4.3. Method	98
4.3.1. Scope of study.....	98
4.3.2. System boundaries: H ₂ production from UCG and SMR with and without CCS.....	102
4.4. Results and discussion	106
4.4.1. Life cycle GHG emissions in SMR-based H ₂ production scenarios.....	106
4.4.2. Life cycle GHG emissions in UCG-based H ₂ production scenarios.....	110
4.4.3. GHG abatement costs in H ₂ production scenarios	112
4.4.4. GHG mitigation potential of UCG-CCS and SMR-CCS technologies for H ₂ production	115
4.5. Conclusions.....	117
Chapter 5.....	118
Conclusions and Recommendations for Future Work	118
5.1. Conclusions.....	118
5.1.1. Research limitations.....	121
5.2. Recommendations for future work	122
References.....	125
Appendix A.....	137
Aspen Plus Simulation Model	137

List of Tables

Table 2.1: Key assumptions in UCG	21
Table 2.2: Composition of the syngas produced from UCG	23
Table 2.3: Key assumptions in SRR and WGSR.....	26
Table 2.4: Key assumptions for CO ₂ capture and removal.....	27
Table 2.5: Key assumptions for a co-generation plant	31
Table 2.6: Power requirement in different unit operations of H ₂ production with CCS and without CCS.....	33
Table 2.7: Key performance parameters of H ₂ production pathways: UCG, surface coal gasification, and SMR with and without carbon capture	48
Table 3.1: Coal composition assumed in the study.....	59
Table 3.2: Key assumptions for calculation of power requirement and production in the different unit operations in scenarios 1 and 2	60
Table 3.3: Power requirement in different unit operations of H ₂ production with and without CCS.....	62
Table 3.4: EOR well reservoir characteristics for CO ₂ sequestration.....	66
Table 3.5: Emission factors associated with fuel and material use and the GWPs of GHGs relative to CO ₂	68
Table 3.6: Life cycle GHG emissions in different unit operations of H ₂ production with and without CCS.....	70

Table 3.7: Description of various H ₂ production pathways considered in a comparative analysis of life cycle GHG emissions	85
Table 4.1: H ₂ production scenarios from UCG and SMR in western Canada.....	96
Table 4.2: UCG-CCS and SMR-CCS plant specifications.....	99
Table 4.3: Emission factors used in this study.....	103
Table 4.4: Life cycle GHG emissions in H ₂ production from SMR with and without CCS (scenarios 1, 2 and 3)	108
Table 4.5: Life cycle GHG emissions in H ₂ production from UCG with and without CCS (scenarios 4, 5, 6 and 7)	111
Table 4.6: GHG abatement costs in H ₂ production scenarios. Note: the reference scenario for GHG abatement costs calculation is scenario 3.	114

List of Figures

Figure 2.1: Unit operations of H ₂ production pathways from UCG with CCS and without CCS.....	18
Figure 2.2: Power distribution for H ₂ production from UCG with CCS.	36
Figure 2.3: Power distribution for H ₂ production from UCG without CCS.	37
Figure 2.4: Energy balance diagram: H ₂ production from UCG with and without CCS..	38
Figure 2.5: The effect of the steam-to-carbon ratio on η_h and η_e in H ₂ production from UCG with CCS with different ground water influx rates and a fixed H ₂ O-to-O ₂ injection ratio of 2.	42
Figure 2.6: The effect of the H ₂ O-to-O ₂ injection ratio on η_h and η_e in H ₂ production from UCG with CCS with different ground water influx rates and a fixed steam-to-carbon ratio of 3.	45
Figure 2.7: Sensitivity analysis for H ₂ production from UCG with CCS. The H ₂ O-to O ₂ -ratio is 2, and the ground water influx rate is 0.4 m ³ per tonne coal.	51
Figure 3.1: System boundary of the study.	57
Figure 3.2: Life cycle GHG emissions distribution in scenario 1 (H ₂ production from UCG with CCS).....	73
Figure 3.3: Life cycle GHG emissions distribution in scenario 2 (H ₂ production from UCG without CCS).....	74

Figure 3.4: Energy balance in scenarios 1 and 2 for base case assumptions i.e. total coal input – 118 tonne/day, H ₂ O-to-O ₂ injection ratio – 2 and ground water influx – 0.4 m ³ /tonne of coal.	76
Figure 3.5: The effect of the steam-to-carbon ratio on H ₂ production and amount of CO ₂ captured using Selexol technology in scenario 1 with different ground water influx rates and a fixed H ₂ O to O ₂ injection ratio of 2. Dash lines represent H ₂ production and solid lines represent total CO ₂ captured.	79
Figure 3.6: The effect of the steam-to-carbon ratio on gross and net life cycle GHG emissions in scenarios 1 and 2 with different ground water influx rates, but a fixed H ₂ O-to-O ₂ injection ratio of 2.	80
Figure 3.7: The effect of the H ₂ O-to-O ₂ injection ratio on H ₂ production and amount of CO ₂ captured using Selexol technology in scenario 1 with different ground water influx rates, but a fixed steam-to-carbon ratio of 3.	82
Figure 3.8: The effect of the H ₂ O-to-O ₂ injection ratio on gross and net life cycle GHG emissions in scenarios 1 and 2 with different ground water influx rates, but a fixed steam-to-carbon ratio of 3.	83
Figure 3.9: Comparative analysis of net life cycle GHG emissions in various H ₂ production pathways.	87
Figure 3.10: Sensitivity analysis on net life cycle GHG emissions for scenario 1.	90
Figure 3.11: Sensitivity analysis on gross life cycle GHG emissions for scenario 1.	91
Figure 4.1: Geographical representation of the H ₂ production scenarios in Alberta.	97
Figure 4.2: System boundary for SMR based-H ₂ production scenarios.	104
Figure 4.3: System boundary for UCG based-H ₂ production scenarios.	105

Figure 4.4: GHG mitigation potential of replacing SMR technology with SMR-CCS and UCG-CCS technologies for H₂ production in bitumen upgrading in western Canada..

..... 116

Nomenclature

ACTL	Alberta Carbon Trunk Line
ASU	air separation unit
bpd	barrel per day
CC	combined cycle
CCS	carbon capture and sequestration
CO ₂ -eq	carbon dioxide equivalent
CRIP	controlled retractable ignition point
CTL	coal-to-liquid
<i>d</i>	depth of well, meter
<i>E</i>	diesel energy consumption in well drilling, megajoule
ECBM	enhanced coal bed methane
EOR	enhanced oil recovery
FUNNEL-EGY-H2-UCG	FUNDamental ENgineering PrinciplEs-based Model for Estimation of EnerGY consumption and production in hydrogen (H ₂) production from Underground Coal Gasification
FUNNEL-GHG-H2-UCG	FUNDamental ENgineering PrinciplEs-based Model for Estimation of GreenHouse Gases in hydrogen (H ₂) production from Underground Coal Gasification
GEMIS	Global Emissions Model for Integrated Systems

GHG	greenhouse gas
GJ	giga Joule
REET	Greenhouse Gases, Regulated Emissions and Energy Use in Transportation Model
GT	gas turbine
GTL	gas-to-liquid
GWP	global warming potential
HP	high-pressure
HRSG	heat recovery steam generator
HT	high-temperature
HX	heat exchanger
IGCC	integrated gasification combined cycle
kg	Kilogram
kWh	kilowatt hour
L/hr	liter per hour
LCIA	life cycle impact assessment
LCA	life cycle assessment
LHV	lower heating value
LP	low-pressure
LT	low-temperature
MDEA	methyl diethanolamine
MEA	Monoethanolamine
MJ	Megajoule

MPa	mega Pascal
Mt	mega tonne
MW	Megawatt
MW	mega Watt
MWh	megawatt hour
NER	net energy ratio
NG	natural gas
NGSR	natural gas steam reforming
η_e	coal to electricity conversion efficiency
η_h	coal to hydrogen conversion efficiency
PSA	pressure swing adsorption
SCG	surface coal gasification
SCO	synthetic crude oil
SMR	steam methane reforming
SR	steam reforming
SRR	syngas reforming reactor
ST	steam turbine
Tt	trillion tonnes
UCG	underground coal gasification
USC	ultra-supercritical
WGSR	water gas shift reactor

Chapter 1

Introduction

1.1. Background

Bitumen, a highly viscous fluid, must be chemically and physically processed to decrease its viscosity, density, sulphur, carbon, and metal concentrations [1, 2]. This process is called bitumen upgrading, and the product obtained is known as synthetic crude oil (SCO) [1]. Bitumen is upgraded for the following reasons. First, upgraded bitumen can be fed to refineries that are designed to process conventional crude oils [3]. Second, upgraded bitumen does not require a solvent in transportation to refineries [1, 3]. Third, the market price of the bitumen increases when upgraded [1, 3]. Canadian crude oil production from the oil sands is projected to rise from 1.9 million barrels per day (bpd) in 2013 to 3.2 and 4.8 million bpd in 2020 and 2030, respectively [4]. SCO or upgraded bitumen production from the Canadian oil sands is anticipated to rise from 0.88 million bpd in 2012 to 1.26 million bpd in 2022 [5]. The production of hydrogen (H_2), required to upgrade bitumen to SCO, will increase in a similar fashion. To put this into perspective, around 21 kg of H_2 is required to upgrade one cubic meter of bitumen to SCO, and this translates to a hydrogen demand of 4.2 thousand tonnes per day to produce 1.26 million bpd of SCO in 2022 [4, 6].

There are two commercial bitumen-to-SCO conversion configurations – coking and hydroconversion [3, 6]. The former has a lower SCO output per unit bitumen feed than the former [3]. Moreover, sulphur, nitrogen, and aromatic concentrations in the SCO produced from the coking-based configuration are higher (leading to low quality) than from the hydroconversion-based configuration [3]. In addition, the H₂ consumption is different in the two upgrading configurations; around 11.7 and 30.3 kg of H₂ are required to upgrade one cubic meter of bitumen in the coking-based and the hydroconversion-based bitumen upgrading configurations, respectively [6].

Steam methane reforming (SMR) is the dominant H₂ production pathway for bitumen upgrading in Alberta and leads to a significant amount of greenhouse house (GHG) emissions, ranging from 8.9-14.2 kg of CO₂-eq per kg of H₂ produced [6-12]. To put things into perspective, H₂ production from SMR accounts for around 43% of the total well-to-upgrading¹ GHG emissions in the Canadian oils sands industry [6]. In 2010, the Alberta oil sands industry contributed around 23% and 8% to Alberta's and Canada's total GHG emissions, respectively [13, 14]. With a focus on reduction of GHG emissions, the Government of Alberta has set a target of a 50% reduction in projected business-as-usual GHG emissions in 2050, which is around 200 million tonnes in GHG emissions reduction [13]. Therefore, there is justification to explore and study an alternate, less GHG-intensive, hydrogen production pathway for the bitumen upgrading industry.

¹ Well-to-upgrading emissions are those associated with bitumen extraction and upgrading to SCO. In absolute numbers, 0.25 tonne of CO₂ will be emitted if SMR is used to produce the required amount of H₂ to upgrade one cubic meter of bitumen [6-10].

Coal reserves in Alberta are estimated to be in the range of 1.8 to 2.7 trillion tonnes (Tt) [15-18]. Of the total reserves, there is the potential to recover around 0.56 Tt (or 25% of total reserves) by surface and underground mining [18]. The remaining 75% of the un-minable coal reserves² can be retrieved through technology like underground coal gasification (UCG) [17, 19]. In UCG, gasifying agents (mainly air, oxygen, water, and steam) are injected into a coal seam, and syngas is produced through chemical reactions that normally occur in surface coal gasifiers [20, 21]. This produced syngas can be used to produce electricity, hydrogen, liquid fuels, etc. [20, 21]. UCG is not only a pragmatic technology for clean coal conversion but also has several economic advantages over surface coal gasification (SCG). UCG significantly reduces the cost of upstream operations such as coal mining, coal handling, coal transport, and coal gasifiers, and leads to low fugitive emissions, low dust, no ash residues, and reduced noise pollution [19, 20, 22, 23].

Furthermore, CO₂ sequestration can be combined with UCG, mainly because of the close proximity of CO₂ sequestration sites with the un-mineable coal reserves [24-26].

Therefore, keeping in mind the abundant coal reserves in Alberta, which are estimated to

² Initial studies have suggested that three coal zones in Alberta – Ardley, Horseshoe Canyon, and upper Mannville – are suitable for UCG. These three zones constitute around 54% of the total coal reserves. Owing to greater depth, upper Mannville (which has around 16% of the total coal reserves) is the most favorable coal zone for UCG in terms of ground water protection and unwanted overburden subsidence [17].

be in the range of 1.8-2.7 Tt, UCG along with carbon capture and sequestration (CCS) is potentially an environmentally benign H₂ production pathway [15-18]. More recently, the feasibility and the operation of UCG for syngas production in Alberta was demonstrated by Swan Hills Synfuels LP [27].

Since coal has the highest CO₂ emissions of all fossil fuels per unit of energy produced, converting syngas to electricity or H₂ produces significant amounts of CO₂ emissions [23, 25, 26]. CCS technology captures CO₂ using a physical solvent within a pre-combustion arrangement and then stores the CO₂ in an underground geological formation for enhanced oil recovery (EOR) or enhanced coal bed methane (ECBM) recovery [20, 25, 26, 28]. Moreover, geological sequestration sites (such as saline aquifers) have been found to co-exist with potential UCG sites [24-26]. The Western Canadian Sedimentary Basin, in which most of Alberta's coal reserves are found, has many favorable CO₂ sequestration sites³ [11]. To put this into perspective, Alberta has the potential to store up to three gigatonnes of CO₂, apart from storing up to 450 megatonnes (Mt) of CO₂ in enhanced oil recovery (EOR) operations [30, 31]. With regard to CCS, over \$C 3 billion

³ Alberta Carbon Trunk Line, a 16 inch, 240 km CO₂ pipeline expected to be operational in 2015, will transport CO₂ collected from current and proposed bitumen upgraders to EOR fields in central and southern Alberta [12]. In another large-scale CCS project – the Shell Canada Energy Quest Project – about one million tonnes of CO₂ per annum, captured from a bitumen upgrading facility located in Fort Saskatchewan, Alberta will be transported and sequestered in a nearby geological site [29].

worth of investments have been made by several provincial governments as well as the Federal Government in various CCS demonstration projects [31].

Interestingly, UCG and CCS can be coupled in a process wherein the captured CO₂ is sequestered into a coal seam cavity created upon gasification by using the same injection and production wells [23, 26]. A similar integrated UCG-CCS process was discussed for a study area in Bulgaria by Nakaten et al. [32]. However, there are energy and cost penalties associated with CCS [31, 33]. Admittedly, with huge un-mineable coal reserves in Alberta and with UCG and CCS potential, a low-carbon H₂ production pathway should be analyzed in terms of sustainable development of the bitumen upgrading industry.

While the UCG and CCS technologies are in development stages in western Canada, it is important to quantify the environmental footprint and the economic assessment in order to provide key insights for decision making for the government and industry regarding such technologies.

1.2. Life cycle assessment

A life cycle assessment (LCA) is a powerful tool that evaluates the environmental impact of a system from cradle to grave [8]. An LCA allows for the characterization of the consequences of possible public policy options or scientific alterations and the development of novel sustainable energy resources [8, 34-36]. LCA is a technique used to evaluate the energy and material use associated with an energy production pathway or product [37]. In order to evaluate the environmental impact of a system, all the inputs and

outputs from raw material extraction to final disposal are aggregated [38]. The results of the LCA can help to identify key processes in an energy production pathway that can be improved to reduce the overall environmental impact of the pathway [34]. Overall, the LCA methodology can be implemented to evaluate the life cycle GHG emissions associated with an energy production pathway. GHG abatement cost estimates are used to evaluate GHG mitigation and the economics of an energy system, and are helpful in making sound policy decisions [39, 40]. These cost estimates are useful in determining which technologies have superior GHG abatement potential or greater economic competency [40].

There are a few studies in the literature that discuss H₂ production from UCG. Yang et al. [41] discussed the fundamentals of H₂ production by analyzing the experimental conditions and the UCG process in China. Rogut et al. [42] discussed the potential of UCG for large-scale integration of H₂ production with on-site geological storage of CO₂ in the European Union. Some studies have described a techno-economic model for electricity and H₂ production from an integrated UCG-CCS process [11, 32]. Nakaten et al. [32] concluded that the UCG-CCS process, integrated with a combined cycle (CC) gas turbine (GT), is an economical, low-carbon option for electricity production in Bulgaria. Prabu et al. [43] developed a model to estimate electrical plant efficiency for an integrated UCG-solid oxide fuel cell system (SOFC) system. Nourozieh et al. [44] conducted a feasibility study for Alberta reservoirs by developing a simulation model for process optimization and prediction of syngas production. Recently, Swan Hills Synfuels

LP has successfully constructed and operated the world's deepest in situ coal gasification pilot facility in Alberta [27].

The system design of converting H_2 from syngas produced from UCG is identical to that of H_2 produced from surface coal gasification [20, 21], and the latter is well described in various studies [45-56]. Following [45-56], a model to estimate and analyze key performance estimates (coal-to- H_2 conversion efficiency (η_h) and coal-to-electricity efficiency (η_e)) of UCG-based H_2 production can readily be developed. While these studies [45-56] focused more specifically on mineable coal and natural gas as a feedstock, the work carried out in this thesis addresses the gap in knowledge in the area of energy balances and the evaluation of plant efficiency in the production of H_2 from unmineable coal resources through UCG.

With regard to implementing an LCA, there are many studies that evaluate environmental competitiveness of various H_2 production pathways (both renewable and non-renewable). Lee et al. [57] conducted an LCA of H_2 production from naphtha steam reforming, natural gas steam reforming (NGSR), liquefied petroleum gas steam reforming, and water electrolysis with wind power. They concluded that the H_2 production from water electrolysis with wind power has the lowest global warming potential (GWP) among the systems studied. Ozbilen et al. [58] concluded that H_2 production from thermochemical water decomposition cycles is less GHG intensive than NGSR. In another study by Ruether et al. [59], an LCA for H_2 fuel production in the United States from liquefied natural gas (LNG) and coal was performed. The results of the analysis showed that

although H₂ production from coal gasification is more GHG intensive than from LNG gasification, the implementation of CCS has a greater environmentally favorable effect with coal than with LNG [59].

Pereira et al. [60] integrated the Greenhouse Gases, Regulated Emissions and Energy Use in Transportation (GREET) model and the Global Emissions Model for Integrated Systems (GEMIS) to conduct a well-to-wheel analysis of H₂ production from wind and solar energy for Portugal. Dufour et al. [61] implemented the LCA of various NG-based H₂ production pathways (i.e., SMR, SMR-CCS, thermal and autocatalytic decomposition of NG) by using SimaPro software. They concluded that H₂ production from SMR-CCS led to 67% lower GHG emissions than conventional SMR. More recently, Dufour et al. [8] compared life cycle GHG emissions in H₂ production from water photo-splitting, solar two-step thermochemical cycles, automated NG decomposition, SMR, SMR-CCS, and electrolysis with different electricity sources (mainly wind, solar, and conventional grid). They concluded that H₂ production from water photo-splitting with cadmium sulphide as a catalyst is the least GHG intensive of all aforementioned pathways. Aspen Plus software was used to conduct a simulation of large-scale H₂ production from the water splitting thermochemical cycle, and the obtained results were then used to implement the LCA [62].

An exergetic LCA of H₂ production from wind and solar energy showed that although the use of wind and energy has lower fossil and mineral consumption, the cost of H₂ production is 2.25-5.25 times higher than SMR-based H₂ production [9]. Cetinkaya et al.

[7] reported that for a large-scale H₂ production operation, NGSR, coal gasification, and thermochemical water splitting with copper-chlorine cycles are more beneficial than wind and solar energy-based pathways. These same authors also compared the LCA outcomes with coal gasification- and coal pyrolysis-based H₂ [7].

There are many studies in the literature that discuss GHG abatement potential and GHG abatement costs of energy efficiency technologies and CCS in various industry sectors [33, 40, 63-65]. Saygin et al. [33] concluded that energy efficient CCS can help reduce 47% of Netherland's industrial GHG emissions in 2040. Xiao et al. [40] evaluated an average GHG abatement costs of \$19.5 (US, 2010) per tonne-CO₂ of 34 energy saving technologies for China's building sector. Garg et al. [64] created marginal abatement cost curves for electricity and CO₂ emissions for Gujarat, India. In a study applicable in South Africa by Telsnig et al. [65], a coal-based integrated gasification combined cycle (IGCC)-CCS plant was found to have the greatest potential for GHG mitigation and the lowest GHG abatement costs among a synthetic fuel coal-to-liquid (CTL)-CCS, a gas-to-liquid (GTL)-CCS, and a coal fired ultra-supercritical (USC)-CCS plant.

There are a lot of gaps in the existing literature with regard to environmental evaluation of UCG as a H₂ production pathway. Numerous motivating factors were identified to conduct the research presented in this research work.

1.3. Research motivation

Several factors spurred this research project. Some of these are listed below.

1. Abundant coal reserves in Alberta, deemed un-recoverable through conventional mining methods, can be recovered through UCG technology. Because UCG technology is still in the infancy stage in western Canada and the information on the operational data for H₂ production from UCG is very limited, a model that would allow its environmental evaluation would be useful. The insight gained from this study could help government in development and formulation of appropriate policy and industry in making investment decisions on large-scale implementation of UCG, especially in a carbon-constrained energy economy such as Alberta's.
2. None of the studies in the literature developed models that provide a holistic evaluation of the energy balances involved in UCG for H₂ production along with the integration of CCS technology. This holistic approach is especially important to characterize the energy conversion efficiency of UCG as a H₂ production pathway, which provides insight into its competitiveness with other conventional options. In addition, the resolution of the energy flows in the H₂ production unit operations and the sensitivity of these unit operations towards key technical parameters will lead to the identification of energy-intensive centers along with improvements in the overall energy and GHG management.

3. While extensive work has been carried out on the LCA of conventional and unconventional H₂ pathways, there is very limited research in the literature on the evaluation of UCG from an LCA perspective and its comparison with other H₂ production pathways. With this in mind, the LCA conducted in this research aims to provide a reliable and comprehensive estimate of the life cycle GHG emissions in H₂ production from UCG along with CCS.

4. None of the existing studies in the literature establish qualitative and quantitative relationships between key UCG process parameters (H₂O-to-O₂ injection ratio, ground water influx, and steam-to-carbon ratio in syngas conversion) and life cycle GHG emissions in H₂ production with and without CCS. Moreover, there is a need to develop a model through which benchmarking of H₂ conversion efficiency from UCG can be carried out with surface coal gasification (SCG)- and SMR-based H₂ production pathways.

5. No study in the literature assesses the GHG reduction potential and GHG abatement costs of UCG technology along with CCS for H₂ production for bitumen upgrading in western Canada. In other words, none of the studies in the literature consider large-scale H₂ production systems in the oil production sector where there is substantial interest in reducing the overall GHG footprint. Furthermore, avenues for efficiency improvements in H₂ production processes need to be explored in order to minimize life cycle GHG emissions and GHG abatement costs.

The estimates developed in this research can contribute to sustainable development in GHG intensive sectors, especially those with considerable hydrogen demand (e.g., western Canada's bitumen upgrading industry).

1.4. Thesis objectives

The principal objective of the research is to evaluate life cycle GHG emissions and GHG abatement costs of producing hydrogen from UCG along with CCS technology for the western Canadian bitumen upgrading industry. The specific objectives of this research are:

1. To develop an integrated and data-intensive simulation-based H₂ production process model and Excel-based spreadsheet model for assessing the life cycle GHG emissions in H₂ production from UCG with and without CCS.
2. To conduct a sensitivity analysis of key UCG parameters and other technical factors involved in different unit operations that impact the life cycle GHG emissions in H₂ production from UCG with and without CCS.
3. To calculate the GHG abatement costs of producing H₂ for the bitumen upgrading industry by SMR- and UCG-based technologies along with CCS. This is done for several practical H₂ production scenarios applicable to western Canada.

1.5. Organization of thesis

This thesis is organized in a paper-based format in the manner described below. It is important to mention that some information in the chapters has been repeated because of this format.

Chapter 2 – *Development of a Process Simulation Model for Energy Analysis of Hydrogen Production from Underground Coal Gasification (UCG)*: This chapter presents the methods and assumptions for developing an Aspen Plus simulation model – FUNNEL-EGY-H2-UCG (**FUN**damental **EN**gineering **Princip**lEs-based **Mode**L for **Est**imation of **Ener**GY consumption and production in hydrogen (**H2**) production from **Underground Coal Gasification**) – in order to perform energy balances and estimate H₂ conversion efficiency from UCG-based syngas. The model is developed for H₂ production from UCG-based syngas with and without CCS, along with the co-production of electricity and steam in a conventional combined cycle plant. In addition, the effect of key UCG parameters like H₂O-to-O₂ injection ratios, ground water influx, and steam-to-carbon ratios in syngas conversion on H₂ production plant efficiencies is investigated in detail. Electricity production from UCG is analyzed to validate the practicality of the model under the stated set of assumptions for different unit operations of the H₂ production pathway presented in the chapter.

Chapter 3 – *Life Cycle Assessment (LCA) of Hydrogen Production from Underground Coal Gasification (UCG) with Carbon Capture and Sequestration (CCS)*: This chapter presents a data-intensive LCA model – FUNNEL-GHG-H2-UCG (**FUN**damental

ENgineering PrinciplEs-based ModeL for Estimation of GreenHouse Gases in hydrogen (H₂) production from Underground Coal Gasification) – to evaluate life cycle GHG emissions in H₂ production from UCG with and without CCS. The model also takes into account the life cycle GHG emissions associated with well drilling, H₂ transportation, and CO₂ transportation and sequestration. Furthermore, to study the effect of key UCG parameters and other technical parameters on the life cycle GHG emissions, a sensitivity analysis is completed.

Chapter 4 – *Greenhouse Gas Abatement Costs of Hydrogen Production from*

Underground Coal Gasification (UCG): This chapter explores GHG abatement costs and GHG abatement potential of producing hydrogen from UCG along with CCS. Seven H₂ production scenarios, applicable to western Canada, are considered to assess the competitiveness of implementing UCG versus steam methane reforming (SMR) along with CCS. The analysis is completed by executing an LCA of large-scale H₂ production from UCG and SMR with and without CCS.

Chapter 5 – *Conclusions and Recommendations for Future Work*: This chapter includes the key conclusions and observations from the research conducted. In the end, recommendations for improvements in the current LCA model and the scope of adapting the current model to evaluate other useful UCG-based products are presented.

Chapter 2

Development of a Process Simulation Model for Energy Analysis of Hydrogen Production from Underground Coal Gasification (UCG)

2.1. Background

Few studies in the literature discuss hydrogen (H_2) production from underground coal gasification (UCG). The fundamentals of H_2 production from UCG in China were discussed in [41] by investigating the experimental conditions and the UCG process. In a study applicable in the European Union, Rogut et al. [42] discussed the potential of UCG for large-scale integration of H_2 production with on-site geological storage of CO_2 . Some studies have completed a techno-economic analysis of electricity and H_2 production from UCG along with carbon capture and sequestration (CCS) [11, 32]. The process design of H_2 conversion from surface coal gasification-based syngas is similar to that of UCG-based syngas [20, 21], and the former is well described in the literature [45-56]. These studies [45-56] focused more on natural gas and mineable coal as a feedstock for H_2 production. Therefore, a model to estimate and analyze key performance estimates of UCG-based H_2 production facility can readily be developed by following these studies [45-56].

This study discusses the development and results of a simulation model to estimate and analyze key performance estimates (coal-to-H₂ conversion efficiency (η_h) and coal-to-electricity efficiency (η_e)) of a UCG-based H₂ production facility with and without carbon capture. The model is called FUNNEL-EGY-H2-UCG (**FUN**damental **EN**gineering **Prin**cipl**Es**-based **Mod**e**L** for **Est**imation of **Ene**r**GY** consumption and production in hydrogen (**H2**) production from **U**nderground **C**oal **G**asification). Furthermore, this study provides a framework through which benchmarking of H₂ conversion efficiency from UCG can be carried out with SCG- and SMR-based H₂ production pathways. This part of the work also establishes the qualitative and quantitative relationships between key UCG process parameters (H₂O-to-O₂ injection ratio, ground water influx and steam-to-carbon ratio) and plant efficiency. The developed model – FUNNEL-EGY-H2-UCG – helps in the assessment of energy balances and the evaluation of plant efficiency in the production of H₂ from un-mineable coal resources through UCG.

2.2. Methodology

2.2.1. Plant layout overview: H₂ production from UCG with and without CCS

The H₂ production pathway from UCG is developed for two different plant configurations: with CCS and without CCS. Figure 2.1 shows all the unit operations

involved in the hydrogen production pathway for the two plant configurations. The difference in the two plant schemes is that CCS uses CO₂ compression, transportation, and sequestration and the configuration without CCS does not. The underground coal seam is gasified by injecting H₂O and O₂ via an injection well. Upon gasification, coal produces syngas, which travels through a production well. This syngas is mainly composed of CO, H₂, CH₄, CO₂, and H₂O. Apart from this, the syngas also contains traces of H₂S, C₂H₆, NH₃, and higher hydrocarbons.

Based on the composition of the syngas, the H₂ production plant scheme can be derived from existing SCG- and SMR-based H₂ production plant schemes. An extensive review of hydrogen production pathways from surface coal gasification and steam methane reforming, provided in [8, 11, 46, 47, 50, 66] was done to determine assumptions for different post-UCG unit operations (see Fig. 2.1). The H₂ production pathway also consists of a co-generation section, which produces electricity and steam to satisfy the requirements of the different unit operations. The underlying assumptions and system components of each unit operation are discussed in the following section of the chapter. The Aspen Plus simulation tool is used to model and perform the energy and mass balance of the different unit operations. The inputs and outputs of the Aspen Plus simulation sheet are integrated with a data-intensive Excel-based spreadsheet and the Aspen Simulation Workbook. Appendix A can be referred for process flow diagram of the individual unit operations that are modeled in Aspen Plus; a brief overview of the unit operations is given in the following section.

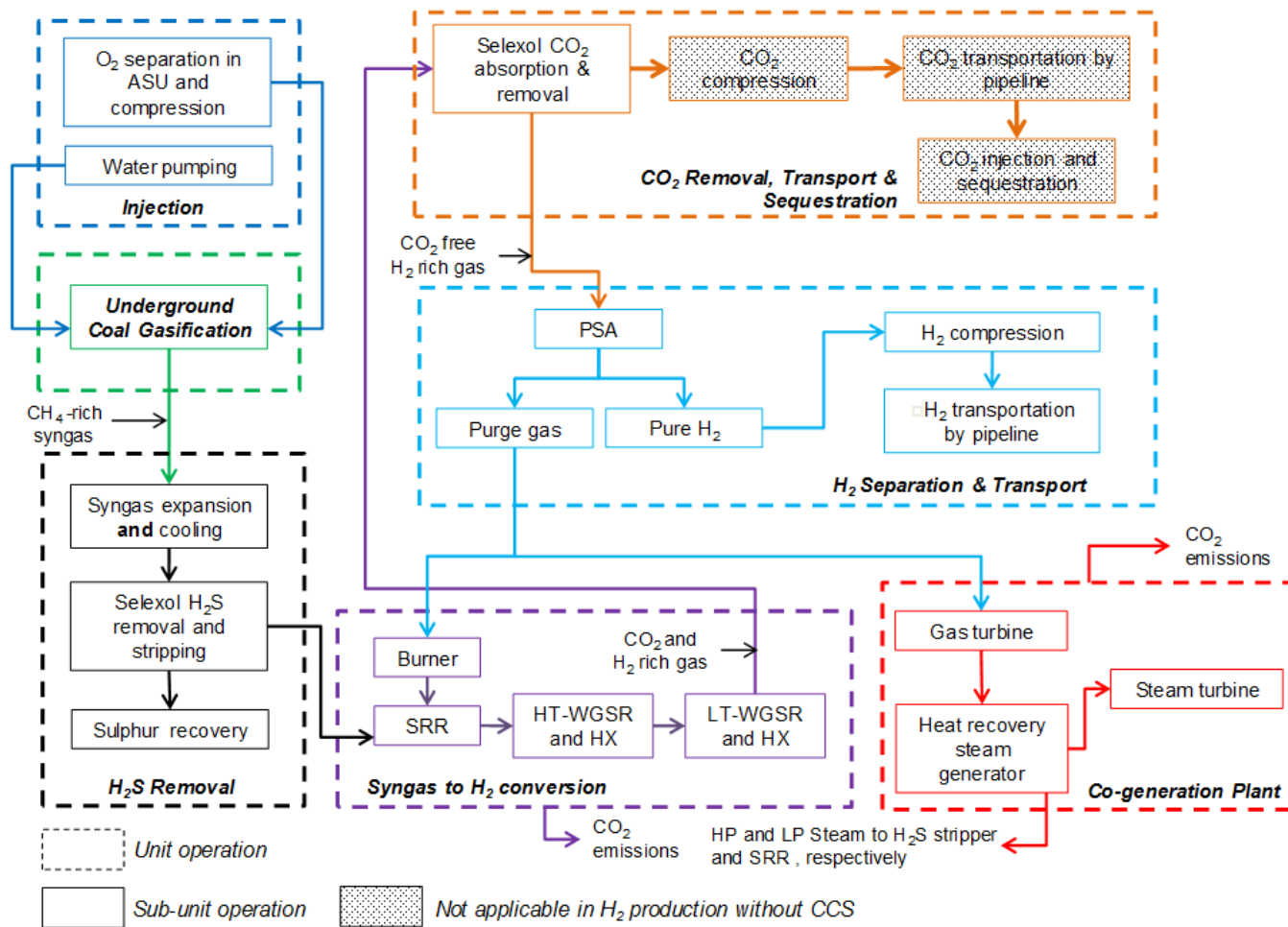


Figure 2.1: Unit operations of H₂ production pathways from UCG with CCS and without CCS. All unit operations, except O₂ production in ASU and sulphur recovery in Claus unit are modeled in Aspen Plus.

2.2.2. H_2 production from UCG – An overview of unit operations

2.2.2.1. *Injection:* This unit operation involves the injection of gasifying agents, mainly oxygen and water, at a pressure of 200 bar and 140 bar, respectively [27]. Oxygen with 95% purity is produced by an air separation unit (ASU) at a pressure of 1.05 bar, which consumes 0.26 kWh of electricity per kg of pure O_2 production [46, 47]. It is assumed that the in situ coal gasification reactor is connected by a pair of wells; an injection well is a 1400 meters deep and is around 1400 meters from a 1400 meter high production well [27]. The well diameter is 4.5 inches [27].

2.2.2.2. *Underground coal gasification:* The specification of coal used for in situ gasification is shown in Table 2.1. Due to a lack of production data for hydrogen production from UCG on a large commercial scale for deep coal seams, in situ coal gasification at a small-scale hydrogen production plant was analyzed. In this study, operational data, mainly type, amount of coal gasified, and injection flow rates of gasifying agents, are taken from a small-scale UCG pilot plant for syngas production operated by Swan Hills Synfuels in Alberta [27]. This pilot project is carried out at a depth of 1400 m, which is one of the deepest of the pilot or commercial UCG projects around the world [22, 27]. Owing to greater coal seam depth, the operating pressure of the UCG reactor in Alberta, Canada ranges from 10 to 12.5 MPa [27, 67]. High operating pressures result in low water influx in the gasification zone of the UCG reactor and high gas losses from the rock formation [20, 21].

The authors in [27] describe a controlled retractable ignition point (CRIP)⁴ technique that was used to gasify coal underground. The CRIP technique and high operating pressure result in the production of high quality syngas, low thermal losses, and improvement of the overall gasification efficiency [22, 68]. Heat loss to the surrounding strata in UCG is difficult to estimate and depends on the properties of the dry rock above the coal seam [20, 22]. Also, the UCG process reaches a heat balance on its own [22]. With that said, a nominal temperature decrease of 100° C in the syngas is assumed in this study to address the heat losses in the UCG reactor. Another factor that is difficult to estimate in UCG is the rate of ground water influx in gasification, which not only affects the composition of the syngas but also the quality and quantity of the syngas [20, 21]. It is also reported in the literature that the influx water will either be part of the gasification reactions or cool the gases in the reactor [21]. It is assumed in the present study that ground water (amounting to 0.4 m³/tonne of coal)⁵ takes part in the gasification reaction, and its effect on η_h , and η_e is addressed.

⁴ The CRIP technique uses coiled tubing for injection through an injection well that is drilled horizontally until it reaches the foot of a production well [22]. Fresh coal is reached by retracting the coil when the cavity has matured (because of which the syngas quality becomes poor) [22].

⁵ A ground water influx rate of 0.4 m³/tonne of coal is assumed for stable and continuous gas production [69].

Table 2.1: Key assumptions in UCG

Parameter/values		Sources/comments	
Coal Type	High Volatile B Bituminous	[27]	
	Manville Coal		
<u>Coal Composition</u>			
Ultimate Analysis		Proximate Analysis	
<i>Parameter</i>	<i>%</i>	<i>Parameter</i>	<i>%</i>
Ash	9.7	Moisture	4.7
Carbon	74.6	Ash	9.3
Hydrogen	3.6	Volatile matter	30.5
Nitrogen	1.1	Fixed carbon	55.5
Sulphur	0.4		
Oxygen	10.7		
LHV of coal (MJ/kg)		28.5	Average of the range 26.8-30.2 MJ/kg [11, 70]
Coal gasified (tonnes/day)		118	[27]
Oxygen injection (tonnes/day)		45	[27]
Water/Oxygen injection mass ratio		2	[27]

One of the most important considerations in estimating H₂ production from UCG is the composition of the syngas collected from the production well. The process of UCG is similar to surface coal gasification, from a chemical and a thermodynamic perspective [71]. The in situ coal will undergo a series of chemical reactions, namely coal drying, pyrolysis, char gasification, boudouard, steam gasification, hydrogen gasification, CO combustion, gas-steam shift, and methane-steam shift⁶ [67, 72]. Coal is characterized in Aspen Plus in the form of products obtained after pyrolysis, that is, char, tar, H₂S, C₂H₆, CO, CH₄, NH₃, CO₂, H₂, ash, and H₂O. The mass flow rates of each of these constituents are estimated in a similar fashion as done by the authors of [67], using a mathematical model provided by [73]. The syngas composition is estimated based on the minimization of the Gibbs free energy of the UCG reactor using the Peng-Robinson equation of state in Aspen Plus. The model developed is predicated upon the assumption that the UCG reactor reaches equilibrium with the following: surrounding strata, ground water influx, heat losses and gasifying agents (H₂O and O₂) at a given point of time. The UCG process is represented by two RGibbs reactors in Aspen Plus. The second RGibbs reactor accounts for heat losses in the UCG reactor by specifying the assumed temperature decrease of 100° C. However, there are limitations with this methodology. The resolution

⁶ Coal drying: Wetcoal → Drycoal + H₂O, ΔH⁰ = 40 kJ/mole; Pyrolysis: Drycoal → Char + Volatiles, ΔH⁰ ~ 0 kJ/mole; Char gasification: C + O₂ → CO₂, ΔH⁰ = -393 kJ/mole; Steam gasification: C + H₂O → H₂ + CO, ΔH⁰ = +131 kJ/mole; Boudouard: C + CO₂ → 2CO, ΔH⁰ = +172 kJ/mole; Hydrogen gasification: C + 2H₂ → CH₄, ΔH⁰ = -75 kJ/mole; CO combustion: CO + 1/2O₂ → CO₂, ΔH⁰ = -283 kJ/mole; Gas-steam shift: CO + H₂O ↔ CO₂ + H₂, ΔH⁰ = -41 kJ/mole; Methane-steam shift: CH₄ + H₂O ↔ CO + 3H₂, ΔH⁰ = +206 kJ/mole

of syngas losses to the surrounding rocks and dynamic temperature-pressure profile in the in situ coal seam and its effect on the syngas composition are beyond the capacity of the model presented in this study.

The composition of the syngas on a dry molar basis based on 118 tonnes per day of coal extracted by UCG for an H₂O-to-O₂ injection ratio of 2 and a ground water influx of 0.4 m³/tonne of coal is given in Table 2.2. The composition of the produced gas obtained from the model is consistent with reported values in the literature for a variety of coal, i.e., H₂: 11-35%; CO: 2-16%; CH₄: 1-8%; CO₂: 12-28%; H₂S: 0.03- 3.5% [22].

Considering the high operating pressures in UCG, there is likely to be considerable CH₄ in the produced gas, unlike in low operating pressures, where the CH₄ percentage is lower than that of other gas constituents [27, 67]. This is mainly due to the fact that the hydrogen gasification reaction ($C + 2H_2 \rightarrow CH_4$) is favorable at a high underground reactor pressure [27, 67]. The product gas is treated with steam to convert CH₄ into water gas (H₂ + CO) in a surface reforming reactor to improve coal to H₂ conversion efficiency (η_h). This reactor is called a syngas reforming reactor (SRR) in this study.

Table 2.2: Composition of the syngas produced from UCG

Dry gas mol%					Total	Calorific
					volume of	value of
					dry gas	syngas
CH ₄	CO ₂	CO	H ₂	H ₂ S	Nm ³ /hr	MJ/m ³

Dry gas mol%					Total	Calorific
					volume of	value of
					dry gas	syngas
10.77%	20.73%	33.69%	34.63%	0.19%	11168.26	10.55

2.2.2.3. *Hydrogen sulphide (H₂S) removal*: Sulphur needs to be removed from the product gas obtained from UCG both for economical operation and to avoid poisoning the catalysts in the reforming reaction of the methane present in the product gas [66]. This is unlike in surface coal gasification plant schemes with CCS, where H₂S is co-captured with CO₂ downstream of water-gas shift reactions [46, 47, 53, 54]. Additionally, prior to H₂S removal, the highly pressurized product gas obtained from UCG is expanded in a turbine to around 30 bar⁷ to generate electricity and then cooled to 25° C [66]. The heat extracted from the hot UCG-syngas is used to raise the temperature of the sulphur-free gas, which is put into the SRR. The polytropic efficiency of the syngas expander is assumed to be 88% [46]. H₂S capture is carried out in an absorption tower with dimethyl ether of polyethylene glycol (Selexol) as a solvent and an operation pressure of 30 bar [46, 47, 50, 66]. The process flow scheme from H₂S absorption to stripping is derived from [50].

⁷ The pressure value of 30 bar is based on values in the literature of steam methane reforming reaction in H₂ production from natural gas plant schemes [66].

The solubility of CO₂ in Selexol is about 8.93 times less than that of H₂S [74]. However, the amount of CO₂ absorbed in Selexol is significantly greater than the amount of H₂S absorbed. This is because of higher mole concentration of CO₂ than of H₂S in the product gas [46] (see Table 2.2). Therefore, after stripping H₂S from Selexol, the solvent is fed to a CO₂ absorption tower downstream of water-gas shift reactors (WGSRs) to capture the CO₂. Close to 99% of H₂S is removed from the product gas, which is consistent with the 99% H₂S removal efficiency reported in the literature [45, 46, 50]. Steam (6 MJ, 6 bar steam per kg of sulphur [46]) required to strip H₂S from the solvent is produced from a heat recovery steam generator (HRSG) in a co-generation plant. The above assumptions are also valid for plant schemes without CCS. Sulphur is recovered in a Claus plant, which consumes 98 kWh of electricity per tonne of sulphur removed⁸ [75]. Additional electricity is required to treat tail gas coming from the Claus plant and is assumed to be 463 kWh per tonne of sulphur removed⁸ [75].

2.2.2.4. Syngas to H₂ conversion: The sulphur-free and CH₄-rich syngas is processed in a series of reactors to produce H₂: a steam reforming reactor (SRR) and high temperature (HT) and low temperature (LT) WGSRs. Table 2.3 shows all the assumptions pertinent to this unit operation. A steam-to-carbon ratio of 3 is assumed in order to get the maximum H₂ output upon syngas conversion [66]. Carbon flow is calculated based on the molar flow of CH₄ and CO in the UCG produced syngas. The syngas is then converted to H₂ in a series of HT and LT WGSRs. A heat exchanger network is modeled in a simplified

⁸ Owing to complexity of the processes involved in the Claus plant, the sulphur recovery and tail gas treatment plants are not modeled in Aspen Plus.

fashion to use the heat recovered from the WGSRs to produce HP and LP steam in an HRSG. A portion of the purge gas, which is produced after the removal of H₂ downstream of CO₂ removal, is burned to satisfy the heat duty of the SRR.

Table 2.3: Key assumptions in SRR and WGSR

Parameter	Value	Sources
<u><i>SRR</i></u>		
Steam-to carbon-ratio	3	[66]
Temperature/pressure in SRR, °C/ bar	800/30	[66]
<u><i>WGSR</i></u>		
Pressure loss in WGSRs	4%	[46]
Temperature of gas inlet to HT-WGSR, °C	350	[45]
Temperature of gas outlet from HT-WGSR, °C	450	[45]
Temperature of gas inlet to LT-WGSR, °C	250	[45]
Temperature of gas outlet from LT-WGSR, °C	275	[45]
Pressure loss in HXs	2%	[46]
Temperature of gas inlet for CO ₂ absorption, °C	25	[45]

2.2.2.5. CO₂ removal and transportation: To integrate H₂ production from UCG with CCS, CO₂ is absorbed, removed, and compressed before its transportation to a sequestration site [45, 47, 76]. CO₂ is absorbed using Selexol as a solvent because

Selexol consumes less energy than other solvents like methyl diethanolamine (MDEA) [47]. The absorbed CO₂ is then separated in a series of flash chambers and finally compressed to a pressure of 150 bar in five stages [47, 76]. The solvent also absorbs H₂ in the absorption tower. Therefore, the solvent coming from the first flash chamber is compressed and recycled back to the absorption tower to avoid loss of H₂ [45]. The pressure drop between the first flash chamber and the absorption tower is achieved with a hydraulic turbine [45]. The work extracted from the hydraulic turbine is then used to satisfy a portion of solvent recycle pump work [45]. Table 2.4 shows key assumptions employed for this unit operation. In H₂ production without CCS, the advantage of CO₂ removal (see Fig. 2.1) is appreciated by achieving a higher heating value of purge gas (55.15 MJ/kg) post H₂ separation than a CO₂-rich purge gas of low heating value (3.15 MJ/kg) when no CO₂ removal takes place [46]. Additionally, the purge gas compression power required in the GT section is likely to be reduced, when CO₂ removal takes place ahead of H₂ separation in PSA.

Table 2.4: Key assumptions for CO₂ capture and removal

Parameter	Value	Sources/comments
<i><u>CO₂ absorption and removal</u></i>		
Solvent pump efficiency	75%	[46]
Recycle compressor isentropic efficiency	85%	[54]

Parameter	Value	Sources/comments
Recycle compressor mechanical efficiency	98%	[54]
Pressure in CO ₂ absorber, bar	50	[46]
Pressure of flash chambers, bar	17, 9.5, 3.2, 1.1	Values indicate pressure level in chambers 1, 2, 3, and 4, respectively [46]
<i><u>CO₂ compressor</u></i>		
Stage 1 discharge pressure, bar	2.4	[76]
Stage 2 discharge pressure, bar	5.6	[76]
Stage 3 discharge pressure, bar	13.2	[76]
Stage 4 discharge pressure, bar	30.2	[76]
Stage 5 discharge pressure, bar	73.8	[76]
Booster pump discharge pressure, bar	150	[76]
Final discharge temperature, °C	25	[76]
Compressor isentropic efficiency	0.75	[76]

Pipeline is assumed to be the mode of transportation of CO₂ to an EOR site. CO₂ is transported as a liquid, and a distance of 100 km from the CO₂ capture site to an EOR site is taken as the base case. CO₂ has a critical pressure of 7.38 MPa; that is, it behaves as a liquid at pressure values greater than 7.38 MPa [76]. Therefore, CO₂ is compressed to a pressure of 150 bar by means of a five-stage compressor power train [46, 54, 76, 77]. Table 2.4 shows the key assumptions pertaining to the CO₂ compressors. With an increase in pressure of the captured CO₂, the temperature also increases in each stage. Since the operating temperature in the compressor power train is assumed to be 31° C, the temperature of the captured CO₂ is decreased through the heat exchanger after each stage. The heat recovered from the heat exchangers is used in the HRSG section to produce steam.

2.2.2.6. H₂ removal and transportation: For plant schemes with and without CCS, H₂-rich gas after CO₂ removal is processed in a PSA unit to separate H₂ at an efficiency of 85% [46]. Since PSA processes require an elaborate and independent model for their assessment, the H₂ separation is represented as a simple separation process, with an efficiency of 85% [46, 66]. The remaining gas, known as purge gas, consists of the inseparable H₂ and some CH₄. A portion of the purge gas is then processed to produce electricity and steam in a co-generation plant, while the other portion is burned to satisfy the heat duty of the SRR. High purity (99.99%) H₂ is delivered at a pressure of 20 bar from PSA [46].

Pipeline is assumed to be the mode of transportation of H₂ to a bitumen upgrading site. A pipeline length of 100 km is used as the base case for H₂ transportation. Typical hydrogen pipeline operating pressures and diameters range from 1 to 3 MPa and 0.25 to 0.30 m, respectively [78]. Considering the exit H₂ gas pressure from PSA, the average of the range is used for the operating pressure in the present analysis. The efficiency of the H₂ compressor is assumed to be 55% [79]. Considering the small-scale H₂ production from UCG and the transportation of H₂, a lower value, 0.25 m, is used for pipeline diameter. The compressor power requirement is calculated using the model developed by Ogden [79].

2.2.2.7. Co-generation plant: This section includes several components, mainly gas turbine (GT), HRSG, and steam turbine (ST). The amount of purge gas fed to the burner is calculated based on the amount of heat duty required in the SRR. The remaining purge gas is compressed, combusted, and then expanded in a GT to produce electricity. The amount of air fed to the GT combustor is specified based on a turbine inlet temperature of 1300° C. The HRSG produces high-pressure (HP) and low-pressure (LP) steam from heat recovered from the SRR and the WGSRs as well as exhaust gas from the GT. The HP steam, at 30 bar, is fed to the SRR, and the LP steam, at 6 bar, is fed to the H₂S stripper. Table 2.5 shows key assumptions employed for this unit operation. The temperature of the exhaust gas is assumed to be 100°C [47]. Based on an average heat exchanger efficiency of 60%; heat losses in heat recovery are assumed to be 40%. Auxiliary power consumption is assumed to be 2% of the gross power output [45, 46]; this makes up for

the power consumption in the process and feed-water pumps [46]. Additionally, a transmission loss of 6.5% of net electricity produced is accounted for in estimating η_e [6].

Table 2.5: Key assumptions for a co-generation plant

Parameter	Value	Sources/comments
<i><u>Gas turbine</u></i>		
Mechanical efficiency	99.5%	[54]
Polytropic efficiency of turbine	88%	[46]
Polytropic efficiency of compressor	85%	[46]
Ambient air temperature/ pressure, °C/ bar	15/1.013	[54]
Turbine inlet temperature, °C	1300	[46]
Pressure ratio	14.8	[46]
Turbine outlet pressure	1.1	[54]
Efficiency of electric generator	98.7	[46]
<i><u>Steam turbine</u></i>		
		Based on steam pressure
Steam pressure (HP/LP), bar	30/6	requirement in SRR, and H ₂ S stripper
Isentropic efficiency of turbine	85%	[47]
Mechanical efficiency of turbine	99.5%	[54]
Pump efficiency	75%	[46]
Efficiency of electric generator	98.7%	[46]

2.3. Results and discussion

2.3.1. Power requirement in different unit operations: H_2 production from UCG with and without CCS

Table 2.6 shows a detailed breakdown of the total power consumption in producing H_2 from UCG with and without CCS. Based on a coal LHV of 28.5 MJ/kg and input of 118 tonnes/day [27, 70] (see Table 2.1), the total rate of coal input energy is calculated as 38.92 MW. This value is the same in H_2 production both with and without CCS. The gross power output from the syngas expander, ST and GT, estimated to be 4.2 MW for a steam-to-carbon ratio of 3, is also the same for both scenarios. The total system power requirement in H_2 production without CCS is less than in H_2 production with CCS; there is a net power output of 0.93 MW and 1.83 MW in H_2 production with CCS and without CCS, respectively. The difference in the net power output is because there is no CO_2 compressor power requirement in the latter scenario, which increases the net power output. η_h , which represents the fraction of the coal energy converted to H_2 energy, is calculated as 58.08 % for both scenarios. Since the net power output is different in the two scenarios, electrical efficiencies are estimated to be 2.4% and 4.7% in H_2 production with CCS and without CCS, respectively. Evidently, the increased η_e in the H_2 production scenario with no CCS is due to the “no CO_2 compressor” power requirement. This increase of 2.3% in η_e is consistent and can be compared with reported values in the literature for H_2 production from SCG with CO_2 capture [46]. CO_2 capture efficiency, calculated as 91.6%, is also found to be in close agreement with existing values in various studies and models [6, 45-48, 52, 55].

Table 2.6: Power requirement in different unit operations of H₂ production with CCS and without CCS

Parameter	Values	
	H ₂ production	H ₂ production
	with CCS	without CCS
Coal input (LHV basis), MW _{th}	38.92	38.92
H ₂ O-to-O ₂ injection ratio	2	2
Ground water influx, m ³ /tonne of coal	0.4	0.4
Steam-to-carbon ratio ¹	3	3
<i><u>Injection</u></i>		
ASU, MW	0.50	0.50
Oxygen compression, MW	0.55	0.55
Water pumping, MW	0.02	0.02
<i><u>Expander and H₂S removal</u></i>		
Syngas expander, MW _e	-1.58 ²	-1.58 ²
Claus and tail gas treatment plant	0.02	0.02
<i><u>CO₂ removal, and transport</u></i>		
Recycle compressor, MW	0.03	0.03
Recycle pump, MW	0.39	0.39
Auxiliary power in CO ₂ absorption unit ³	0.72	0.72
CO ₂ compressor, MW	0.96	0
CO ₂ capture efficiency ⁴	91.6%	0

Parameter	Values	
	H ₂ production	H ₂ production
	with CCS	without CCS
Purity of captured CO ₂ (mol %)	97.4% ⁵	0
Total CO ₂ emissions, kg/hr	1031.3	12207.4
<i><u>H₂ separation and transport</u></i>		
H ₂ compressor, MW	0.02	0.02
<i><u>Co-generation section</u></i>		
Gas turbine, MW	-1.16 ²	-1.16 ²
Steam turbine, MW	-1.46 ²	-1.46 ²
Gross power ⁶ , MW	-4.20	-4.20
Net power ⁷ , MW _e	-0.93	-1.83
H ₂ output (LHV basis), MW	22.61	22.61
H ₂ conversion efficiency, η_h ⁸	58.08%	58.08%
Electrical efficiency, η_e ⁹	2.39%	4.69%

¹ Represents the amount of steam required for syngas reforming in SRR, calculated based on the molar flow of carbon (CO+CH₄) in the syngas

² Negative value indicates power output

³ Power consumption of solvent pump and gas compressors

⁴ Represents the ratio of the amount of CO₂ captured to the amount of CO₂ in the feed gas

⁵ Remaining gas consists of CH₄ and other gases

⁶ Sum of electricity output from gas turbine, syngas expander, and steam turbine; this value includes auxiliary power consumption (2% of gross power output) and losses in the electrical generator (1.3% of gross power output)

⁷ Difference of gross power output and electricity requirement in all other unit operations. Also includes a transmission loss of 6.5%

⁸ Ratio of H₂ output (MW, LHV basis) to coal input (MW, LHV basis); LHV of H₂ is 120 MJ/kg

⁹ Ratio of net power output (MW) to coal input (MW, LHV basis)

Figures 2.2 and 2.3 show the power distribution in different unit operations of H₂ production from UCG with and without CCS. Injection, which comprises an ASU, O₂ compressor, and water pump, consumes around 33.4% and 47.7% of the total power requirement in H₂ production with and without CCS, respectively. The power requirement in the CO₂ removal is also significant and contributes 35.7% and 50.9% to the total power consumption in H₂ production with CCS and without CCS, respectively. CO₂ compressors contribute around 29.9% and 0% of the total power requirement in H₂ production with and without CCS, respectively. This zero power requirement in the “no CCS” scenario is because there is no CO₂ compression. Only a fraction of the total energy consumption is taken for H₂ compression and sulphur recovery, with values of approximately 1% in H₂ production with CCS and 1.4% in H₂ production without CCS.

Unarguably, with an increase in the scale of operation or pipeline transportation distance, the pipeline configuration may require additional booster stations to overcome the increased friction losses and keep the flow in a liquid state. In that case, the total power requirement is likely to increase. The H₂ compressor requirement in both scenarios is, however, insignificant compared to other system components’ power requirements. This

is mainly because the small-scale H₂ pipeline operation requires less pressure increase in the inlet pipeline compressor station in order to maintain the assumed operating pressure of the pipeline. Conversely, for a large-scale H₂ production plant, the power requirement is likely to increase to overcome the increased friction losses in the pipeline.

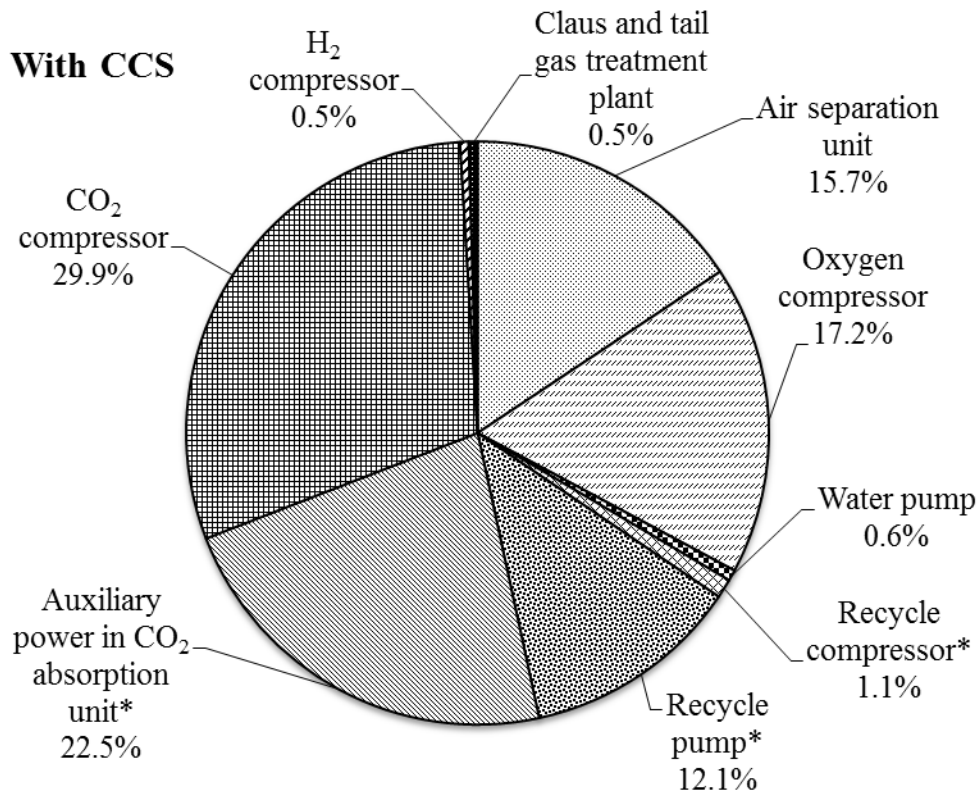


Figure 2.2: Power distribution for H₂ production from UCG with CCS

*Applies to the CO₂ removal section

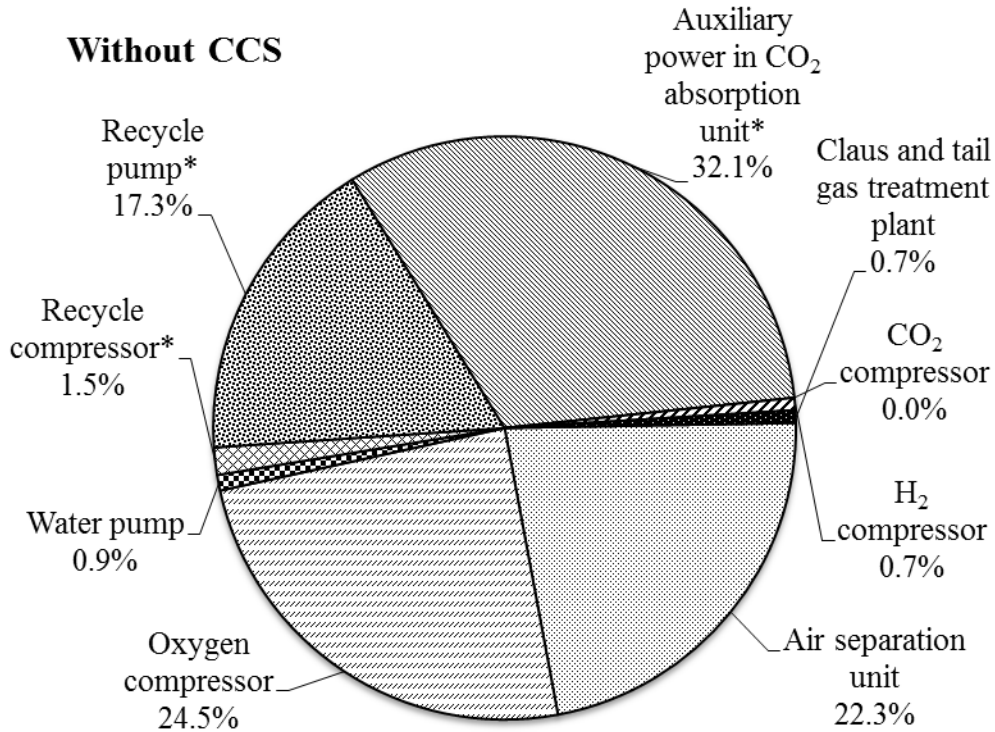


Figure 2.3: Power distribution for H₂ production from UCG without CCS.

*Applies to the CO₂ removal section

Figure 2.4 depicts energy input and energy output associated with different operations in the two H₂ production scenarios (with and without CCS). The only noticeable difference in the energy balance diagram for the two scenarios is in the CO₂ compressor requirements, the consequence of which is realized in a higher export of electricity to the grid in H₂ production without CCS than with. The losses, which are the difference of total energy inputs and total energy outputs, are estimated as 16.01 MW and 15.05 MW in H₂ production with and without CCS, respectively.

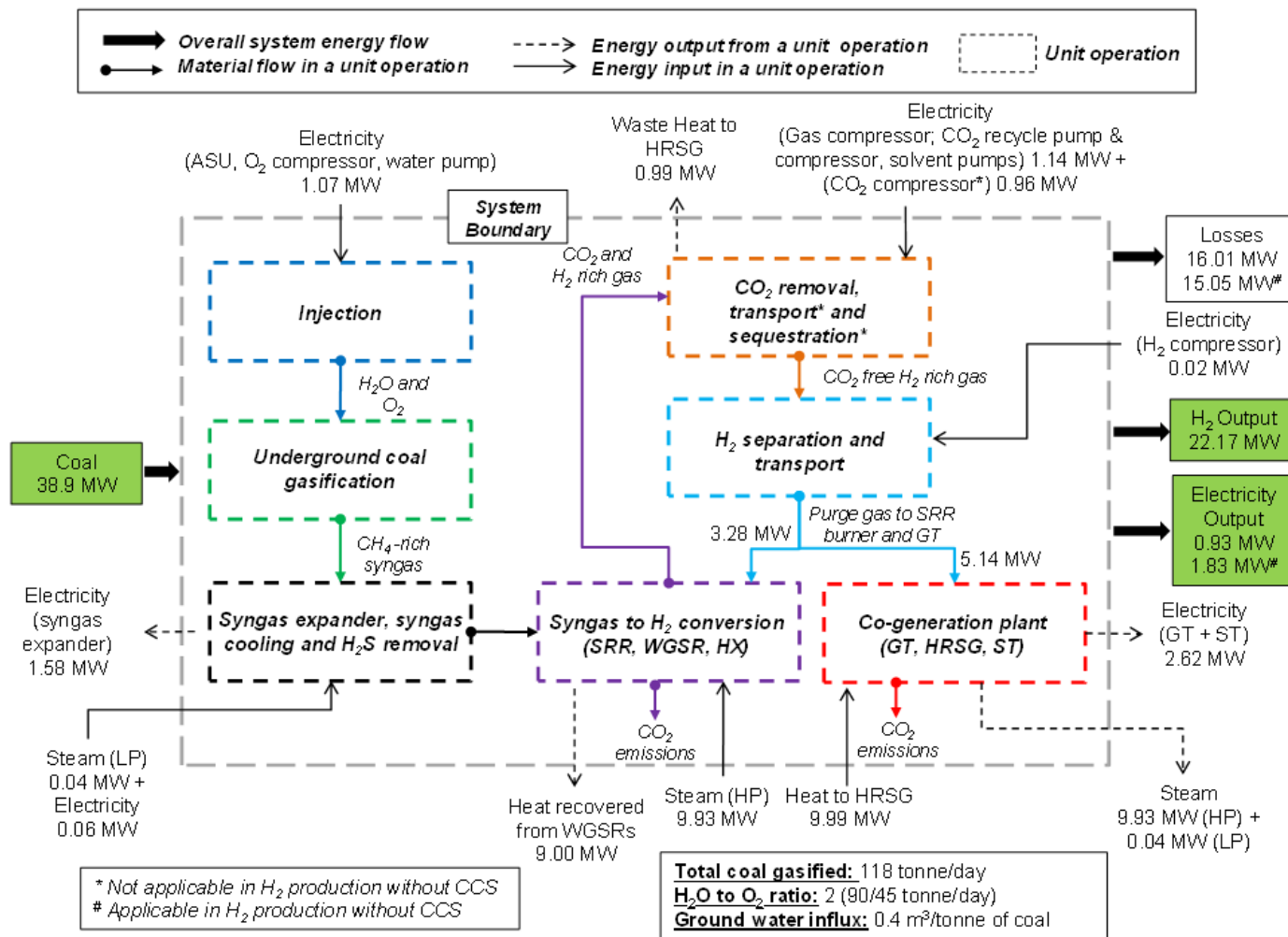


Figure 2.4: Energy balance diagram: H₂ production from UCG with and without CCS

2.3.2. Effect of the steam-to-carbon ratio on η_h and η_e

The steam-to-carbon ratio plays an important role in the conversion of syngas into H_2 in an SCG-based H_2 production plant [46]. Chiesa et al. [46] demonstrated that by increasing the steam to carbon from 0.55 to 1.48 in the SCG-based H_2 production plant increases the H_2 production by 26%. Therefore, it becomes equally important to investigate the effect of this parameter in UCG-based H_2 production plant efficiencies. The steam-to-carbon ratio is defined as the ratio of steam molar flow in the SRR and molar flow carbon (in the form of CH_4 , and CO) in the UCG-based syngas. Figure 2.5 shows the effect of the steam-to-carbon ratio on η_h and η_e in H_2 production from UCG with and without CCS. Considering the fact that the ground water influx rate in the UCG reactor is difficult to estimate, the analysis was done for various ground water influx rates ranging from 0 to 0.4 m^3 per tonne of coal. Carbon molar flow is calculated based on the product gas available from the production well of the UCG plant. For a ground water influx of 0.4 m^3 per tonne of coal, with an increase in the steam-to-carbon ratio from 2 to 4, η_h increases from 51.4% to 62.6%. This is because a higher flow of steam is favorable for converting CH_4 into H_2 in SRR and CO into H_2 in WGSRs, ultimately increasing the net H_2 output. It is important to note that this trend is identical in both scenarios – H_2 production with and without CCS – because the unit operations and their conditions are the same until H_2 separation and transport (see Fig. 2.1).

However, there is a counter effect on η_e with an increase in the steam-to-carbon ratio. With an increase in steam flow to the SRR, the unconverted CH_4 concentration decreases, and the CO_2 flow rate increases in the product gas downstream of WGSRs. These

increases result in a lower heating value of the purge gas after CO₂ removal and H₂ separation in the PSA and ultimately lower GT power output. Additionally, the amount of heat recovered from the WGSRs decreases with an increase in steam flow, resulting in lower ST power output. Overall, the gross power output decreases with an increase in steam flow. However, the power required to remove and compress CO₂ for sequestration increases because of the increased CO₂ flow rate. Overall, the net power output decreases with an increase in the steam-to-carbon ratio. For a fixed ground water influx rate of 0.4 m³ per tonne of coal, with an increase in the steam-to-carbon ratio from 2 to 4, η_e decreases from 5.4% to 0.4% in H₂ production with CCS, whereas the decrease in the magnitude of η_e ranges from 7.6% to 2.8% in H₂ production without CCS.

It is interesting to note that for a fixed steam-to-carbon ratio, η_h decreases with an increase in ground water influx in the UCG reactor (see Fig. 2.5). This stems from the fact that with a rise in ground water influx, the CH₄ content in the syngas obtained from the production well increases, whereas its H₂ content decreases. As a consequence, the steam consumption in the SRR unit rises in order to maintain the fixed steam to carbon ratio, thus compensating for the shortfall in H₂ content of the syngas. The aggregate effect of this amounts to a slight drop in the H₂ output as shown in Fig. 2.5. On the other hand, the rise in CH₄ content of the syngas results in a small appreciation in the value of η_e . The reason for this trend is two-fold. First, the increase in CH₄ content of the syngas results in an increase in the total flow of the purge gas. At the same time, due to increased steam consumption, the heat duty requirement in the SRR unit also rises. Since a greater portion of the purge gas is burned in a combustor to satisfy this heat requirement, the

flow of the purge gas fed to the GT is only slightly increased. As a result, only a small increase in the GT power output is observed. Second, the rise in the steam consumption imposes a penalty in the power output of the ST.

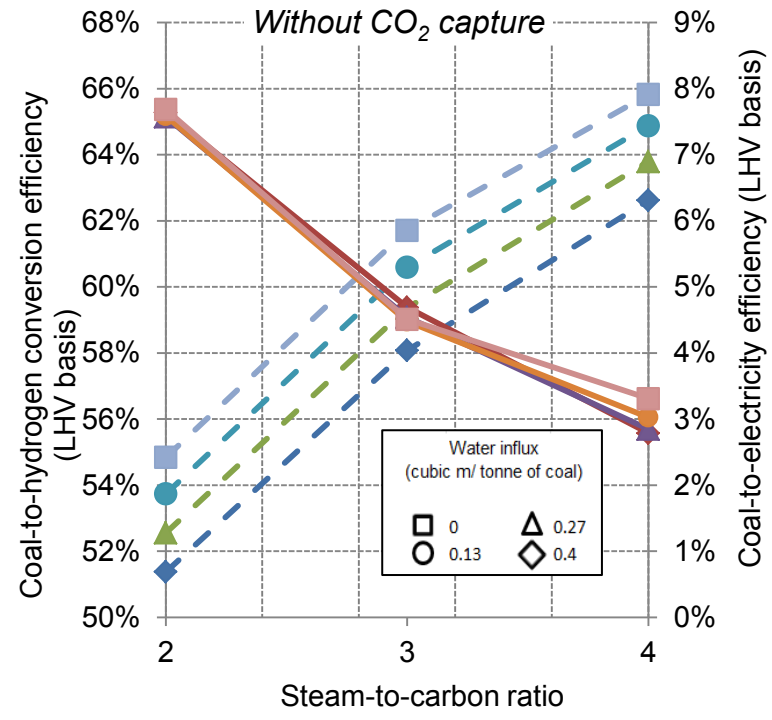
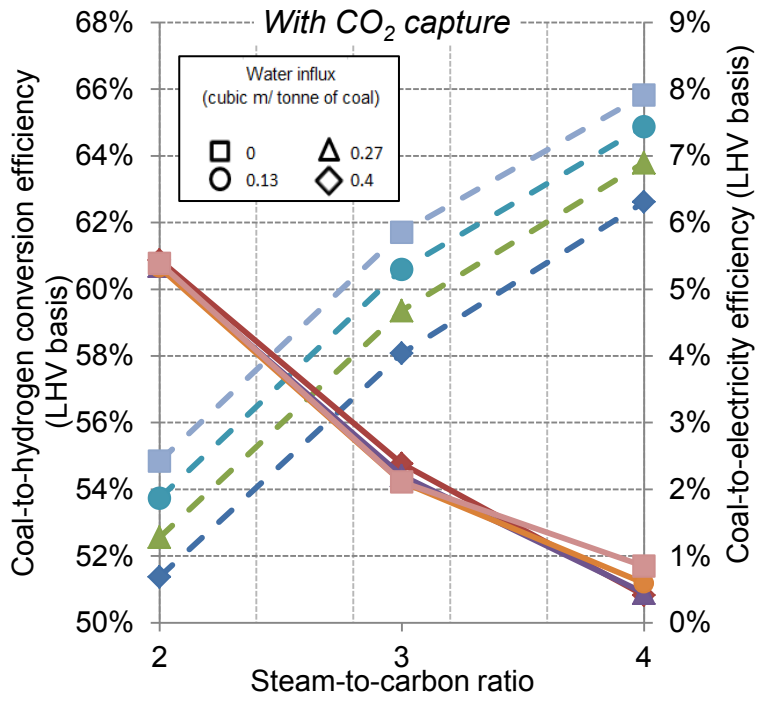


Figure 2.5: The effect of the steam-to-carbon ratio on η_h and η_e in H₂ production from UCG with CCS with different ground water influx rates and a fixed H₂O-to-O₂ injection ratio of 2. Dash lines represent η_h and solid lines represent η_e

2.3.3. The effect of H₂O-to-O₂ injection flow ratio on coal-to-H₂ conversion efficiency, η_h

Stability of the UCG operation in relation to the quality of the syngas can be achieved by controlling the H₂O-to-O₂ injection ratio [27]. At the same time, the H₂O-to-O₂ ratio was found to have a significant influence on the product gas composition [44]. Clearly, it is imperative to appreciate and analyze the sensitivities of variable H₂O-to-O₂ injection ratios on H₂ production from UCG-based syngas. Figure 2.6 shows the effect of the H₂O-to-O₂ injection ratio on η_h and η_e in H₂ production from UCG with and without CCS. Again, due to the uncertainty of the ground water influx in the UCG reactor, the sensitivity of the H₂O-to-O₂ ratio for different influx rates is investigated. For the same reasons mentioned in the above section, η_h increases as ground water influx increases. Other parameters remain the same. At the same time, the effect of ground water influx on η_e is negligible.

However, with an increase in H₂O-to-O₂ ratio, η_h decreases. This is mainly due to an increase in CH₄ content and a decrease in H₂ content in the product gas after UCG, resulting in a lower H₂ flow rate for the same flow rate of steam in the SRR and the WGSRs. The findings of the effect of the H₂O-to-O₂ ratio on the product gas composition provided by the present model – FUNNEL-EGY-H2-UCG – are found to be consistent with a simulation study done for a similar type and depth of in situ coal gasification by the authors in [44]. Overall, the η_h decreases from 58.1% to 54.4% as the H₂O-to-O₂ ratio is increased from 2 to 3 for a fixed ground water influx rate of 0.4 m³ per tonne of coal. Contrastingly, η_e increases marginally with an increase in the H₂O-to-O₂ ratio, with values ranging from 2.1% to 3.1% and 4.4% to 5.4% for a range of ground water influx

rates (0 to 0.4 m³ per tonne of coal) in H₂ production with and without CCS, respectively. This counter effect is justified by a slight increase in net power output by the GT due to an increase in the CH₄ flow in the purge gas on increase in the H₂O-to-O₂ injection ratio.

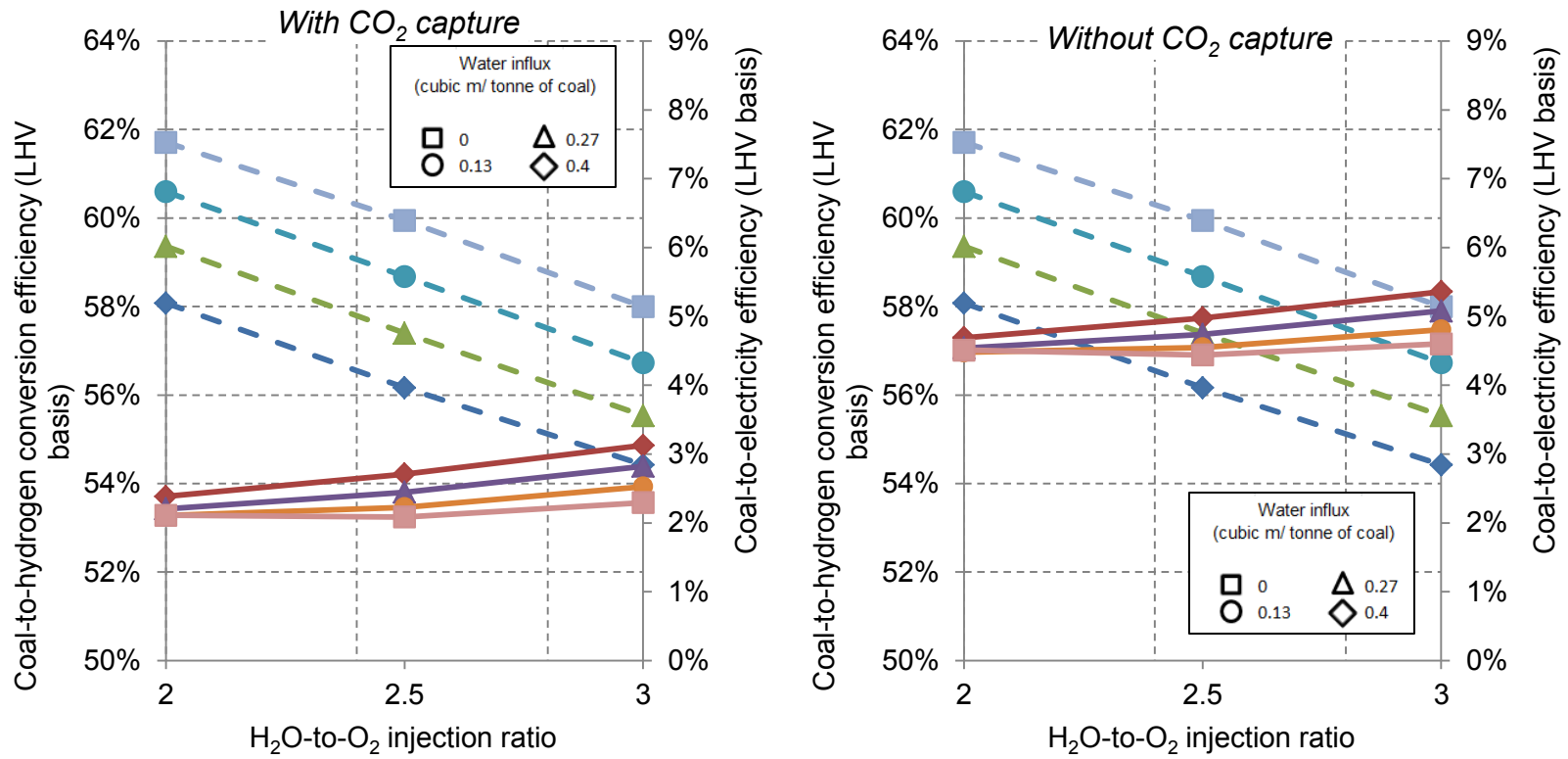


Figure 2.6: The effect of the H₂O-to-O₂ injection ratio on η_h and η_e in H₂ production from UCG with CCS with different ground water influx rates and a fixed steam-to-carbon ratio of 3. Dash lines represent η_h and solid lines represent η_e

2.3.4. Electricity production from UCG with and without CCS

The present analysis illustrates the use of product gas obtained from the UCG process for H₂ production with and without CCS. Taking into account the immaturity of large commercial-scale UCG technology, the literature on the UCG product gas processing for a variety of end uses, i.e., electricity production, H₂ production, etc., is, therefore, limited. However, the authors in [19, 32, 80] predict η_e from a combined UCG-IGCC plant producing only electricity in a range of 36% to 43% without carbon capture and 29% to 30% with carbon capture. Prabu et al. [43] estimated a net coal-to-electricity efficiency of 32.3 % for an integrated UCG-SOFC-CCS plant. But none of these studies evaluates η_h . If the same set of assumptions employed in this study is applied, and the PSA unit is removed from the H₂ production pathway, it becomes easy to derive a plant configuration that produces only electricity from the produced syngas of the UCG process. The coal-to-electricity efficiency (η_e) in plants producing only electricity is evaluated to be 32% with CCS and 38% without CCS. The results from this scenario are found to be in close agreement with the numbers reported in existing studies. The decrease of 5.9% in η_e for adopting a CCS plant configuration against a non-CCS plant configuration is also found to be consistent with the value of 6% reported in [32]. This analysis validates the practicality of FUNNEL-EGY-H₂-UCG presented in the study under the stated set of assumptions for different unit operations of the H₂ production pathway.

2.3.5. Comparative analysis: H_2 production from UCG vs. SCG vs. SMR

Table 2.7 shows typical H_2 plant efficiencies in fossil-fuel based H_2 production pathways (SCG, SMR, and UCG with and without CCS) derived from various studies. Carbon capture technology in most of the listed studies is through physical absorption by Selexol and amines for surface coal gasification and SMR, respectively. The competitiveness of H_2 production of UCG over SCG can be appreciated, given that η_h in UCG ranges from 51.4% to 65.8% versus a range of 44.5% to 69% in SCG [6, 46, 48, 49, 52, 55]. It is evident from the table that there is also a wide range of η_h – 61% to 73% in H_2 production from SMR [48, 51, 56]. Unarguably, a wide range of efficiency values of H_2 production from SCG and SMR may be attributed to the disparity in the assumptions and the methodology adopted by the authors in the respective studies. Considering the complexity of the H_2 production pathway and the lack of detail in the various studies, it is difficult to outline and justify the dissimilarities that lead to variable outputs [46]. With regard to CO_2 capture efficiency, the value varies from 86.8% to 92% and 85% to 90% for H_2 production from surface coal gasification and SMR, respectively. The CO_2 capture efficiency estimated from FUNNEL-EGY-H2-UCG – 87% to 95.7% – is in close agreement with the values evaluated in various studies for other H_2 production pathways listed in Table 2.7. Another observation that can be made for H_2 production from surface coal gasification with CCS is the trade-off between η_h , and η_e . The higher the η_h , the lower the η_e . This trend is also true for H_2 production from UCG (see Figs. 2.5 and 2.6).

Table 2.7: Key performance parameters of H₂ production pathways: UCG, surface coal gasification, and SMR with and without carbon capture

H ₂ production pathway	With or without CCS (CO ₂ capture technology)	H ₂ conversion efficiency, %	Electrical efficiency, %	CO ₂ capture efficiency, %	Sources/ comments
<i>UCG</i>	With CCS (Selexol)	51.4-65.8 ¹	0.8-5.4 ¹	87-95.7 ¹	Present model (FUNNEL-EGY-H2-UCG)
	Without CCS (Selexol)	51.4-65.8 ¹	3.3-7.6 ¹	0	Present model (FUNNEL-EGY-H2-UCG)
<i>SCG</i>	With CCS (Selexol)	51.9	1.4	92	[46, 52]
	Without CCS (Selexol)	51	4.5	0	[46, 52]
	With CCS (Selexol)	44.5	12.8	86.8	[46, 49]
	With CCS (Selexol)	57.3	2.8-3.8 ²	91.1-91.3 ²	[46]
	Without CCS	57.5	4.2-6.2 ²	0	[46]

H₂	With or without	H₂	Electrical	CO₂	Sources/
production	CCS	conversion	efficiency,	capture	comments
pathway	(CO₂ capture	efficiency,	%	efficiency,	
	technology)	%		%	
	(Selexol)				
	With CCS	62	2.3	91	[48]
	(Selexol)				
	With CCS	69	-3.7 ³	90	[48, 55]
	(Selexol)				
	With CCS	73	0	85	[48, 51]
	(MDEA)				
<i>SMR</i>	With CCS	61	-3.9 ³	90	[48, 56]
	(MEA)				

¹ Range of values for different ground water influx rates, steam-to-carbon ratio, and H₂O-to-O₂ injection ratio

² The author in [46] present results for different gasification pressures (70-120 bar) and syngas cooling modes (quench or syngas cooler)

³ A negative value indicates net import of electricity from the grid

2.3.6. Sensitivity analysis

Figure 2.7 depicts the sensitivity analysis done for H₂ production from UCG with CCS, wherein the ground water influx rate is 0.4 m³ per tonne of coal and the H₂O-to-O₂ ratio is 2. It is important to mention that the same trend is observed when the analysis is conducted for H₂ production without CCS; the only difference is in the absolute values of electrical efficiencies because there is no CO₂ compressor power requirement in this scenario.

η_h is most sensitive to H₂ separation efficiency in the PSA unit. A 10% reduction in the H₂ separation efficiency would result in a decrease of η_h from 58.1% to 52.3 %, while η_e would increase from 2.4% to 4.4% because of increased GT power output. Conversely, a 10% increase in the H₂ separation efficiency would result in a rise of η_h from 58.1% to 63.9% and a decline in η_e from 2.4% to 0.4%. All the other variables, namely heat exchanger efficiency, GT inlet temperature and pressure ratio, CO₂ compressor isentropic efficiency, and H₂ and CO₂ pipeline transportation distance, have no effect on η_h . However, a temperature decrease in the UCG reactor has a marginal effect on η_h . The greater the temperature decrease in the UCG reactor, the lower the η_h . This is mainly because of increased CH₄ content in the produced gas after the UCG process [22, 69].

The sensitivity of the heat exchanger efficiency on η_e can be appreciated; because of an increase in total heat available in the HRSG, steam production increases, ultimately resulting in increased ST power output, and vice-versa. η_e increases from 2.4% to 4.2% with a 20% increase in heat exchanger efficiency. Conversely, η_e decreases from 2.4% to

0.9% with a 20% decrease in heat exchanger efficiency. A moderate non-linear increasing trend is observed for η_e with an increase in the GT inlet temperature. This is mainly because of the non-linear relationship between the GT inlet temperature and the power delivered by the GT. All the other parameters have a marginal effect on η_e .

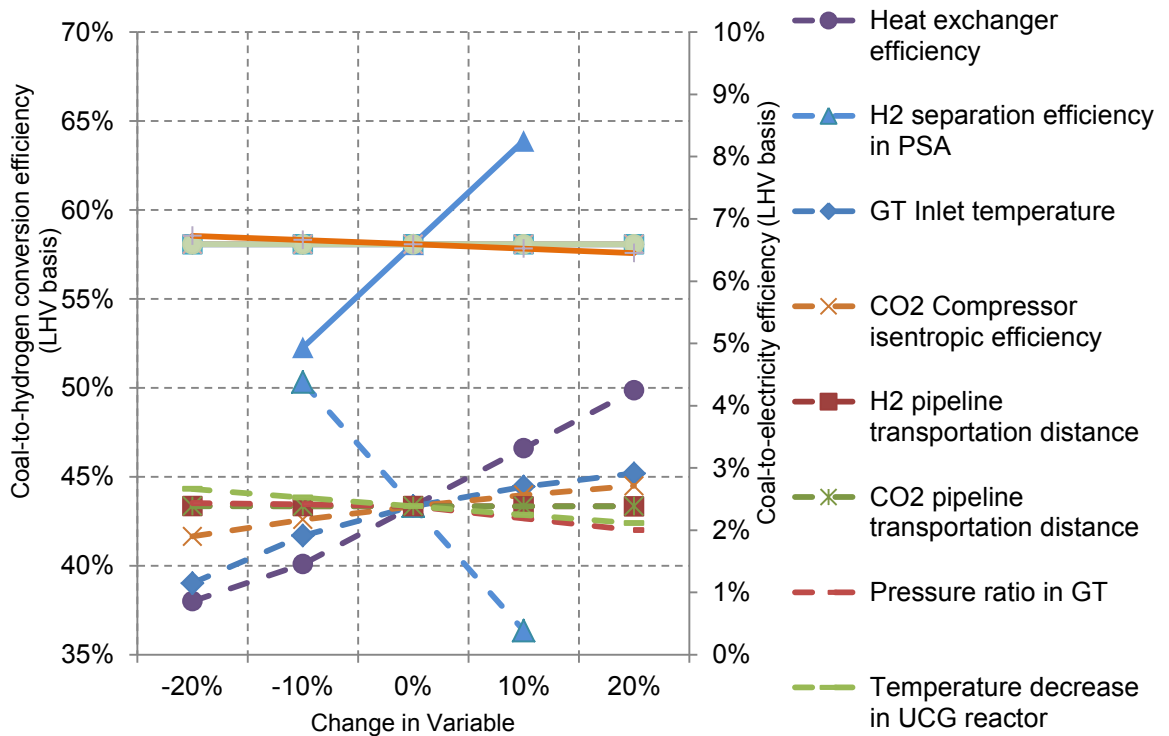


Figure 2.7: Sensitivity analysis for H₂ production from UCG with CCS. The H₂O-to O₂-ratio is 2, and the ground water influx rate is 0.4 m³ per tonne coal. Dash lines represent η_e , and solid lines represent η_h

2.4. Conclusions

This research provides insight on the energy balances involved in hydrogen production from UCG with and without CCS. In particular, the authors have developed the relationship between key process variables and η_h and η_e . For base case assumptions, η_h is calculated to be 58.1% for both plant configurations, while η_e is estimated to be 2.4% and 4.7% with and without CCS, respectively. The effect of ground water influx on both η_h and η_e is small. Furthermore, the hydrogen conversion efficiency falls with a rise in the H₂O-to-O₂ injection ratio and increases with an increase in steam-to-carbon ratio. An opposite trend is observed for η_e , where an appreciation of its value occurs with a rise in the injection ratio. However, a decrease in the value of η_e is observed with an increase in steam-to-carbon ratio. In addition, the sensitivity analysis showed that η_e is most sensitive to the efficiency of the heat exchanger and the separation efficiency of the PSA.

Chapter 3

Life Cycle Assessment (LCA) of Hydrogen Production from Underground Coal Gasification (UCG) with Carbon Capture and Sequestration (CCS)⁹

3.1. Background

Numerous studies in the literature have evaluated the environmental competitiveness of producing hydrogen (H₂) from renewable (wind, solar, hydro) and non-renewable pathways (natural gas, liquid natural gas, ex-situ coal gasification) by using a life cycle assessment (LCA) approach. However, the environmental evaluation of underground coal gasification (UCG) as a H₂ production pathway and its comparison with other pathways in the literature is scarce.

In this study, two configurations – H₂ from UCG with carbon capture and sequestration (CCS) and without CCS – are considered to quantify the environmental competitiveness

⁹ A version of this chapter has been submitted as Verma A., Kumar A. Life Cycle Assessment (LCA) of Hydrogen Production from Underground Coal Gasification (UCG) with Carbon Capture and Sequestration (CCS). *Applied Energy*. (in review).

over conventional H₂ production methods such as steam methane reforming (SMR), SMR-CCS, surface coal gasification (SCG) and SCG-CCS. A life cycle assessment (LCA) model – FUNNEL-GHG-H₂-UCG (FUNDamental ENgineering PrinciplEs-based Model for Estimation of GreenHouse Gases in hydrogen (H₂) production from Underground Coal Gasification) – is developed to estimate the GHG emissions in H₂ production from UCG with and without CCS. In addition, FUNNEL-GHG-H₂-UCG takes into account the life cycle GHG emissions associated with CO₂ transportation and sequestration. A process modeling approach is applied to estimate the operation emissions in the two UCG-based H₂ production configurations. This chapter also discusses the effect of key UCG process parameters (H₂O-to-O₂ injection ratio, ground water influx and steam-to-carbon ratio) on life cycle GHG emissions, both quantitatively and qualitatively. More importantly, the life cycle GHG emissions are estimated based on pertinent data inputs to represent western Canadian conditions as closely as possible.

3.2. Methodology

A life cycle assessment (LCA) is a technique used to estimate energy, material use and environmental impacts associated with a pathway or product [37]. In order to evaluate the environmental impact of a system, all inputs and outputs from raw material extraction to final disposal are aggregated [38].

3.2.1. Goal and Scope

The purpose of this analysis is to evaluate life cycle GHG emissions from H₂ production from UCG. This study evaluates two scenarios, H₂ production from UCG with CCS (scenario 1) and H₂ production from UCG without CCS (scenario 2) in Alberta. A geological sequestration method – enhanced oil recovery (EOR) – is used for carbon storage in scenario 2¹⁰.

3.2.1.1. Functional unit: The functional unit chosen in this analysis is 1 kg of H₂. This analysis reports GHG emissions and energy use associated with different unit operations involved in the H₂ production pathway. GHG emissions are reported as kg-CO₂-eq/kg-H₂. The net energy ratio (NER) is defined in Eq. 3.1.

$$\text{NER} = \frac{\text{H}_2 \text{ energy output} + \text{Electricity export}}{\text{Fossil energy input}} \quad (3.1)$$

¹⁰ EOR was purposefully selected to put into perspective the Government of Alberta's decision to fund a large-scale CCS project, the Alberta Carbon Trunk Line (ACTL) [12]. The ACTL will include a 16 inch, 240 km CO₂ pipeline, which will transport CO₂ from Fort Saskatchewan, Alberta to an EOR site in Clive, Alberta [12].

3.2.1.2. *System boundaries*: Figure 3.1 depicts system boundaries for scenario 1 and scenario 2. The starting point of both scenarios is the injection of gasifying agents (mainly H₂O and O₂) through an injection well in an underground coal reactor, which upon gasification produces syngas. The syngas is collected by a production well and is converted to H₂ using conventional technologies employed in SMR- and SCG-based H₂ production pathways. It is important to mention that both scenarios are characterized with capture of CO₂ using a physical solvent – Selexol¹¹. Pure H₂ reaches a bitumen upgrading facility by a pipeline after its separation in a PSA unit, and compression. Downstream of the PSA unit, the remaining un-separated gas, called purge gas, is combusted in a combined cycle plant to produce electricity and steam. A portion of the purge gas is burned separately to satisfy the heat duty of a syngas reforming reactor (SRR) in the syngas-to-H₂ conversion section. The underlying difference between the two scenarios is the absence of CO₂ compression, transportation, and sequestration in scenario 2. In scenario 1, the captured CO₂ is compressed till it reaches a supercritical state and then transported through a pipeline to the sequestration site. The system boundary termination point is the bitumen upgrading facility for both scenarios. It is worth mentioning that the emissions associated with CO₂ capture, compression, and transportation are allocated to H₂ production.

¹¹ A higher calorific value of purge gas – 55.15 KJ/kg – is achieved in scenario 2 upon CO₂ removal against a calorific value of 3.15 MJ/kg when no CO₂ removal takes place in scenario 2. In addition, the purge gas compression power requirement ahead of the GT is also reduced (for more information, refer to section 2.2.2.5 of the thesis).

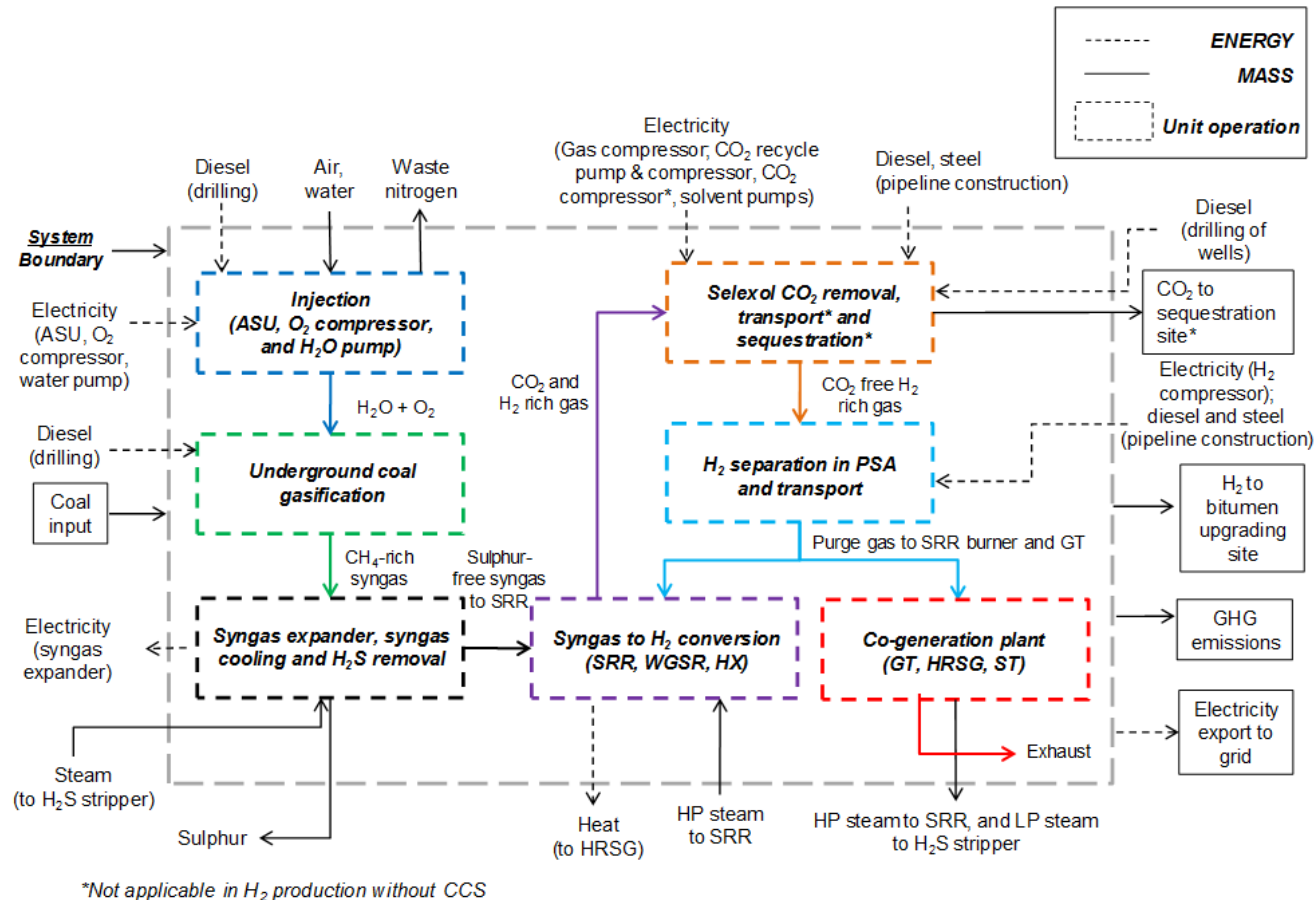


Figure 3.1: System boundary of the study. The boundaries are the same for scenarios 1 and 2, except for the absence of CO₂ transport, and sequestration in the latter scenario. Notes: ASU-air separation unit; SRR-syngas reforming reactor; WGSR-water gas shift reactor; HX-heat exchanger; GT-gas turbine; HRSG-heat recovery steam generator; ST-steam turbine.

3.2.2. Life cycle inventory (LCI)

This step includes identification of all unit operations within the system boundary and the quantification of corresponding inputs and outputs [37]. Of the several methodologies for data collection e.g. direct measurement, literature review and process modeling [37], the life cycle inventory (LCI) is conducted by incorporating the results of FUNNEL-EGY-H2-UCG (FUNDamental ENgineering PrinciplEs-based ModeL for Estimation of EnerGY consumption and production in hydrogen (H₂) production from Underground Coal Gasification) developed and presented in Chapter 2. However, in some unit operations of the presented work, the data is collected from the literature and developed as required.

3.2.2.1. *H₂ production from UCG*: The plant size for H₂ production is based on gasification of a deep highly volatile B bituminous Manville coal seam. This is typical of Alberta's un-minable coal seam. The total gasified coal amount is 118 tonnes per day¹² [27]. The H₂ output is estimated to be 16.28 tonnes per day for a H₂O-to-O₂ injection ratio of 2, and a ground water influx of 0.4 m³/tonne of coal (as discussed in section 2.3 of the thesis). The energy consumption in various unit operations involved in the H₂ conversion pathway was derived from FUNNEL-EGY-H2-UCG presented in Chapter 2 of the thesis. Tables 3.1 and 3.2 show the composition of coal chosen in the study and the

¹² UCG at a small-scale H₂ production plant was analyzed due to lack of production data for H₂ production from UCG on a large commercial scale for deep coal seams. See section 2.2.2.2 of the thesis for more information.

key assumptions associated with different unit operations of the H₂ production pathway from UCG for both scenarios. The H₂ production plant lifetime is assumed to be 40 years and is applicable for both scenarios [11]. The details on the process modeling of the unit operations are given in Chapter 2. It is worth noting that owing to the complexity of the unit operations in the PSA, H₂ separation was modeled as a simple separation process¹³ by assuming a separation efficiency of 85% [46, 66]. Furthermore, the heat exchanger network for steam generation was modeled in a similar fashion¹⁴ as employed by authors in [66].

Table 3.1: Coal composition assumed in the study. Data adapted from [11, 27]

<u>Ultimate Analysis</u>		<u>Proximate Analysis</u>	
<i>Parameter</i>	<i>%</i>	<i>Parameter</i>	<i>%</i>
Ash	9.7	Moisture	4.7
Carbon	74.5	Ash	9.3
Hydrogen	3.6	Volatile Matter	30.5

¹³ Post CO₂ capture, the constituents of the H₂-rich and CO₂-free gas (input gas stream to PSA unit) (see Fig. 3.1) were split into two gas streams – H₂-rich gas, containing 85% of the H₂ in the input gas stream, and purge gas, containing the remaining constituents of the input gas stream [66].

¹⁴ Refer to section 2.2 of the thesis. The heat recovered from different unit operations was aggregated and then used for steam production in the co-generation section. A heat exchanger efficiency of 60% was assumed for the base case conditions.

<u>Ultimate Analysis</u>		<u>Proximate Analysis</u>	
<i>Parameter</i>	<i>%</i>	<i>Parameter</i>	<i>%</i>
Nitrogen	1.1	Fixed Carbon	55.5
Sulphur	0.4		
Oxygen	10.7		
LHV of coal, MJ/kg		28.5	

Table 3.2: Key assumptions for calculation of power requirement and production in the different unit operations in scenarios 1 and 2

Parameter	Applicable scenario	Values	Sources/comments
<u>UCG, syngas to H₂ conversion</u>			
H ₂ O to O ₂ injection ratio in UCG	1, 2	2	[27]. Refer to section 2.2 of the thesis.
Ground water influx, m ³ /tonne of coal	1, 2	0.4	[69]. Refer to section 2.2 of the thesis.
Steam-to-carbon ratio in SRR ¹	1, 2	3	[66]. Refer to section 2.2 of the thesis.
<u>CO₂ compressor²</u>			
Compressor isentropic efficiency	1	0.75	[76]
<u>GT</u>			
Mechanical efficiency	1, 2	99.5%	[54]

Parameter	Applicable scenario	Values	Sources/comments
Isentropic efficiency	1, 2	88%	[46]
Turbine inlet temperature, °C	1, 2	1300	[46]
Pressure ratio	1, 2	14.8	[46]
<i><u>HRSG, ST</u></i>			
HP steam temperature, °C	1, 2	510	Based on steam energy requirement in the SRR [66]. Refer to section 2.2 of the thesis.
HP steam pressure, bar	1, 2	30	
LP steam temperature, °C	1, 2	302	Based on steam energy requirement in the H ₂ S stripper [46]. Refer to section 2.2 of the thesis.
LP steam pressure, bar	1, 2	6	
Isentropic efficiency	1, 2	85%	[47]
Mechanical efficiency	1, 2	99.5%	[54]
Pump efficiency	1, 2	75%	[46]
Heat exchanger efficiency	1,2	60%	Refer to section 2.2 of the thesis.

¹ Calculated based on the molar flow of CO and CH₄ in the syngas, which is fed to SRR

² Applicable for compression of CO₂ that is captured using Selexol technology, in a five-stage compressor train

Table 3.3 shows the key energy inputs and outputs associated with various unit operations in scenarios 1 and 2. The total H₂ output was estimated to be 16.28 tonne/day in both scenarios (see section 2.3 of the thesis). In scenario 1, nearly 91.6% CO₂ was captured; the total flow of CO₂ is evaluated to be 247.8 tonne/day (see section 2.3 of the thesis). It is important to mention that, of the total gas captured, around 97.4% is CO₂, 0.8% is CH₄, while the remaining gases are non-GHGs. In scenarios 1 and 2, GHG emissions were mainly associated with combustion of the purge gas in the GT and the burner in the syngas to H₂ conversion section. However, scenario 2 has additional GHG emissions from CO₂ venting which is captured in the CO₂ removal section.

Table 3.3: Power requirement in different unit operations of H₂ production with and without CCS

Parameter	Values ⁵		Source/
	Scenario 1	Scenario 2	Comment
Coal input, tonne/day	118	118	[27]
H ₂ output, tonne/day	16.28	16.28	
Injection (ASU, O ₂ compressor, H ₂ O pump) ¹ , MW	1.07	1.07	

Parameter	Values ⁵		Source/
	Scenario 1	Scenario 2	Comment
Syngas expander power output	1.58	1.58	
H ₂ S removal (Claus and tail gas treatment plant) ² , MW	0.02	0.02	
Selexol CO ₂ removal, MW	1.14	1.14	
CO ₂ compressor ³ , MW	0.96	0	
H ₂ compressor, MW	0.02	0.02	
Gas turbine power output, MW	1.16	1.16	
Steam turbine power output, MW	1.46	1.46	
Total power consumption, MW	3.21	2.25	
Total power output, MW	4.20	4.20	
Net electricity export to grid ⁴ , MW	0.93	1.83	

¹ Based on an O₂ input of 45 tonne/day; O₂ and H₂O injection pressure is 200 bar and 140 bar, respectively

² H₂S captured with using Selexol. Sulphur is recovered in a Claus plant after stripping of H₂S from the solvent

³ The captured CO₂ is compressed above its critical pressure to around 150 bar using a five-stage compressor train for suitable pipeline transportation

⁴ Difference of total power output and total power consumption. A loss of 6.5% is assumed while transmission of electricity from the H₂ production plant to the grid

⁵ See section 2.3 of the thesis for more information.

3.2.2.2. *Drilling*: UCG involves drilling for the formation of an injection well and a production well. A horizontal drilling technique is used to connect both wells. Injection and production well depth are both assumed to be 1400 m, whereas the length of the horizontal section is 1400 m [27]. Diesel is used for drilling the wells. Total energy consumption in well drilling is calculated based on a correlation developed by Brandt [81] for drilling operations in Canada. Brandt [81] discussed two correlations for diesel use to represent low intensity (Eq. 3.2)¹⁵, and high intensity (Eq. 3.3)¹⁵ drilling operations. An average of the results obtained from the two correlations was used to account for diesel use in drilling in this analysis.

$$E = 128.765 * d * \exp(0.469 * d/1000) \quad (3.2)$$

$$E = 366.707 * d * \exp(0.399 * d/1000) \quad (3.3)$$

3.2.2.3. *CO₂ pipeline design and EOR well characteristics for sequestration*: It is important to reiterate that the operating and infrastructure emissions associated with CO₂ capture, compression, transport, and sequestration are allocated to H₂ production. This is mainly because the primary objective of CO₂ sequestration through EOR is to store the unwanted CO₂ and not to produce more oil from depleted oil reservoirs¹⁶.

¹⁵ d is the depth of well, meters; E is the diesel energy consumed in drilling a well of depth d , in MJ.

¹⁶ See footnote 10.

Pipeline is assumed to be the mode of transportation of CO₂ to the geological sequestration site. CO₂ is transported as a fluid in its supercritical state; a distance of 100 km from the H₂ production plant to an enhanced oil recovery (EOR) site is taken as the base case. Based on a pipeline operating pressure of 10.3 MPa [82], the pipeline diameter is calculated by a model developed by Ogden [79]. An iterative methodology is adopted to match an assumed diameter value with the calculated value obtained from the model [79]. CO₂ pipeline is manufactured from carbon steel, with a wall thickness of 15 mm [77, 83, 84]. Pipeline construction is also associated with use of a trencher. A trencher model Vermeer T555, suitable for CO₂ pipeline construction is chosen and a trench depth of 3 feet is assumed [85]. Diesel fuel consumption for the given trencher model is 36.6 L/hr [85]. GHG emissions associated with pipeline construction are amortized over a lifetime of 30 years [83].

After reaching the EOR site, CO₂ is then injected in an EOR well reservoir. Table 3.4 shows EOR well reservoir characteristics considered in the present analysis. Given that reservoir characteristics are site-specific [86], it is worth mentioning that an average of a range of values is used. With the assumed reservoir characteristics and the CO₂ flow rate, the total number of wells required is calculated by using a method developed by McCollum et al. [76]. The GHG emissions associated with drilling EOR wells were calculated using the methodology discussed in section 3.2.2.2.

Table 3.4: EOR well reservoir characteristics for CO₂ sequestration

Parameter	Value	Sources/comments
Depth of reservoir ¹ , m	1635.4	[86]
Reservoir thickness ¹ , m	27.2	[86]
Reservoir pressure ¹ , MPa	14.7	[86]
Permeability of reservoir, md	5	[76]
CO ₂ leakage rate per annum	0.01%	Applicable over 100 years [28, 87]
Life of EOR well, years	25	Average life of an oil well ranges from 20 to 30 years [88]

¹ Average of range of values for different EOR pilot projects in Alberta

3.2.2.4. *H₂ pipeline design:* Highly pure (99.99%) H₂ is delivered at a pressure of 20 bar after its separation in PSA [46]. Pipeline is assumed to be the mode of transportation of H₂ to a bitumen upgrading site. A pipeline length of 100 km is considered as the base case for H₂ pipeline transportation. Typical hydrogen pipeline operating pressure and diameter range from 10 to 30 bar and 0.25 to 0.30 m, respectively [78]. Considering small-scale H₂ production from UCG and its transportation, a lower value of diameter – 0.25 m is used for pipeline diameter. The compressor power requirement is calculated using Panhandle equation adopted in a similar model developed by Ogden [79]; compressor efficiency is assumed to be 55% [79]. Pipeline construction material and wall

thickness are assumed to be steel and 0.75 mm, respectively [89]. Diesel consumption for trenching up to a depth of 4 feet is calculated using the same assumptions discussed in section 3.2.2.3. [89]. GHG emissions associated with H₂ pipeline construction were amortized over a lifetime of 22 years [78].

3.2.3. Life cycle impact assessment (LCIA)

For both scenarios, all material and energy use values were totaled to obtain gross life cycle GHG emissions. Operation emissions are mainly associated with combustion of the purge gas. Diesel is used for drilling the UCG injection and production wells, injection wells for CO₂ sequestration (only applicable in scenario 1), and trenching in the construction of H₂ pipeline and CO₂ pipeline (only applicable in scenario 1). Steel is used in the CO₂ and H₂ pipeline infrastructure. The steam requirement in the various unit operations is fulfilled by an in-house co-generation facility. It is important to mention that average emission factors of 0.048 and 0.040 kg-CO₂.eq/kg-H₂ were used to account for construction and manufacturing of the H₂ production plant in scenarios 1 and 2, respectively [59]. The GHG emissions associated with infrastructure are aggregated to evaluate non-operation GHG emissions. The gross life cycle GHG emissions are the sum of operation and non-operation GHG emissions (see Eq. 3.4). A credit is given for the export of electricity (in the case of a net positive electricity production) to the grid. Net life cycle GHG emissions are then calculated using Eq. 3.5. Table 3.5 summarizes emission factor values associated with fuel and material use and the GWP of various GHGs. The GHG emissions associated with construction materials and diesel use during

well drilling and trenching in pipeline construction were amortized over the lifetime of respective construction sections.

$$\begin{aligned} \text{Gross life cycle GHG emissions} = & \hspace{15em} (3.4) \\ \text{Operation emissions} + \text{Non-operation GHG emissions} \end{aligned}$$

$$\begin{aligned} \text{Net life cycle GHG emissions} = \\ (\text{Gross life cycle GHG emissions}) - (\text{Emissions credit for electricity export to grid}) \end{aligned} \quad (3.5)$$

Table 3.5: Emission factors associated with fuel and material use and the GWPs of GHGs relative to CO₂

Parameter	Value	Source
<i>Emission factors</i>		
Grid-electricity use ¹ , tonnes-CO ₂ -eq/MWh	0.88	[90]
On-site electricity production ² , tonnes-CO ₂ -eq/MWh	-0.65 ²	[90]
Diesel use, kg-CO ₂ -eq/MJ	0.074	[6]
Production of virgin steel, kg-CO ₂ -eq/kg-steel	4.972	[6]
<i>GWP</i>		
CO ₂	1	[6]
CH ₄	25	[6]
N ₂ O	298	[6]

¹ Applicable for Alberta, Canada

² Negative value indicates a credit will be given for electricity supply from the site to the grid

3.3. Results and discussion

3.3.1. Life cycle GHG emissions

Table 3.6 shows a detailed breakdown of operation and non-operation emissions in scenario 1 and 2 estimated by FUNNEL-GHG-H₂-UCG. Since the H₂ production pathway in both scenarios is self-sufficient in terms of electricity consumption (see Table 3.3), there are no GHG emissions for electricity use. The operation emissions in scenario 1 comprise purge gas combustion emissions, whereas in scenario 2, in addition to purge gas combustion emissions, there are emissions associated with venting of gases in the CO₂ removal section. The advantage of the co-generation is realized in both scenarios; the H₂ production pathway is self-sufficient in terms of steam production. This ultimately negates the GHG emissions associated with steam use in different process units – SRR, WGSRs and H₂S stripper.

In scenario 1, approximately 91.6% of CO₂ is captured; around 204 kWh of electricity is required to capture and compress one tonne of CO₂. Non-operation emissions are mainly associated with steel and diesel use in H₂ and CO₂ pipeline construction and with diesel use in drilling. Gross life cycle GHG emissions are estimated to be 1.8 and 19.8 kg-CO₂-eq/kg-H₂ in scenarios 1 and 2, respectively. Contrastingly, net life cycle GHG emissions, which are calculated using Eq. 3.5, are lower than the gross life cycle GHG emissions

because of a credit for net positive electricity production in scenarios 1 and 2. It is worth mentioning that the credit awarded in scenario 1 is less than in scenario 2 because of higher net electricity production in scenario 2 than in scenario 1 (see Table 3.3). The net life cycle emissions are evaluated to be 0.9 and 18.0 kg-CO₂-eq/ kg-H₂ in scenarios 1 and 2, respectively.

Table 3.6: Life cycle GHG emissions in different unit operations of H₂ production with and without CCS. The results are presented for the base case of an H₂O-to-O₂ injection ratio of 2, steam-to-carbon ratio of 3 and ground water influx of 0.4 m³/tonne-coal.

Parameter	Values (kg-CO ₂ -eq/ kg-H ₂)	
	Scenario 1	Scenario 2
<i>Operation emissions</i>		
Emissions from the CO ₂ removal section	0	17.998
Purge gas combustion ¹	1.521	1.521
Electricity use in H ₂ production	0	0
<i>Non-operation emissions</i>		
Drilling of injection and production well in UCG	0.001	0.001
Drilling and leakage in EOR	0.001	0
CO ₂ pipeline construction	0.038	0

Parameter	Values (kg-CO₂-eq/ kg-H₂)	
	Scenario 1	Scenario 2
H ₂ pipeline construction	0.193	0.193
H ₂ production plant construction	0.048	0.040
Emissions credit for electricity supply to grid	0.890	1.750
Gross life cycle GHG emissions	1.801	19.752
Net life cycle GHG emissions	0.912	18.003

¹This value represents emissions associated with combustion of purge gas both in the GT and the burner of the SRR unit

Figures 3.2 and 3.3 show a detailed distribution of operation and non-operation GHG emissions in scenarios 1 and 2, respectively. The operation emissions in scenario 1 are mainly associated with combustion of the purge gas, which contribute around 84.4% to gross life cycle GHG emissions. On the other hand, non-operation emissions are around 15.6% of gross GHG emissions. Of the total non-operation emissions, 68.8% are associated with H₂ pipeline construction, while the remaining 31.2% are attributed to CO₂ pipeline construction, drilling of wells in the UCG plant and the EOR site, EOR well leakage, and H₂ production plant construction. Since the diameter of the H₂ pipeline is greater than the diameter of the CO₂ pipeline, the GHG emissions associated with steel use is greater in the former case than the latter case.

Apart from emissions associated with purge gas combustion in scenario 2 (which contribute only 7.4% to gross life cycle GHG emissions), the operation emissions also

include emissions from venting of gases in the CO₂ removal section (contributing around 91.1% to gross life cycle GHG emissions). Non-operation emissions contribute only 1.2%. Of the total non-operation emissions in scenario 2, 83% are associated with H₂ pipeline construction, while the remaining 17% are from drilling the UCG wells and H₂ plant construction. Clearly, there are no GHG emissions associated with drilling, leakage in the EOR well, and CO₂ pipeline construction in scenario 2. Overall, the significance of non-operation emissions with respect to gross life cycle GHG emissions can be appreciated in scenario 1 more than in scenario 2. This is because adoption of CCS technology in the former scenario results in lower operation emissions than in the latter scenario. It is worth noting that emissions associated with coal surface mining, coal mine development, and coal transport are negated in H₂ production from UCG, unlike in H₂ production from surface coal gasification (SCG) [7, 22]. The notion of similarity of processes of syngas to H₂ conversion in UCG and SCG is complimented by the fact that the contribution of the operation emissions in the gross life cycle emissions (around 97.8%) in UCG is almost equivalent to reported values of 97% in SCG [7]. A higher percentage in UCG may be attributed to zero emissions associated with coal transport and coal mining.

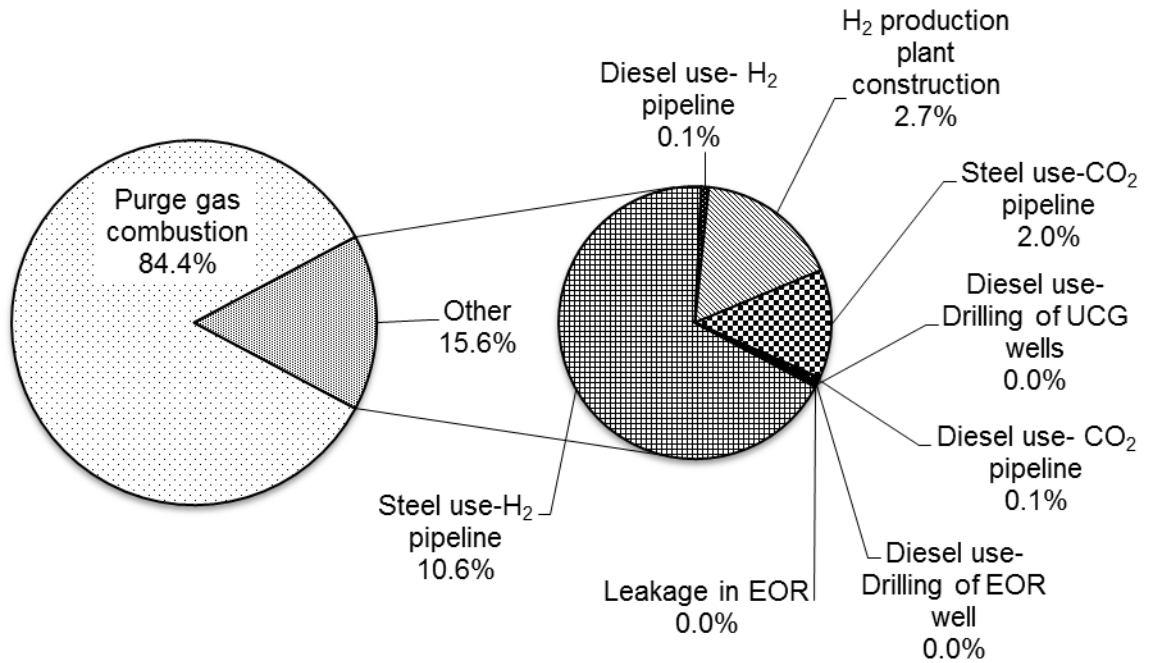


Figure 3.2: Life cycle GHG emissions distribution in scenario 1 (H₂ production from UCG with CCS). “Other” indicates non-operation GHG emissions. Note: the distribution is based on gross life cycle GHG emissions.

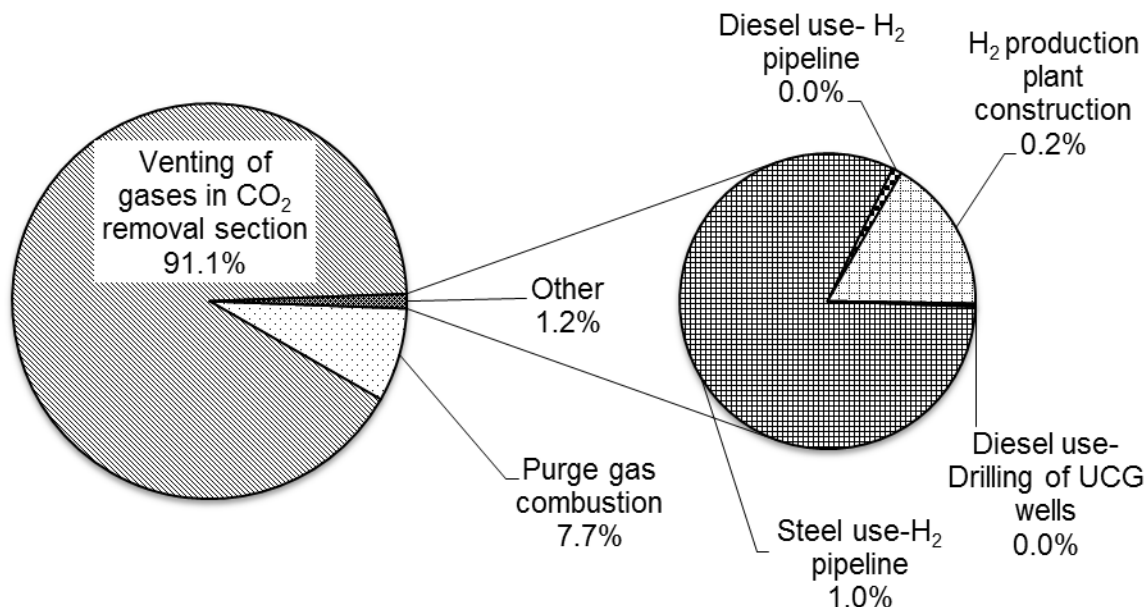


Figure 3.3: Life cycle GHG emissions distribution in scenario 2 (H₂ production from UCG without CCS). “Other” indicates non-operation GHG emissions. Note: the distribution is based on gross life cycle GHG emissions.

3.3.2. Net energy ratio (NER)

NER is a measure of “useful energy” (i.e., H₂ and electricity) production by the system per unit energy consumption of the fossil fuel (i.e., coal). In simpler terms, NER is calculated using Eq. 3.1. Figure 3.4 shows the energy balance for scenarios 1 and 2. This energy balance allows for identification of key energy consumption within and outside the system boundary for scenarios 1 and 2. NER is calculated as 0.59 and 0.61 for scenarios 1 and 2, respectively. The aforementioned NER values indicate that, the aggregate amount of energy extracted from coal is less than the energy content of the

coal. This NER also accounts for the energy used in the production of electricity and steam required for operating the H₂ plant in scenarios 1 and 2. Furthermore, the NER in scenario 2 is greater than in scenario 1; this is mainly due to zero energy consumption in CO₂ compression in scenario 2, which ultimately leads to higher electricity export to grid.

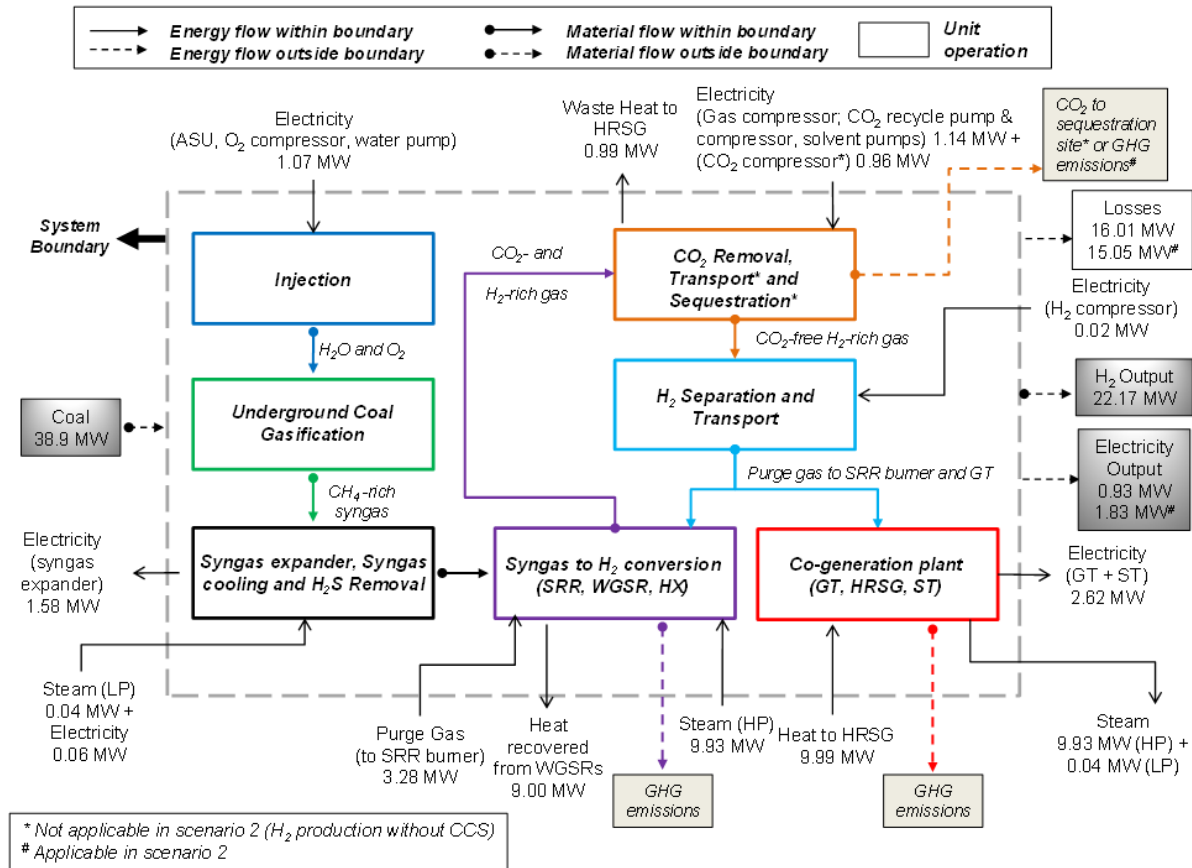


Figure 3.4: Energy balance in scenarios 1 and 2 for base case assumptions i.e. total coal input – 118 tonne/day, H₂O-to-O₂ injection ratio – 2 and ground water influx – 0.4 m³/tonne of coal.

3.3.3. *The effect of steam-to-carbon ratio on life cycle GHG emissions*

The steam-to-carbon ratio is an important process parameter for syngas-to-H₂ conversion in a conventional SCG-based H₂ production plant [46]. Chiesa et al. [46] examined the effect of steam-to-carbon ratio at the inlet of a high temperature WGSR in H₂ production from SCG; reducing the value of the steam-to-carbon ratio from 1.48 to 0.55 increases the emissions by 45%. Figure 3.5 shows the effect of the steam-to-carbon ratio on the H₂ production and the amount of CO₂ captured in scenario 1. It is important to note that a similar trend is obtained for H₂ production in scenario 2 because the unit operations up to H₂ production are the same in both scenarios.

However, for a fixed steam-to-carbon ratio, H₂ production falls slightly with increase in ground water influx¹⁷ (see Fig. 3.5). The reason is two-fold. First, H₂ content in the syngas from UCG falls, while CH₄ content rises. Second, steam consumption in the SRR unit increases to maintain a fixed steam-to-carbon ratio; this makes up for the deficit in H₂ content in the syngas by converting CH₄ into H₂ in the SRR unit. In addition, the amount of CO₂ captured also falls with an increase in ground water influx. Ultimately, an increasing trend of the gross and net life cycle GHG emissions in both scenarios is seen with increase in ground water influx (see Fig. 3.6).

¹⁷ Ground water influx in the UCG affects the quality and the quantity of the produced syngas, which ultimately affects the H₂ output [20, 21]. Since the ground water influx is difficult to estimate, a range of values – 0-0.4 m³/tonne-coal is considered for analysis [20, 21].

The effect of the steam-to-carbon ratio can be appreciated over gross and net life cycle GHG emissions in both scenarios (see Fig. 3.6). With a rise in the steam-to-carbon ratio, H₂ production increases; this stems from the fact that an augmented flow of steam will favor CH₄ conversion into H₂ in the SRR unit. At the same time, increased CH₄ conversion also escalates the amount of CO₂ in the reformed syngas post SRR and WGSR units, the effect of which is eventually realized in improved CO₂ capture. However, the percentage increase in H₂ production (13%) is greater than the percentage increase in CO₂ captured or vented (5%) in both scenarios. As a result, gross life cycle GHG emissions drop with a rise in steam-to-carbon ratio in both scenarios.

Contrastingly, the effect of the steam-to-carbon ratio on the net life cycle GHG emissions is not straightforward in either scenario. With an increase in the steam-to-carbon ratio, an increasing trend is observed in the net life cycle GHG emissions in scenario 1, as compared to a decreasing trend in scenario 2. With a rise in the steam-to-carbon ratio from 2 to 4, net life cycle GHG emissions reduce from 20.4 to 16.6 kg-CO₂-eq/kg-H₂ in scenario 2, while it increases from 0.6 to 1.1 kg-CO₂-eq/kg-H₂ in scenario 1. The reason for the observed trends is multifold. First, with an increase in the steam-to-carbon ratio, the GT power output decreases; due to decreased CH₄ flow in the purge gas, the calorific value of the purge gas falls, which results in lower GT power output for a higher steam-to-carbon ratio. Second, a penalty is enforced on the output of the ST because of rise in steam consumption in the SRR unit. Third, there is an increased energy penalty in capture and compression of CO₂ in scenario 1; the CO₂ content of the syngas after it's processing in SRR and WGSRs increases with increase in steam-to-carbon ratio (see Fig. 3.5).

These three factors (drop in power output of ST and GT, and energy penalty for CCS) result in lower net power output for a higher steam-to-carbon ratio. Eventually, the emissions credit for the export of electricity to the grid declines with a rise in the steam-to-carbon ratio. Since the values of gross life cycle GHG emissions in scenario 1 are much lower than in scenario 2 (see Fig. 3.6), the effect of the emissions credit on net life cycle GHG emissions is greater in scenario 1. A marginal increasing trend in net life cycle GHG emissions is therefore, achieved in scenario 1 compared to a significant decreasing trend in scenario 2 with increase in steam-to-carbon ratio.

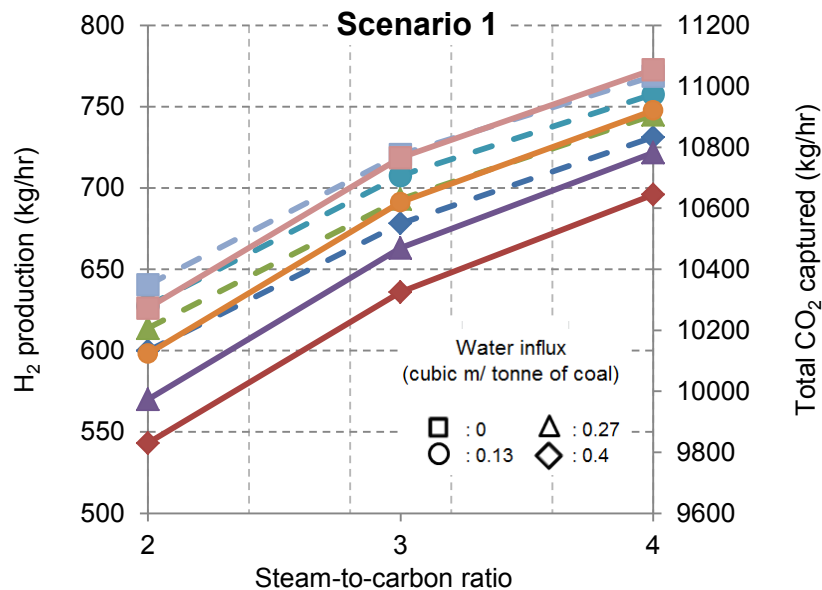


Figure 3.5: The effect of the steam-to-carbon ratio on H₂ production and amount of CO₂ captured using Selexol technology in scenario 1 with different ground water influx rates and a fixed H₂O to O₂ injection ratio of 2. Dash lines represent H₂ production and solid lines represent total CO₂ captured.

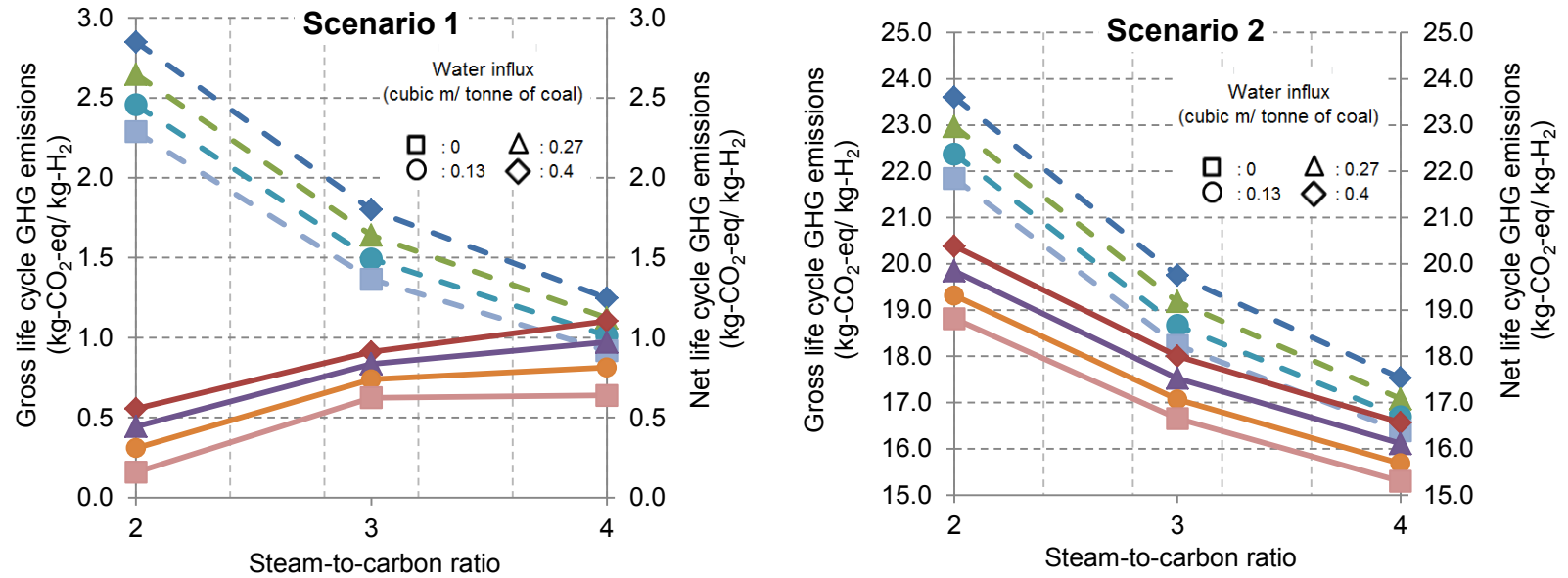


Figure 3.6: The effect of the steam-to-carbon ratio on gross and net life cycle GHG emissions in scenarios 1 and 2 with different ground water influx rates, but a fixed H₂O-to-O₂ injection ratio of 2. Dash lines represent gross life cycle GHG emissions and solid lines represent net life cycle GHG emissions.

3.3.4. The effect of the H₂O-to-O₂ injection ratio on life cycle GHG emissions

The H₂O-to-O₂ ratio plays a significant role in the composition of syngas and stability of the UCG operation [27, 44]. Therefore, it is important to understand the effect of this ratio on H₂ production output and life cycle GHG emissions. Figure 3.7 shows the effect of the H₂O-to-O₂ injection ratio on the H₂ production output and the total CO₂ captured for a fixed steam-to-carbon ratio of 3. Clearly, both output variables have great sensitivity towards the H₂O-to-O₂ injection ratio; with an increase in H₂O-to-O₂ injection ratio from 2 to 3, the H₂ output and the flow rate of captured CO₂ decrease by around 3.4% and 6.3%, respectively. This trend is mainly attributable to an increase in CH₄ content, while a decrease in H₂ flow in the syngas after UCG is observed.

The effect of the H₂O-to-O₂ injection ratio is clearly transferred to the gross life cycle GHG emissions in scenarios 1 and 2 (see Fig. 3.8). The decrease in flow of “captured CO₂” results in an increase in CO₂ content of the purge gas. This combined effect of a rise in CO₂ content of purge gas and fall in H₂ production output, eventually increases the gross life cycle GHG emissions from 1.8 to 2.3 kg-CO₂-eq/kg-H₂ in scenario 1 and 19.8 to 21.7 kg-CO₂-eq/kg-H₂ in scenario 2, with rise in the H₂O-to-O₂ injection ratio from 2 to 3. Contrastingly, the increase in net life cycle GHG emissions is marginal in scenario 1. This is mainly because the GHG emissions credit award for increased power output compensates for decreased flow of “captured CO₂” in scenario 1.

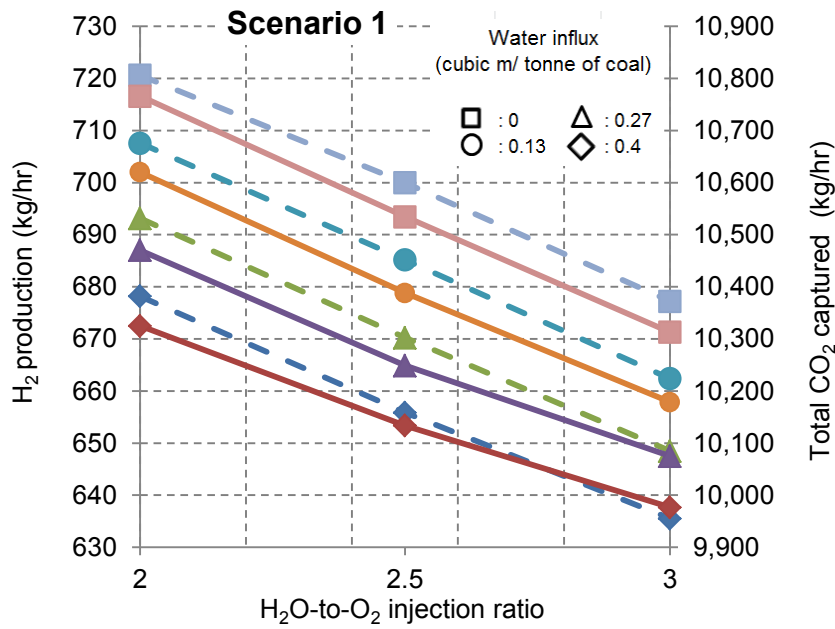


Figure 3.7: The effect of the H₂O-to-O₂ injection ratio on H₂ production and amount of CO₂ captured using Selexol technology in scenario 1 with different ground water influx rates, but a fixed steam-to-carbon ratio of 3. Dash lines represent H₂ production and solid lines represent total CO₂ captured.

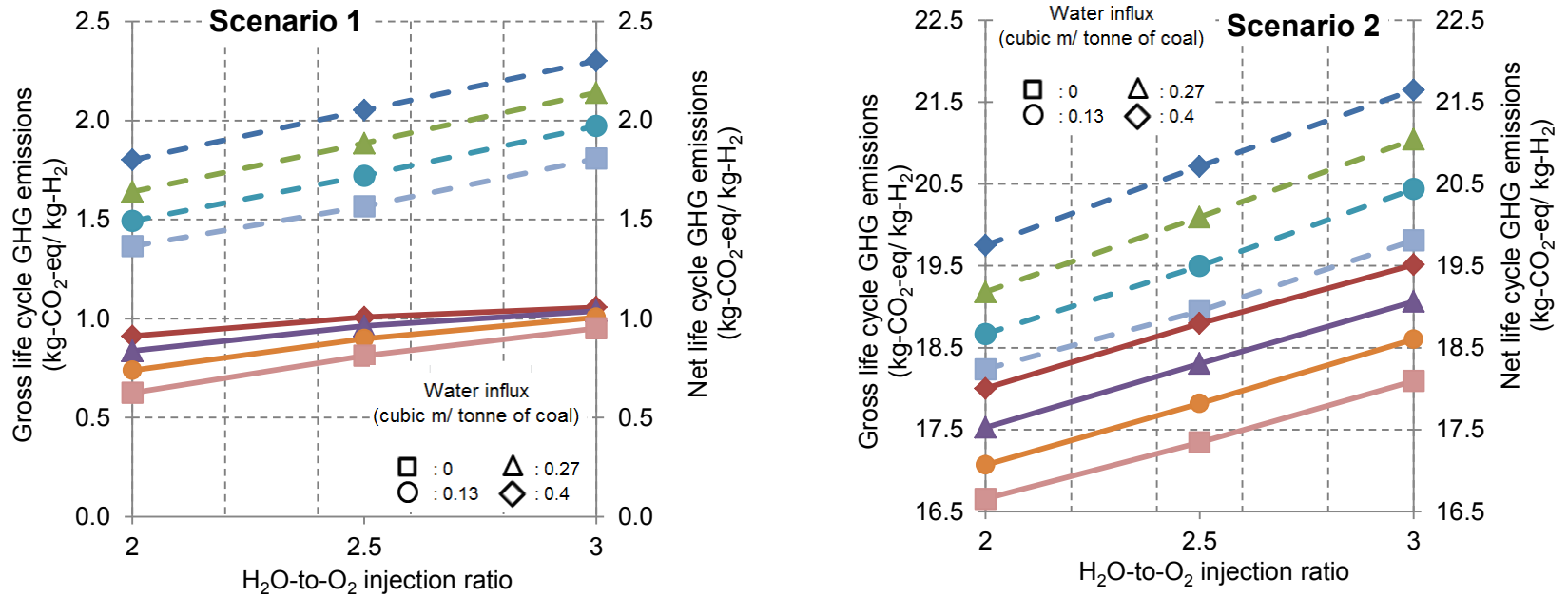


Figure 3.8: The effect of the H₂O-to-O₂ injection ratio on gross and net life cycle GHG emissions in scenarios 1 and 2 with different ground water influx rates, but a fixed steam-to-carbon ratio of 3. Dash lines represent gross life cycle GHG emissions and solid lines represent net life cycle GHG emissions.

3.3.5. Comparative assessment of life cycle GHG emissions in H₂ production from UCG with other H₂ production pathways

H₂ production from UCG-CCS is found to be more environmentally competitive than H₂ production without CCS. The competitiveness of H₂ production from UCG in terms of GHG emissions can be appreciated when the life cycle GHG emissions are compared with other H₂ production pathways. For the comparative assessment, a number of fossil fuel and renewable energy based H₂ production pathways are considered; they are listed in Table 3.7. Clearly, a wide range of scenarios is present in SCG and SMR, with regards to different plant configurations and schemes (with or without co-generation, only electricity co-production and only steam co-production).

Figure 3.9 shows a comparison of life cycle GHG emissions between UCG, SCG, SMR, wind, hydro, and solar energy based H₂ production pathways. It is evident from Fig. 3.9 that there exists a wide range of values for life cycle GHG emission in the literature for SCG and SMR. This might be due to the consideration of a different system boundary, coal composition, set of assumptions, jurisdiction, etc.¹⁸. The UCG-CCS pathway has a significantly lower GHG footprint than other fossil fuel based H₂ production pathways

¹⁸ These reasons can also be used to explain higher value of net life cycle GHG emissions in H₂ production from UCG without CCS than some reported values in the literature for SCG-based H₂ production pathway without CCS (see Fig. 3.9). To put this into perspective, the emissions associated with electricity production from UCG are evaluated to be 0.843 tonnes-CO₂-eq/MWh as compared to 0.88 tonnes-CO₂-eq/MWh from SCG in Alberta (see Table 3.5).

for all plant configurations, except SCG-CCS with steam co-production. The advantage of integrating CCS technology with UCG can be realized as this pathway becomes competitive with even renewable energy-based H₂ production pathways – wind, solar and hydro.

Table 3.7: Description of various H₂ production pathways considered in a comparative analysis of life cycle GHG emissions

Pathway Number	Pathway description	Source
Pathway 1	Water electrolysis using electricity generated by wind turbines	[34]
Pathway 2	Integrated photo voltaic system	[7]
Pathway 3.1	Water electrolysis using electricity generated by a hydro plant	[34]
Pathway 3.2		[7]
Pathway 4.1	SCG without co-generation	[6]
Pathway 4.2	SCG with co-generation	[7]
Pathway 4.3	SCG with electricity co-production	[6]
Pathway 4.4	SCG with steam co-production	[6]
Pathway 5.1	SCG-CCS without co-generation	[6]
Pathway 5.2	SCG- CCS with electricity co-production	[6]
Pathway 5.3	SCG-CCS with steam co-production	[6]

Pathway Number	Pathway description	Source
Pathway 6.1.1		[9]
Pathway 6.1.2	SMR without co-generation	[34]
Pathway 6.1.3		[8]
Pathway 6.1.4		[6]
Pathway 6.2	SMR with co-generation	[7]
Pathway 6.3	SMR with electricity co-production	[6]
Pathway 6.4.1	SMR with steam co-production	[10]
Pathway 6.4.2		[6]
Pathway 7.1	SMR-CCS	[8]
Pathway 7.2	SMR-CCS without co-generation	[6]
Pathway 7.3	SMR-CCS with electricity co-production	[6]
Pathway 7.4	SMR-CCS with steam co-production	[6]
Pathway 8	UCG with co-generation	Present model (FUNNEL-GHG-H2-UCG)
Pathway 9	UCG-CCS with co-generation	Present model (FUNNEL-GHG-H2-UCG)

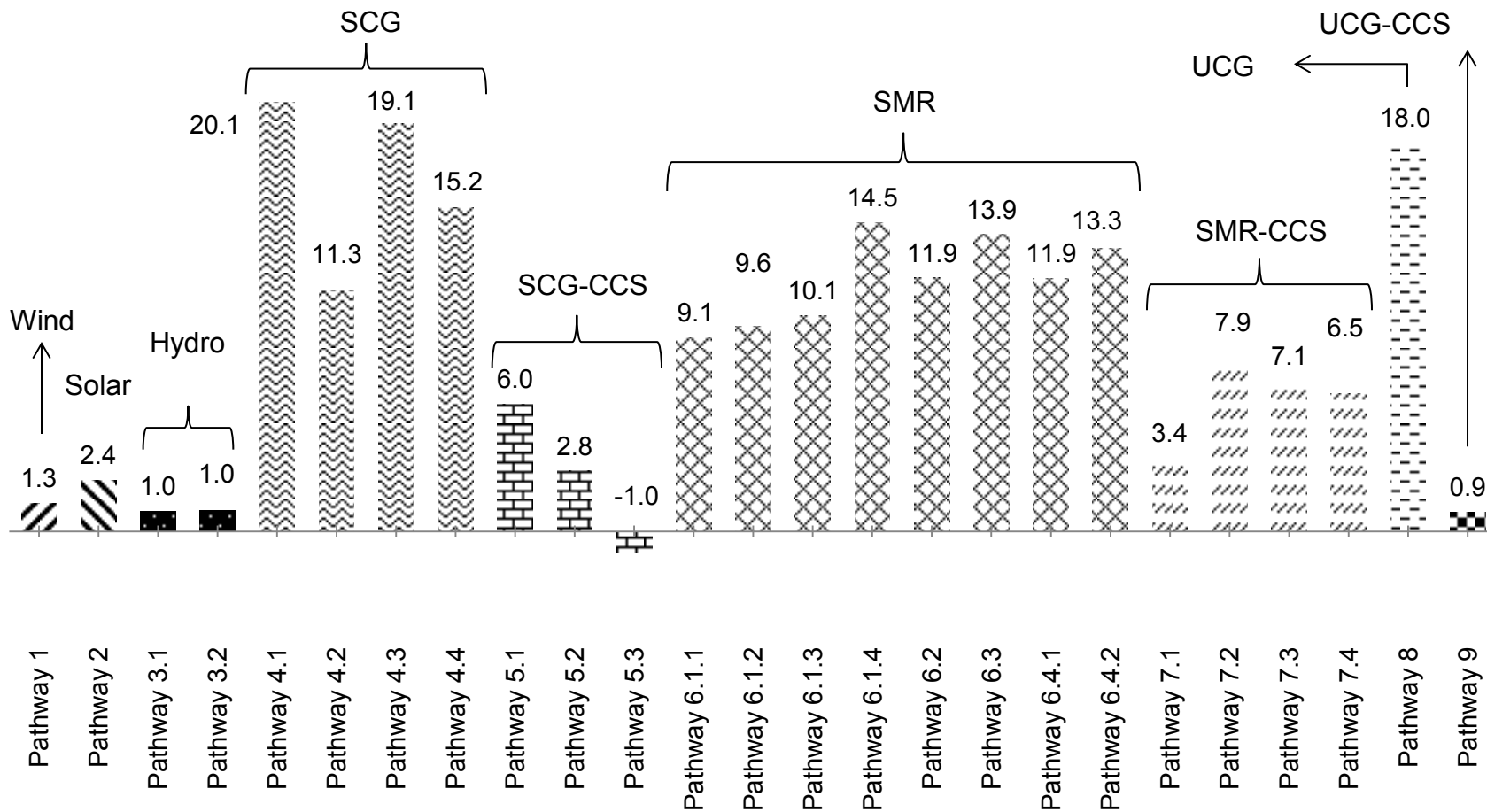


Figure 3.9: Comparative analysis of net life cycle GHG emissions in various H₂ production pathways. Pathways 1-3 are renewable energy-based, while pathways 4-9 are fossil-fuel based H₂ production pathways.

3.3.6. Sensitivity analysis

3.3.6.1 Sensitivity analysis on net life cycle GHG emissions: A sensitivity analysis was conducted to understand the influence of various input parameters on net life cycle GHG emissions. A variation of $\pm 20\%$ in the input parameters was done to appreciate their effects on the results. Figure 3.10 shows the sensitivity analysis completed for scenario 1 using base case assumptions. CO₂ and H₂ pipeline transportation distance are found to have weak sensitivities towards net life cycle GHG emissions owing to their low contribution towards the total values. Nevertheless, the net life cycle GHG emissions increase slightly with an increase in transportation distance owing to an increase in diesel and steel use in pipeline construction. The isentropic efficiency of the CO₂ compressor and the pressure ratio in GT are found to have a moderate effect on the net life cycle GHG emissions. The net life cycle GHG emissions moderately increase in a non-linear fashion with increase in pressure ratio in GT owing to the decreased power output of the GT. Due to reasonable contribution of the CO₂ compressors in the total power consumption (around 30%) in scenario 1, the net life cycle GHG emissions decrease with an increase in the CO₂ compressor efficiency; with an increase in the efficiency, the power consumption decreases, ultimately increasing the net power output and emissions credit for export of electricity to the grid.

It is challenging to estimate the syngas losses to the surrounding rocks in the UCG process. Therefore, a sensitivity analysis is conducted for this parameter (see Fig. 3.10). A 10% syngas production loss inside the UCG cavity increases the net life cycle GHG emissions by around 14%. This is mainly due to reduction in the H₂ output and the net

electricity export to the grid. The significance of H₂ separation efficiency in the sensitivity analysis is realized on observing a sharp increasing trend in the net life cycle GHG emissions. The observed trend is counterintuitive as an increase in the H₂ separation efficiency will not only increase the H₂ output but cause a significant decrease in the power output of the GT and the ST. With an increase in the H₂ separation efficiency by 10%, the power output of the GT and ST decreases by 44% and 27%, respectively, and ultimately the emissions credit is reduced by 85%. Overall, the net life cycle GHG emissions increase from 0.9 to 1.5 kg-CO₂-eq/kg-H₂ with an increase in the H₂ separation efficiency in the PSA by 10%.

The heat exchanger efficiency also has a major effect on the net cycle GHG emissions, with values increasing by 62.3% upon a drop in the efficiency by 10%. This is mainly due to reduced ST power output in the co-generation plant, eventually resulting in a lower emissions credit. Lastly, GT inlet temperature has a high sensitivity towards the net life cycle GHG emissions. A non-linear decreasing trend is observed due to low GT power output upon decreasing the GT inlet temperature.

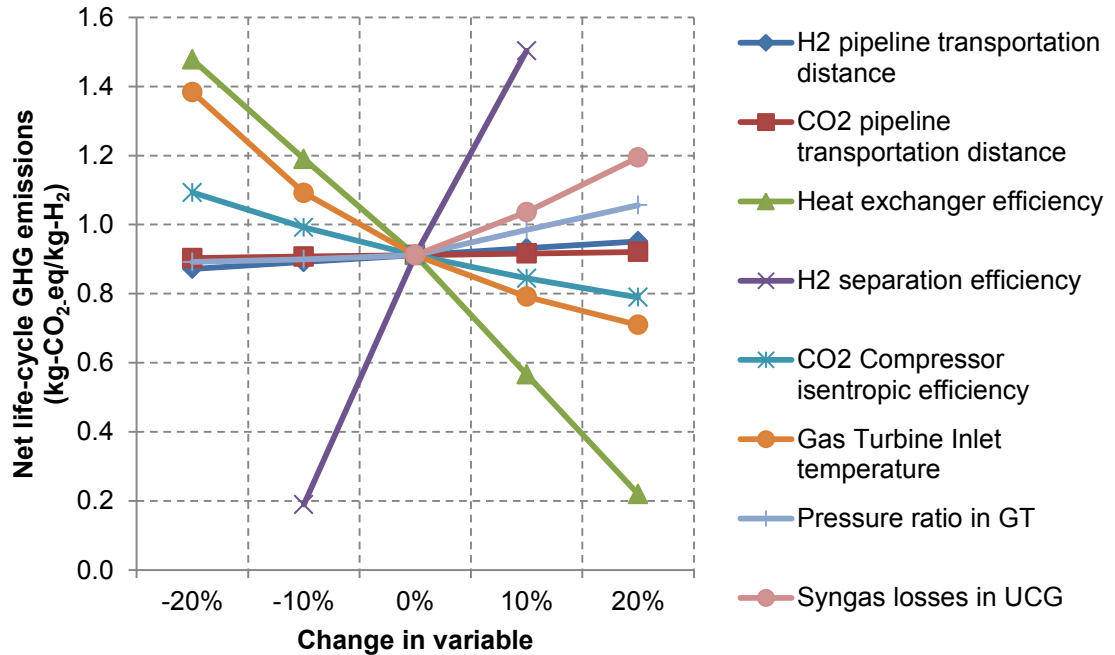


Figure 3.10: Sensitivity analysis on net life cycle GHG emissions for scenario 1. The analysis is done for base case assumptions (the H₂O-to-O₂ injection ratio is 2, ground water influx is 0.4 m³/tonne of coal, and the steam-to-carbon ratio is 3).

3.3.6.2 *Sensitivity analysis on gross life cycle GHG emissions:* Figure 3.11 shows the sensitivity analysis of the various parameters on gross life cycle GHG emissions. The gross life cycle GHG emissions in scenario 1 are the sum of operation and non-operation GHG emissions (see Eq. 3.4) and mainly composed of purge gas combustion emissions (see Fig. 3.2). Moreover, there are no GHG emissions associated with the steam and electricity use since the pathway is self-sufficient both in terms of steam and electricity use. Therefore, the parameters that affect the electricity production or consumption in the H₂ production pathway (e.g. GT inlet temperature and pressure ratio, CO₂ compressor

efficiency, heat exchanger efficiency) impact only the net life cycle GHG emissions, and not the gross life cycle GHG emissions. However, the separation efficiency of H₂ in the PSA unit impacts the gross life cycle GHG emissions. Increasing the H₂ separation efficiency by 10% decreases the gross life GHG emissions by 10%; a 10% increase in the H₂ production output is achieved upon a 10% rise in the H₂ separation efficiency.

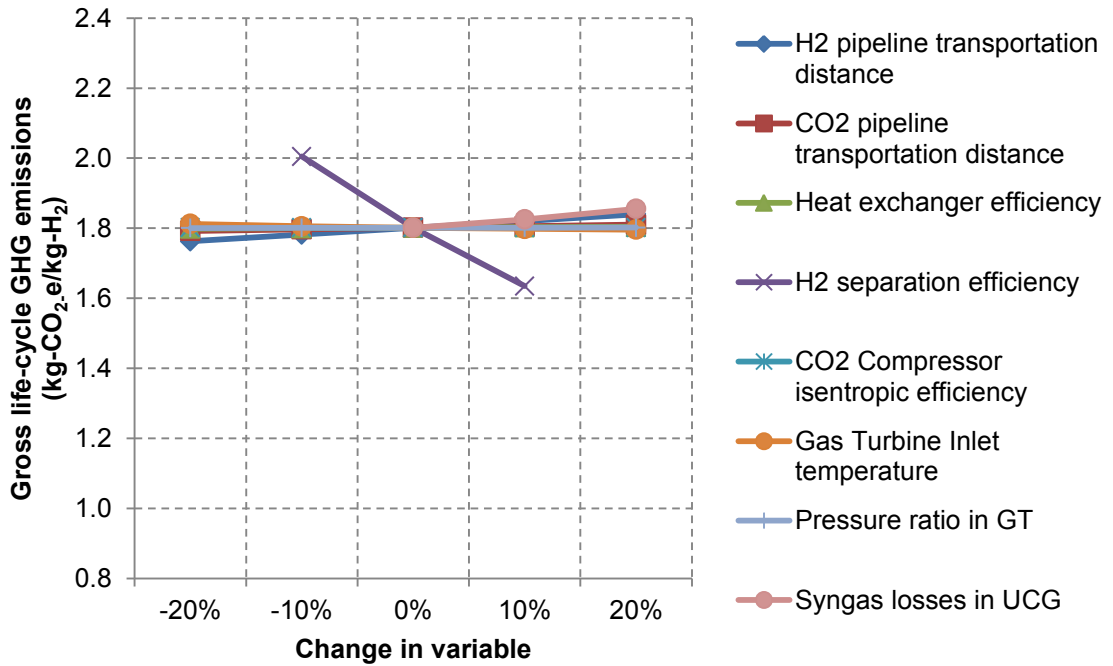


Figure 3.11: Sensitivity analysis on gross life cycle GHG emissions for scenario 1. The analysis is done for base case assumptions (the H₂O-to-O₂ injection ratio is 2, ground water influx is 0.4 m³/tonne of coal, and the steam-to-carbon ratio is 3).

3.4. Conclusions

This study examined life cycle GHG emissions of H₂ production from UCG for two scenarios with and without CCS by developing FUNNEL-GHG-H₂-UCG. The net life cycle GHG emissions are estimated to be 0.9 and 18.0 kg-CO₂-eq/kg-H₂ in H₂ production from UCG with and without CCS, respectively. Adoption of CCS technology leads to a substantial (91.1%) reduction in total life cycle emissions in H₂ production from UCG. Purge gas combustion and venting of gases in the CO₂ removal section are the major contributing factors in the net life cycle GHG emissions. On the other hand, energy and material use in drilling, H₂ and CO₂ pipeline transportation, and other construction contributed around 15.6% and 1.2% towards life cycle GHG emissions in H₂ production with and without CCS, respectively.

Furthermore, the net life cycle GHG emissions increase marginally with a rise in the H₂O-to-O₂ injection ratio and the steam-to-carbon ratio in H₂ production from UCG with CCS. In addition, the sensitivity analysis showed that the net life cycle GHG emissions are most sensitive to the separation efficiency of the PSA and the efficiency of the heat exchanger.

UCG-CCS is found to have a lower life cycle GHG emissions footprint in comparison to other conventional H₂ production pathways (SCG, SCG-CCS, SMR and SMR-CCS). UCG-CCS based H₂ is also comparable with wind, hydro, and solar based H₂ in terms of GHG emissions.

Chapter 4

Greenhouse Gas Abatement Costs of Hydrogen Production from Underground Coal Gasification (UCG)¹⁹

4.1. Background

Greenhouse gas (GHG) abatement costs assessments are helpful to evaluate GHG mitigation and the economics of an energy system, and are useful in making sound policy decisions [39, 40]. These cost estimates are useful in determining which energy production technologies have higher GHG abatement potential or superior economic competency [40]. As discussed in Chapter 1, there are several studies in the literature that discuss GHG abatement potential and GHG abatement costs of energy efficiency technologies and carbon capture and sequestration (CCS) in different industry sectors [33, 40, 63-65]. However, none of these studies have considered large-scale energy systems for H₂ production especially in the oil production sector where there is substantial interest to reduce the overall GHG footprint.

¹⁹ A version of this chapter has been as Verma A., Olateju B., Kumar A. Greenhouse Gas Abatement Costs of Hydrogen Production from Underground Coal Gasification (UCG). *Energy*. (in review).

The principal objective of this study is to estimate the GHG abatement costs of H₂ production from fossil fuel based pathways – SMR and UCG – for a variety of feasible scenarios applicable in western Canada. Out of the total seven scenarios assessed in this study, five scenarios include the consideration of CCS with the distinctions of – (1) type of CO₂ sequestration method, (2) transportation distance or location of CO₂ sequestration from the H₂ production plant, and (3) sale of CO₂ to an EOR operator.

This study uses the results of the techno-economic model developed in an earlier study [11], to estimate the GHG abatement costs for the seven scenarios. The GHG emissions for various scenarios are evaluated using a life cycle assessment (LCA) method. The life cycle GHG emissions for UCG-based H₂ production scenarios are evaluated from the LCA model – FUNNEL-GHG-H₂-UCG (FUNdamental ENgineering PrinciplEs-based Model for Estimation of GreenHouse Gases in hydrogen (H₂) production from Underground Coal Gasification) – discussed in Chapter 3. On the other hand, the life cycle GHG emissions for SMR-based scenarios are calculated by using – (1) the energy and material inputs of a life cycle assessment (LCA) model as developed earlier in the literature [10], and (2) the earlier developed process model for the SMR process [66]. The key contribution is in development of emission factors for material and energy use, and data inputs in the SMR-LCA model to represent western Canadian conditions²⁰.

²⁰ For instance, Spath et al. [10] considered an electricity emissions factor based on the mid-continental United States electricity generation mix, which is not applicable to western Canada, especially Alberta. Ultimately, the GHG emissions associated with electricity use or export will

Furthermore, life cycle GHG emissions in H₂ production from SMR along with CCS are estimated. The GHG abatement costs are in 2014 Canadian dollars. The following section gives a brief description of the H₂ production scenarios developed in this study.

4.2. Western Canadian H₂ production scenarios

Table 4.1 shows the seven H₂ production scenarios that can be implemented in western Canada and are likely to be considered by the bitumen upgrading industry [11]. Figure 4.1 provides a geographical representation of these seven scenarios and a high-level system boundary. These scenarios are similar to those considered earlier [11] in a techno-economic evaluation of UCG- and SMR-based H₂ production with and without CCS developed for western Canada. Scenarios 1-3 represent SMR-based H₂ production pathways; scenarios 1 and 2 have CCS with the different locations of sequestration (see Table 4.1). In scenarios 1-3, the H₂ production site is the same as the bitumen upgrading site and is located at Fort Saskatchewan, Alberta. Scenarios 4-7 represent UCG-based H₂ production pathways; scenario 6 is without CCS and the others are with CCS. Again, the discerning feature in the scenarios with CCS is the location of the CO₂ sequestration; in scenario 7, the captured CO₂ is sold to an EOR well operator located in close proximity to the UCG plant at a price of \$47/tonne-CO₂ [11]. The revenues for the sale of CO₂ are calculated based on the incremental flow of CO₂ in the UCG-CCS over the SMR-CCS case [11].

vary. Moreover, existing studies in the literature [7-10, 34] did not evaluate or oversimplify the assumptions while calculating life cycle GHG emissions in H₂ production along with CCS.

Table 4.1: H₂ production scenarios from UCG and SMR in western Canada (Adapted from [11])

Scenario number	Pathway	H ₂ supply chain			CO ₂ supply chain		
		Production site	Delivery site	Transportation distance and mode	With or Without CCS, and sequestration type	Delivery site	Transportation distance and mode
Scenario 1	SMR	Fort Saskatchewan, Alberta	Fort Saskatchewan, Alberta	-	With CCS – geological sequestration	Shell Quest; Thorhild, Alberta	84 km via pipeline
Scenario 2	SMR	Fort Saskatchewan, Alberta	Fort Saskatchewan, Alberta	-	With CCS – geological sequestration	Swan Hills, Alberta	225 km via pipeline
Scenario 3	SMR	Fort Saskatchewan, Alberta	Fort Saskatchewan, Alberta	-	Without CCS	-	-
Scenario 4	UCG	Swan Hills, Alberta	Fort Saskatchewan, Alberta	225 km via pipeline	With CCS – geological sequestration	Swan Hills, Alberta	10 km via pipeline
Scenario 5	UCG	Swan Hills, Alberta	Fort Saskatchewan, Alberta	225 km via pipeline	With CCS – geological sequestration	Shell Quest; Thorhild, Alberta	184 km via pipeline
Scenario 6	UCG	Swan Hills, Alberta	Fort Saskatchewan, Alberta	225 km via pipeline	Without CCS	-	-
Scenario 7	UCG	Swan Hills, Alberta	Fort Saskatchewan, Alberta	225 km via pipeline	With CCS – EOR	Swan Hills, Alberta	10 km via pipeline

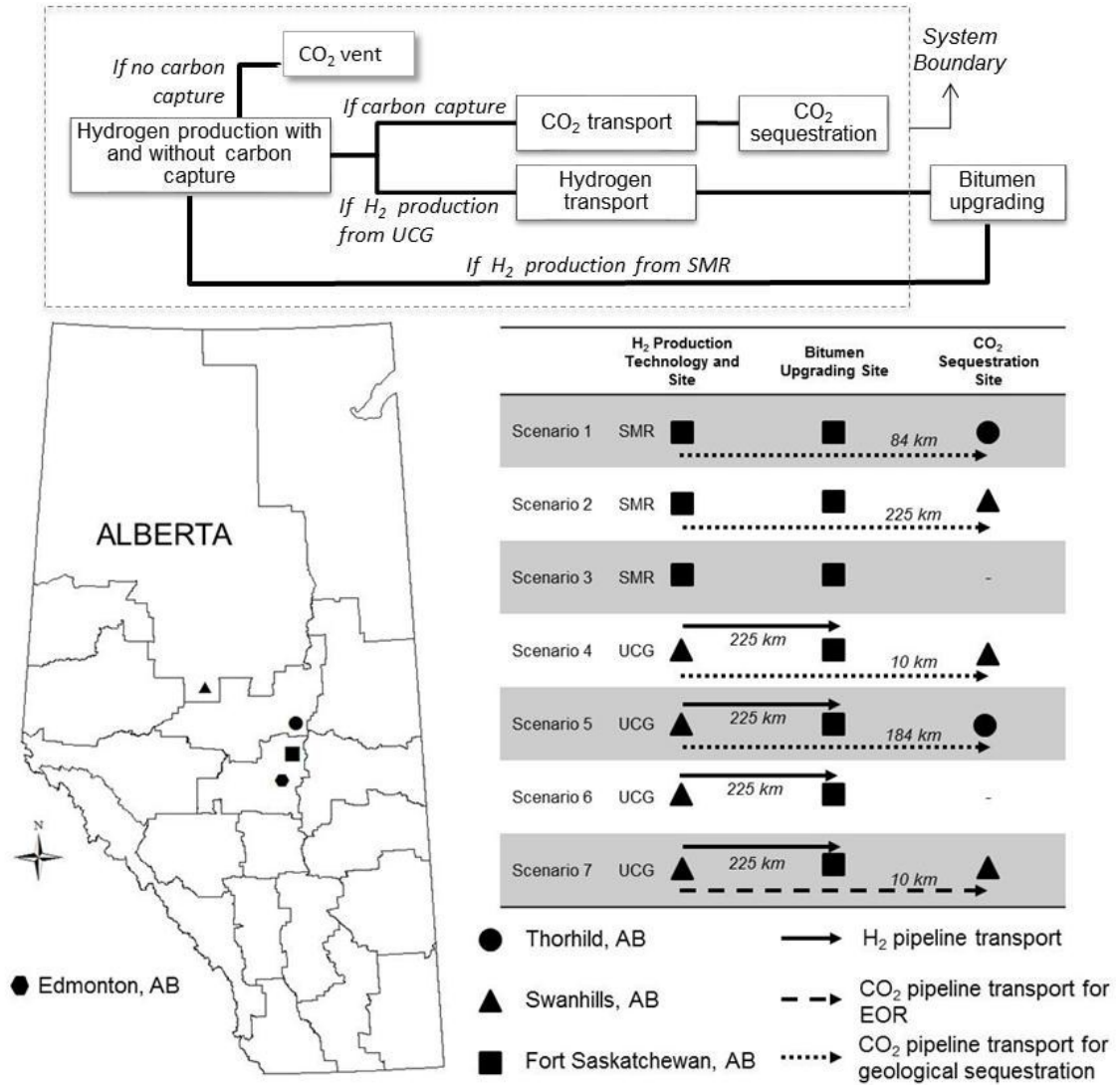


Figure 4.1: Geographical representation of the H₂ production scenarios in Alberta

4.3. Method

4.3.1. Scope of study

The purpose of this analysis is to estimate the GHG abatement costs in different scenarios of H₂ production in western Canada (see Table 4.1). The characteristics of the bitumen upgrading plant, UCG-CCS plant, and SMR-CCS plant are listed in Table 4.2. The GHG abatement costs (\$/tonne-CO₂-eq) are evaluated using Eq. 4.1; the value of 'i' indicates the scenario number for which the abatement costs are being calculated, 'ref' is the reference scenario number, the costs of H₂ production are in \$/kg-H₂, and the life cycle GHG emissions are in kg-CO₂-eq/kg-H₂; the functional unit selected in the LCA is 1 kg of H₂. The choice of the reference scenario has a considerable impact on the GHG abatement costs. The GHG abatement costs are calculated by comparing scenarios with the two H₂ production technologies, i.e., UCG and SMR with and without CCS; the reference technology for calculating the GHG abatement costs for all scenarios is SMR (scenario 3). The system boundaries considered for the H₂ production technologies (UCG, UCG-CCS, SMR, and SMR-CCS) are described in the following section.

Table 4.2: UCG-CCS and SMR-CCS plant specifications

Parameter	Value	Sources/ comments
<i><u>Bitumen upgrader</u></i>		
Capacity, bitumen-barrels/day	290,000	Based on Shell Canada's planned upgrader capacity [11].
H ₂ requirement in upgrading, kg/m ³ -bitumen	21	Based on an average value of 11.7 kg-H ₂ /m ³ in coking-based bitumen upgrading configuration and 30.3 kg H ₂ /m ³ in hydroconversion-based bitumen upgrading configuration [6]
H ₂ demand, tonnes/day	828.2	[11]
<i><u>UCG-CCS plant</u></i>		
H ₂ production capacity, tonnes/day	660	[11]
Coal consumption, tonnes/day	4784.3	Based on a coal-to-hydrogen conversion efficiency of 58.1% (LHV basis) (see section 2.3 of the thesis) and coal calorific value of 28.5 MJ/kg [11, 70].
Capacity factor	85%	[91]
Number of well pairs required	70	Based on coal thickness (7.5 m), width (80 m), and length (1400 m) of a coal seam gasified in a pilot scale project by Swan Hills Synfuels in Alberta; a coal

Parameter	Value	Sources/ comments
		utilization factor of 50% is employed [27, 44]. The coal bulk density and well lifetime are assumed to be 1.205 gm/cm ³ [44] and 20 years [32], respectively.
Total CO ₂ captured, tonnes/day	8540.1 ¹	Based on the results of FUNNEL-EGY-H2-UCG (FUNDamental ENgineering PrinciplEs-based ModeL for Estimation of EnerGY consumption and production in hydrogen (H ₂) production Underground Coal Gasification) developed in Chapter 2 of the thesis; Selexol technology is employed for CO ₂ capture.
<i><u>SMR-CCS plant</u></i>		
H ₂ production capacity, tonnes/day	607	[91]
Capacity factor	90%	[91]
Natural gas (NG) consumption (fuel and feedstock), tonnes/day	1762.3 ²	Based on energy consumption of NG feedstock and fuel equivalent to 137 MJ/kg-H ₂ and 15 MJ/kg-H ₂ , respectively [10]. The lower heating value (LHV) of NG and H ₂ is taken as 47.14 and 120 MJ/kg, respectively [6].
Total CO ₂ captured, tonnes/day	3235.6 ²	Calculated based on the CO ₂ content of the H ₂ -rich gas fed to the PSA unit [66]

Parameter	Value	Sources/ comments
		<p>and a CO₂ capture efficiency of 91.6% achieved by using Selexol technology [46, 48] (Also see results section of Chapter 2). While other traditional technologies (i.e., MEA and MDEA) can be applied for CO₂ capture in H₂ production from SMR [48], the Selexol technology is purposefully chosen for benchmarking SMR-CCS with the UCG-CCS-based H₂ production technology.</p>

¹ Capacity factor of 85% is applied to estimate this value. Around 15.2 kg-CO₂ is captured per kg of H₂ produced (see section 2.3 of the thesis).

² Capacity factor of 90% is applied to estimate this value.

$$(\text{GHG abatement cost})_i = \left(\frac{(\text{Levelised cost of H}_2 \text{ production})_i - (\text{Levelised cost of H}_2 \text{ production})_{\text{ref}}}{(\text{Life cycle GHG emissions})_{\text{ref}} - (\text{Life cycle GHG emissions})_i} \right) * 1000 \quad (4.1)$$

4.3.2. System boundaries: H₂ production from UCG and SMR with and without CCS

The emission factors for material and energy use in different unit operations of the H₂ production pathway are listed in Table 4.3. The life cycle GHG emissions in the SMR process (scenarios 1-3) are evaluated for the system boundary shown in Fig. 4.2. The key energy and material inputs in SMR-based H₂ production plant operations are derived from the LCA study from literature [10] and the results of an earlier developed process model [66]. In SMR-based H₂ production scenarios with CCS (scenarios 1 and 2), the CO₂ pipeline design for transportation and injection well design for sequestration are derived from the method developed by Ogden [79]. The emissions related to pipeline construction and sequestration (the use of steel in pipelines and diesel in trenching and well drilling) are then evaluated using the method and assumptions incorporated in the LCA model – FUNNEL-GHG-H₂-UCG – developed in Chapter 3 of the thesis. An SMR-based H₂ production pathway can be self-sufficient in terms of electricity or steam use depending on the final use of the heat recovered by the heat exchangers in the NG-to-H₂ conversion section (see Fig. 4.2); the "electricity co-production" scenario represents the former case and "steam co-production" scenario represents the latter. Appropriate credits are given for the export of electricity and steam.

The life cycle GHG emissions in UCG-based H₂ production scenarios (scenarios 4-7) are evaluated using the results of FUNNEL-GHG-H₂-UCG developed in Chapter 3 of the thesis; the system boundary for UCG-based H₂ production scenarios is depicted in Fig. 4.3. The syngas is collected from the UCG production wells and fed to a surface syngas-to-H₂ production plant; this plant is assumed to be located near the UCG wells and any energy inputs in transporting or storing syngas are not considered. Moreover, this pathway is found to be self-sufficient in terms of steam and electricity use; a credit is given for the export of electricity to the grid.

Table 4.3: Emission factors used in this study

Parameter	Value	Sources/comments
Electricity use, kg-CO ₂ -eq/kWh	0.88	Applicable for Alberta [90]
Electricity export, kg-CO ₂ -eq/kWh	0.65	Applicable for Alberta [90]
NG use, gm-CO ₂ -eq/MJ-NG	56.24	[6]
NG recovery, processing, transmission and distribution, gm-CO ₂ -eq/MJ-NG	5.12	[6]
Steam export, gm-CO ₂ -eq/MJ-steam export	81.79	Calculated based on the NG use in a boiler to produce an equivalent amount of steam energy; a boiler efficiency of 75% is assumed [10].
Steel use, kg-CO ₂ -eq/kg-steel	4.97	[6]
Diesel use, gm-CO ₂ -eq/MJ-diesel	73.96	[6]

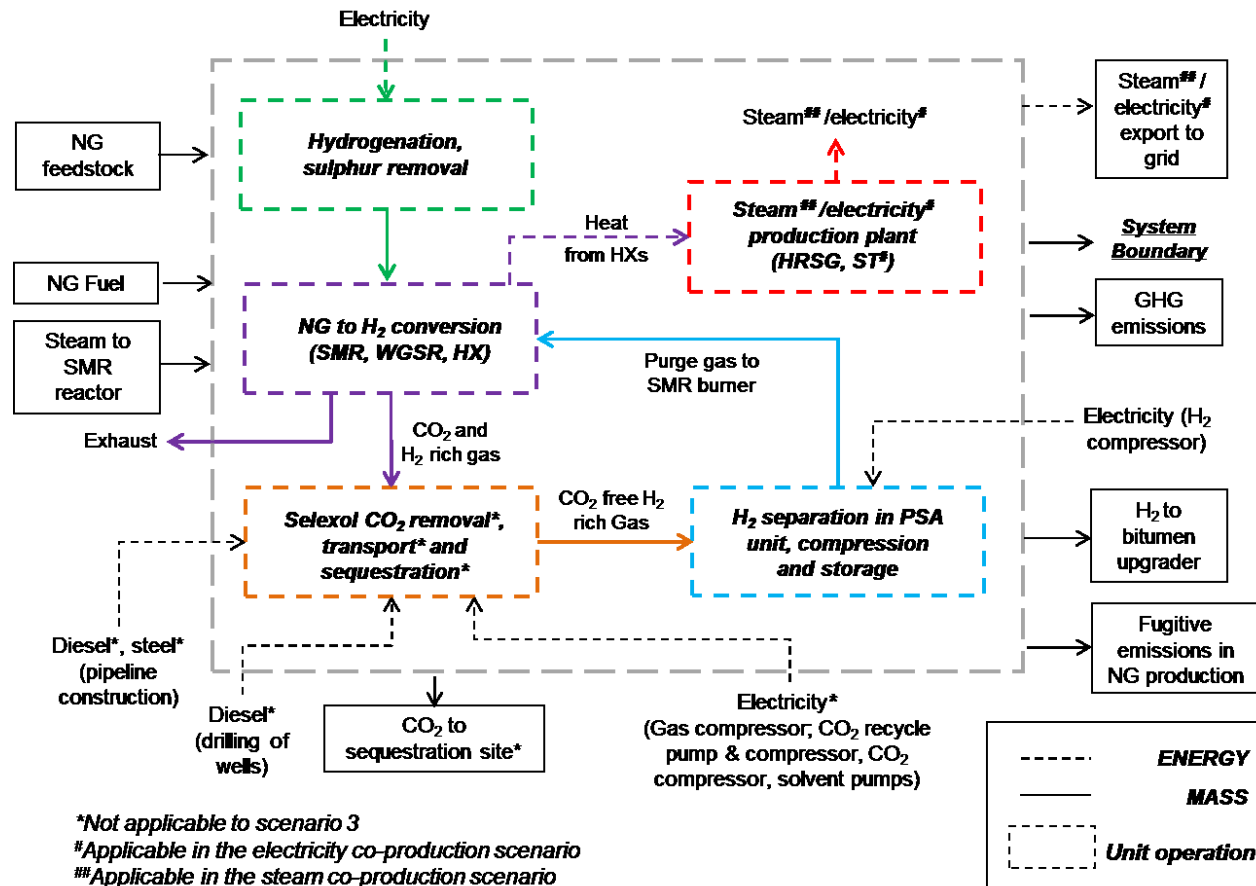


Figure 4.2: System boundary for SMR based-H₂ production scenarios. Note: SMR=steam methane reforming; WGSR=water gas shift reactor; HX=heat exchanger; PSA=pressure swing adsorption; HRSG=heat recovery steam generator; ST=steam turbine.

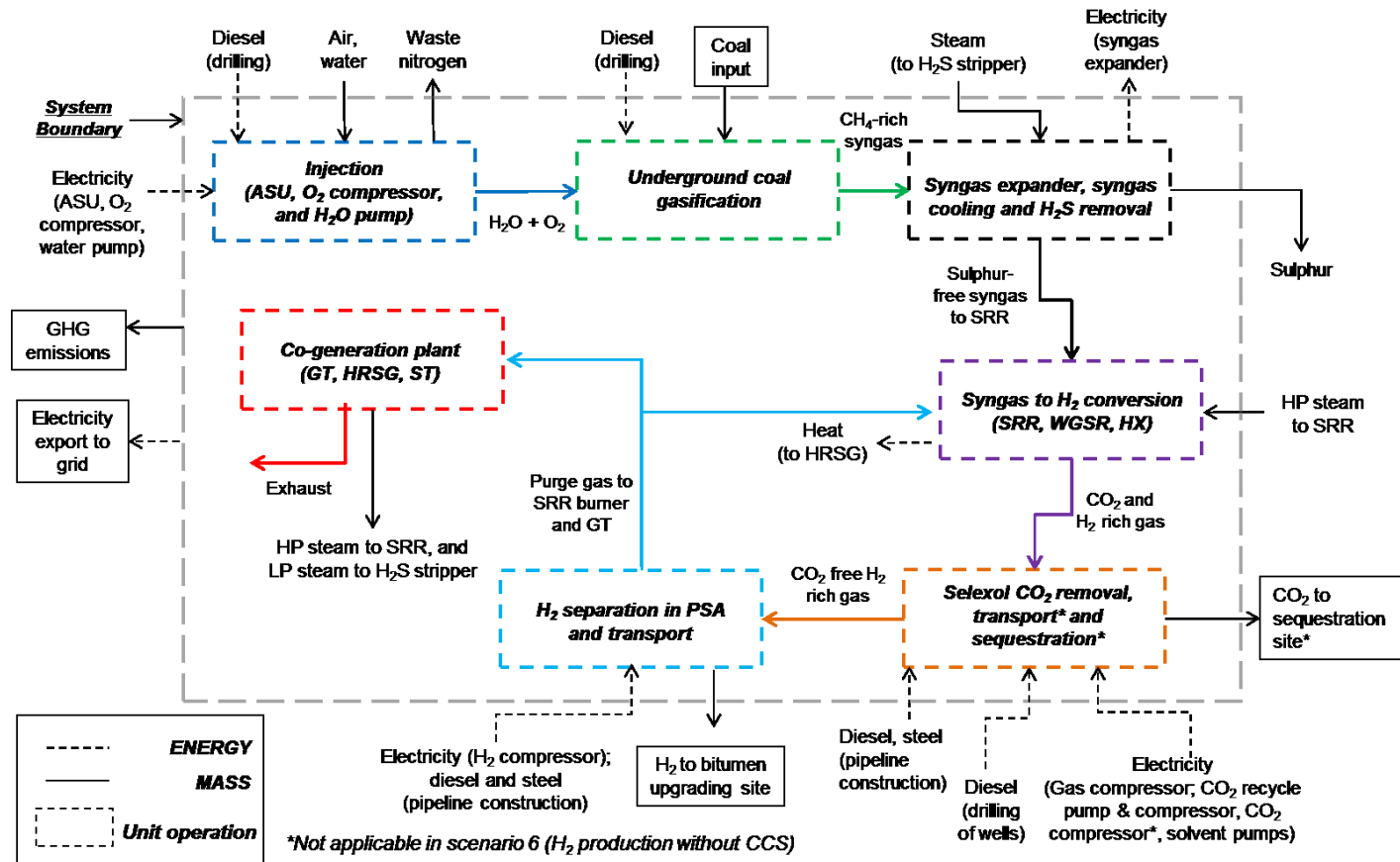


Figure 4.3: System boundary for UCG based-H₂ production scenarios. Note: ASU=air separation unit; SRR=syngas reforming reactor; WGSR=water gas shift reactor; HX=heat exchanger; PSA=pressure swing adsorption; HRSG=heat recovery steam generator; ST=steam turbine; GT=gas turbine.

4.4. Results and discussion

The GHG abatement costs are a function of the life cycle GHG emissions for a given scenario (see Eq. 4.1). Therefore, it is important to quantify the life cycle GHG emissions for energy and material inputs in different unit operations over the life cycle of the operation. As mentioned earlier, the life cycle GHG emissions are reported in kg-CO₂-eq/kg-H₂.

4.4.1. Life cycle GHG emissions in SMR-based H₂ production scenarios

Table 4.4 lists the life cycle GHG emissions from scenarios 1, 2, and 3 for the system boundary presented in Fig. 4.2. It is important to reiterate that the H₂ production capacity in these scenarios is 607 tonnes per day (see Table 4.2). Moreover, for each of these scenarios, there are two sub-scenarios or plant schemes considered in this analysis – steam co-production and electricity co-production (see Fig. 4.2). In both plant schemes, the emissions associated with all energy and material uses are the same, except electricity use, steam use, electricity export, and steam export. While there are no emissions associated with the electricity use and there is no emissions credit for the steam export from the plant scheme with electricity co-production, these emissions are considered in the plant scheme with steam co-production. However, the emissions associated with the steam use and the electricity export in the steam co-production plant scheme are considered.

The advantage of electricity co-production over steam co-production in the SMR-based H₂ production pathway is clearly evident in terms of the total life cycle GHG emissions (see Table 4.4); in the former scenario, the excess steam produced from the heat recovered in the syngas-to-H₂ conversion section is used to produce electricity from a steam turbine. This is mainly because producing electricity from the excess steam not only offsets the grid electricity use, but also results in electricity export to the grid. This advantage is complemented by the fact that the emission factor for electricity use (244.4 gm-CO₂-eq/MJ-electricity [90])²¹ and the emissions credit for electricity export to the grid (180.6 gm-CO₂-eq/MJ-electricity [90]) in Alberta is greater than NG use (61.3 gm-CO₂-eq/MJ-NG [6]). Moreover, replacing coal with other, cleaner fuels like natural gas or even renewable energy production methods like hydro, wind, etc., for electricity production would result in lower GHG emissions.

It is also evident from Table 4.4 that the CCS technology results in a significant reduction in the amount of GHG emissions in scenarios 1 and 2 compared to 3. The total life cycle GHG emissions in scenario 2 are slightly greater than in scenario 1. This is mainly due to the lower contribution of CO₂ construction emissions (steel and diesel use in pipeline construction and trenching, respectively) in the total life cycle GHG emissions. It is interesting to note that in spite of a 91.6% CO₂ capture (see Table 4.2) using Selexol solvent in a pre-combustion plant configuration, the total life cycle GHG emissions decrease only by around 44% (see Table 4.4). This is mainly because there is an energy

²¹ A relatively high electricity emission factor is attributed to the use of coal for electricity production in Alberta, Canada.

penalty in terms of increased electricity use to deploy CCS in this H₂ production pathway. Moreover, the GHG emissions associated with this increased use of electricity partially offset the advantage of CO₂ capture in the total life cycle GHG emissions calculation. In addition, post CO₂ capture, the purge gas contains significant amounts of CH₄ (around 33.6% by mol) [66], which results in GHG emissions on combustion in the burner (see Fig. 4.2).

Table 4.4: Life cycle GHG emissions in H₂ production from SMR with and without CCS (scenarios 1, 2 and 3)

Parameter	With steam			With electricity		
	co-production			co-production		
	(kg-CO ₂ -eq/kg-H ₂)			(kg-CO ₂ -eq/kg-H ₂)		
Applicable scenarios	1	2	3	1	2	3
<i>H₂ production</i>						
Losses in the NG production ¹	1.129	1.129	1.129	1.129	1.129	1.129
Electricity use	1.908 ³	1.908 ³	0.990 ²	0	0	0
NG fuel use and upstream emissions	0.922	0.922	0.922	0.922	0.922	0.922
NG feedstock upstream emissions	0.700	0.700	0.700	0.700	0.700	0.700
Emissions from purge gas	2.981	2.981	8.904	2.981	2.981	8.904

Parameter	With steam			With electricity		
	co-production			co-production		
	(kg-CO ₂ -eq/kg-H ₂)			(kg-CO ₂ -eq/kg-H ₂)		
Applicable scenarios	1	2	3	1	2	3
combustion ⁴						
Steam use	0	0	0	2.723	2.723	2.723
Steam export	-1.168	-1.168	-1.168	0	0	0
Electricity export ⁵	0	0	0	-2.549	-2.549	-3.182
Construction and						
decommissioning of H ₂	0.041	0.041	0.041	0.041	0.041	0.041
production plant ⁶						
<u>CCS</u>						
CO ₂ pipeline infrastructure, well drilling and leakage	0.077	0.244	-	0.077	0.244	-
Total life cycle GHG emissions	6.590	6.757	11.518	6.024	6.191	11.237

¹ Assumed to be 1.4% of NG production [10]. A global warming potential (GWP) of 25 is taken for CH₄ to calculate GHG emissions [6].

² The H₂ is delivered at a pressure of 14 bar and compressed to 70 bar for storage [11]. The value in the table is inclusive of electricity use in compression of H₂ from 14 bar to 70 bar; the power requirement is calculated using a model developed by Ogden [79].

³ The value includes electricity use in H₂ compression from 14 bar to 70 bar and CO₂ capture using Selexol technology and compression in a five-stage compression train up to 150 bar.

Electricity use in CO₂ capture and compression is taken as 203.8 kWh/tonne-CO₂ (see section 2.3 of the thesis).

⁴ Calculated based on a purge gas composition (mol %) – CO-0.3%, CO₂-49.4%, H₂-29.7%, H₂O-1.1%, CH₄-18.4%, N₂-1.1% in scenario 3 [66]; PSA efficiency for H₂ separation is reported in a range of 82-90% [66, 92]. It is assumed to be 85%, which is also consistent with UCG-based H₂ production scenarios and appropriate for benchmarking purpose.

⁵ Estimated based on electricity production by a gas turbine with a thermal efficiency of 36.1% [93]; the NG input is calculated based on equivalent amount of NG required to produce steam that would otherwise be exported, in a boiler with an efficiency of 75% [10]. Moreover, the value includes the electricity requirement in the H₂ plant operation and a transmission loss of 6.5% in export of electricity to the grid [6].

⁶ The difference in this value is negligible for H₂ production with and without carbon capture [59]; a value of 0.041 kg-CO₂-eq/kg-H₂ [10] is, therefore, used for both cases.

4.4.2. Life cycle GHG emissions in UCG-based H₂ production scenarios

The life cycle GHG emissions for scenarios 4, 5, 6, and 7 are listed in Table 4.5. As mentioned earlier, the results for the respective scenarios are based on FUNNEL-GHG-H₂-UCG developed in Chapter 3 of the thesis, with the difference being the scale of H₂ production considered in the present analysis. Moreover, the H₂ production capacity in these scenarios is 660 tonnes per day as compared to a H₂ production capacity of 607 tonnes per day in SMR-based H₂ production scenarios (see Table 4.2). Because the H₂ production scales in the two pathways (SMR and UCG) are similar, the scenarios can be

reasonably compared with each other. It is important to mention that the life cycle GHG emissions in the present analysis are slightly greater than the results presented in Chapter 3 (see section 3.3.1 for more information), mainly due to the increased scale of H₂ pipeline transport from the UCG plant to the bitumen upgrading facility. A larger scale of H₂ pipeline operation results in more electricity consumption at the inlet pump station compared to a lower scale of pipeline operation; electricity consumption increases to account for increased friction losses in the pipeline. This rise in electricity consumption lowers the emissions credit for electricity export to the grid and ultimately the total life cycle GHG emissions increase.

Table 4.5: Life cycle GHG emissions in H₂ production from UCG with and without CCS (scenarios 4, 5, 6 and 7)

Parameter	Life cycle GHG emissions (kg-CO ₂ -eq/kg-H ₂)			
	4	5	6	7
Applicable scenarios				
UCG well drilling	0.003	0.003	0.003	0.003
<i>H₂ production and transport</i>				
Purge gas combustion and venting of gases from CO ₂ removal section	1.521	1.521	19.519	1.521
Steam use	0	0	0	0
Electricity use	0	0	0	0
Electricity export	-0.341	-0.458	-1.318	-0.341
H ₂ pipeline construction	0.015	0.015	0.015	0.015

Construction and decommissioning of H ₂ production plant	0.048	0.048	0.040	0.048
<u>CCS</u>				
CO ₂ pipeline infrastructure, well drilling and leakage	0.010	0.275	0	0.010
Total life cycle GHG emissions	1.255	1.404	18.258	1.255

4.4.3. GHG abatement costs in H₂ production scenarios

The GHG abatement costs for the seven scenarios listed in Table 4.1 are estimated using Eq. 4.1, and include the additional cost of using a technology per unit savings in the life cycle GHG emissions. Table 4.6 lists the GHG abatement costs calculated for various H₂ production scenarios. The reference scenario chosen for the analysis is scenario 3, which uses an SMR-based H₂ production technology without CCS. As mentioned in section 4.3.2, two plant configurations – electricity co-production and steam co-production – are chosen for the analysis of SMR-based scenarios. The GHG abatement costs are negative and hence lowest for scenario 7; they range from -\$C 12.91 to -\$C 13.27 per tonne-CO₂-eq. This observation can be explained by the lower costs of H₂ production in scenario 7 than in scenario 3. It is important to reiterate that the sale of captured CO₂ to an EOR operator (at \$47/tonne-CO₂) not only negates the additional cost of CCS but also lowers the levelised cost of H₂ production in scenario 7 [11]. Another important observation is that in spite of higher levelised cost of H₂ production, the GHG abatement costs in all the

UCG-CCS-based scenarios (scenarios 4, 5, and 7) are lower than those in the SMR-CCS-based scenarios (scenario 1 and 2). This is attributable to higher life cycle GHG emissions in the SMR-CCS scenarios than in the UCG-CCS scenarios^{22,23}.

It is important to note that despite different plant configurations and equipment, there is no significant difference in the levelised cost of H₂ production in scenarios 3 (SMR without CCS) and 6 (UCG without CCS). This is mainly because the incremental levelised cost of H₂ production due to the higher total capital costs in the UCG-based H₂ production plant than the SMR-based H₂ production plant is compensated by the negligible feedstock cost of coal in the former case versus a feedstock cost of \$5/GJ-NG in the latter case. That being said, the costs of GHG emissions mitigation in SMR-CCS and UCG-CCS-based scenarios are mainly due to the capital costs of the additional infrastructure required for CCS – CO₂ capture equipment, CO₂ compressors, CO₂

²² In a pre-combustion carbon capture scheme, as considered in the present LCA analysis of SMR-based H₂ production, a significant amount of natural gas that is not converted to H₂ in the reformer is burned in the burners as purge gas (see section 4.4.1 and Fig. 4.2). On the other hand, in UCG-CCS, around 90% of the carbon in coal is converted to CO₂ after UCG and syngas-to-H₂ conversion (see Fig. 4.3), leading to high CO₂ capture efficiency as compared in the SMR-CCS pathway.

²³ Note that the CO₂ capture rate in a UCG-CCS plant is higher than in a SMR-CCS plant (see Table 4.2) resulting in increased capital costs of CO₂ capture, compression and transport in the former case than in the latter. This leads to higher levelised H₂ production costs in the UCG-CCS than in the SMR-CCS (see results for scenario 2 and 5 in Table 4.6).

pipeline, and CO₂ sequestration costs. Moreover, for a fixed H₂ production scale in SMR- and UCG-based scenarios, the GHG abatement costs are highly sensitive to the transportation distance of the captured CO₂ to the sequestration site; with an increase in transportation distance from 84 km (scenario 1) to 225 km (scenario 2), the GHG abatement costs rise by around 71%.

Table 4.6: GHG abatement costs in H₂ production scenarios. Note: the reference scenario for GHG abatement costs calculation is scenario 3.

Scenario number	H ₂ production cost (\$C/kg-H ₂) ³	Life cycle GHG emissions (kg-CO ₂ -eq/kg-H ₂)		GHG abatement costs (\$C/tonne-CO ₂ -eq)	
		<i>Lower</i>	<i>Upper</i>	<i>Lower</i>	<i>Upper</i>
		<i>limit</i> ¹	<i>limit</i> ²	<i>limit</i> ¹	<i>limit</i> ²
Scenario 1	2.36	6.024	6.590	86.83	91.83
Scenario 2	2.66	6.192	6.758	148.79	157.67
Scenario 3	1.91	11.237	11.518	-	-
Scenario 4	2.33	1.255	-	40.87	42.03
Scenario 5	2.98	1.404	-	105.86	108.90
Scenario 6 ⁴	1.96	18.258	-	-	-
Scenario 7	1.78	1.255	-	-12.91	-13.27

¹ Applies in SMR-based H₂ production with electricity co-production (see Table 4.2).

² Applies in SMR-based H₂ production with steam co-production (see Table 4.2).

³ Derived from the techno-economic model developed for a similar H₂ production plant size by [11]. The costs are corrected to 2014 Canadian dollars using an inflation rate of 2.5% [11].

⁴ The GHG abatement costs are not calculated for this scenario because the life cycle GHG emissions in this scenario are greater than the life cycle GHG emissions in the reference scenario (scenario 3).

4.4.4. GHG mitigation potential of UCG-CCS and SMR-CCS technologies for H₂ production

Figure 4.4 shows the GHG mitigation potential of H₂ production scenarios with CCS in 2022. The GHG mitigation potential is estimated for SMR-CCS and UCG-CCS technologies for H₂ production in order to satisfy the projected SCO production of 73.53 million m³ per annum in 2022 [5]. The base scenario for the analysis is scenario 3.

Moreover, based on the type of bitumen upgrading configuration, i.e., coking-based and hydroconversion-based²⁴, the lower limits and the upper limits for emissions mitigation in each scenario are assessed. Based on the present analysis, the GHG abatement potential is highest for UCG-CCS-based H₂ production scenarios and varies from 8.58 to 22.55 Mt of GHG emissions per year. This abatement potential can contribute significantly to the Government of Alberta's plan to reduce GHG emissions by around 50 Mt per year in 2020 [13]. The GHG abatement potential is lower if one of the SMR-CCS-based scenarios (scenario 1 or 2) is adopted for H₂ production; the potential varies from 4.22 to

²⁴ The H₂ requirement in upgrading of bitumen in coking-based and hydroconversion-based configurations is estimated to be around 11.7 and 30.3 kg/m³-bitumen, respectively [6].

11.30 Mt of GHG emissions per year. This is mainly attributable to higher life cycle GHG emissions in scenarios 1 and 2 than in scenarios 4, 5, and 7.

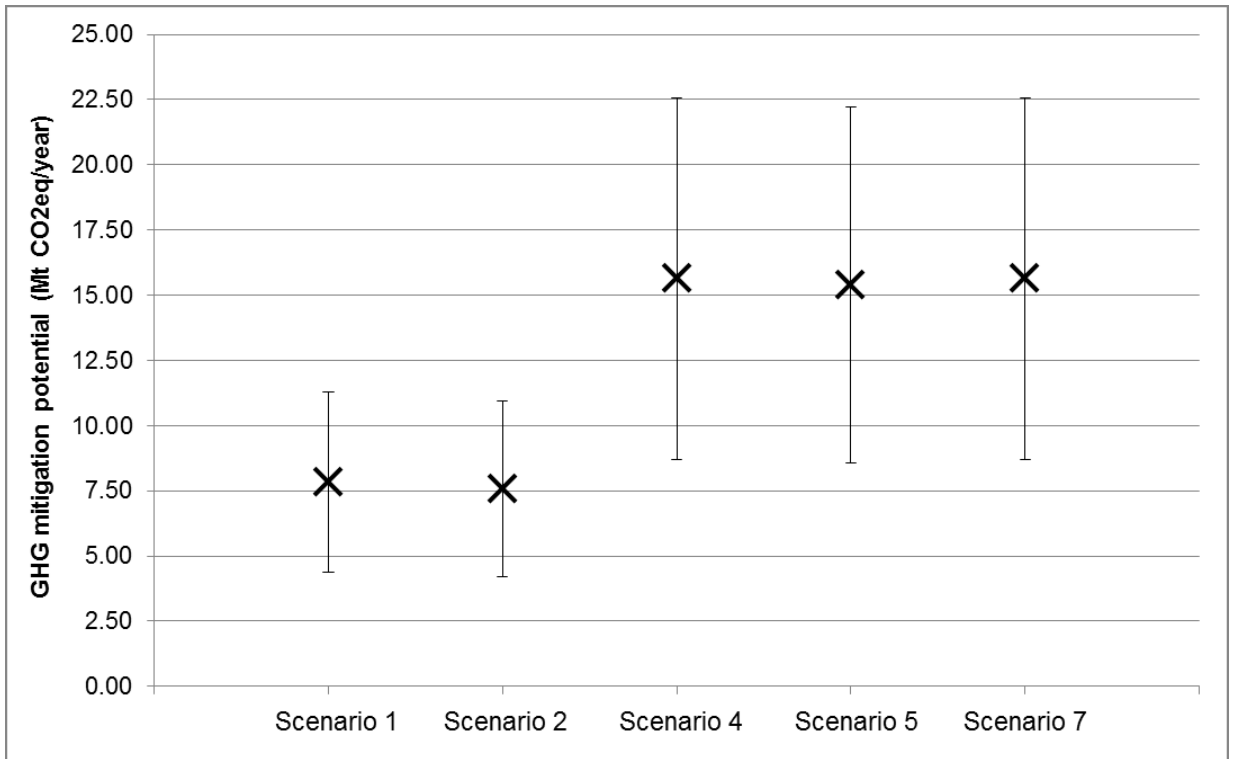


Figure 4.4: GHG mitigation potential of replacing SMR technology with SMR-CCS and UCG-CCS technologies for H₂ production in bitumen upgrading in western Canada. The upper limit corresponds to 100% SCO production (projected in 2022) by employing a hydroconversion-based bitumen upgrading configuration, whereas the lower limit corresponds to SCO production in a coking-based bitumen upgrader.

4.5. Conclusions

This study provides insight on the GHG abatement costs of replacing SMR technology with SMR-CCS and UCG-CCS technologies for H₂ production for bitumen upgrading in Alberta's oil sands. A number of valuable conclusions can be drawn from this analysis. First, the life cycle GHG emissions in a large-scale SMR-CCS-based H₂ production (6.024-6.758 kg-CO₂-eq/kg-H₂) are higher than in a large-scale UCG-CCS-based H₂ production (1.255-1.404 kg-CO₂-eq/kg-H₂). However, the life cycle GHG emissions in H₂ production without CCS from SMR (calculated as 11.237 kg-CO₂-eq/kg-H₂) are lower than in H₂ production from UCG without CCS (11.258 kg-CO₂-eq/kg-H₂). Second, the application of the CCS technology in a UCG-based pathway is more beneficial, both with regard to GHG abatement costs and potential, than in an SMR-based pathway. The GHG abatement costs are calculated to be 40.87-42.03 and 105.86-108.90 \$C/ tonne-CO₂-eq for UCG-CCS-based scenarios. For SMR-CCS-based scenarios the costs vary from 86.83-91.83 and 148.79-157.67 \$C/ tonne-CO₂-eq. However, CCS could play a major role in reducing the GHG emissions in the bitumen upgrading industry.

Third, sale of incremental flows of captured CO₂ for EOR operations in a UCG-CCS-based scenario (scenario 7) compared to the SMR-CCS alternative has the maximum advantage, and an opportunity for revenue generation is recognized. Fourth, for a fixed H₂ production scale, the GHG abatement costs are highly sensitive to the transportation distance of the captured CO₂ to a sequestration site. Finally, large-scale H₂ production from UCG-CCS for SCO production can help reduce Alberta's annual GHG emissions by 22.6 mega tonnes in 2022.

Chapter 5

Conclusions and Recommendations for Future Work

5.1. Conclusions

This study presented a model for a comprehensive evaluation of the energy balances involved in different unit operations to produce hydrogen from UCG-based syngas along with the integration of CCS technology, a model that is not found in existing studies in the literature. This holistic approach was adapted to develop and integrate a data-intensive process model – FUNNEL-EGY-H2-UCG (FUNDamental ENgineering PrinciplEs-based Model for Estimation of EnerGY consumption and production in hydrogen (H₂) production from Underground Coal Gasification) – with a spreadsheet-based LCA model – FUNNEL-GHG-H2-UCG (FUNDamental ENgineering PrinciplEs-based Model for Estimation of GreenHouse Gases in hydrogen (H₂) production from Underground Coal Gasification) – to estimate life cycle GHG emissions. An Aspen Plus model was developed for H₂ production from UCG-based syngas along with carbon capture using Selexol solvent and the co-production of steam and electricity.

In addition to the quantification of operational GHG emissions in the H₂ production, life cycle GHG emissions associated with drilling of UCG wells, H₂ and CO₂ pipeline transportation, and H₂ plant construction materials were evaluated by FUNNEL-GHG-H2-UCG. The flexibility of the FUNNEL-EGY-H2-UCG lies in the user's ability to

change the key UCG process parameters like coal type, injection ratio, injection feed rates, steam-to-carbon ratios, equipment efficiencies, etc., in the user friendly spreadsheet without entering into the process simulation environment in Aspen Plus. Moreover, qualitative and quantitative relationships between key UCG process variables and coal-to-H₂ conversion efficiency, coal-to-electricity efficiency, and life cycle GHG emissions were developed.

This study is helpful in characterizing the energy conversion efficiency and the life cycle GHG footprint of UCG as a H₂ production pathway, along with providing insight into UCG's competitiveness with other conventional options, i.e., SMR. Furthermore, GHG abatement costs and the mitigation potential of replacing SMR technology with SMR-CCS and UCG-CCS technologies for H₂ production to upgrade bitumen from the Canadian oil sands were estimated. This was done for several viable H₂ production scenarios applicable to western Canada.

A number of conclusions can be drawn from this research. Some of the main observations and conclusions include the following:

1. In a combined cycle UCG-syngas-based H₂ production plant configuration, the H₂ production pathway was found to be self-sufficient in terms of electricity and steam use, both with and without CCS. The net energy ratios were estimated to be 0.59 and 0.61 in H₂ production with and without CCS, respectively.

2. The life cycle GHG emissions for a small-scale UCG-syngas-based H₂ production plant (16.3 tonnes/day) with and without CCS were estimated to be 0.91 and 18.0 kg-CO₂-eq/kg-H₂, respectively. UCG-CCS was found to have a lower life cycle GHG emissions footprint in comparison to other conventional fossil fuel based H₂ production pathways (SCG, SCG-CCS, SMR and SMR-CCS).

3. In H₂ production from UCG with CCS, the life cycle GHG emissions increased slightly from 0.91 to 1.0 kg-CO₂-eq/kg-H₂ with a rise in the H₂O-to-O₂ injection ratio from 2 to 3. The increase in life cycle GHG emissions was also marginal (from 0.56 to 1.1 kg-CO₂-eq/kg-H₂) with a rise in the steam-to-carbon ratio from 2 to 4. In addition, the sensitivity analysis showed that the life cycle GHG emissions were most sensitive to the separation efficiency of the PSA unit and the efficiency of the heat exchangers.

4. The GHG abatement costs were calculated to be in the range 41-109 \$C/ tonne-CO₂-eq for UCG-CCS-based large-scale H₂ production (660 tonnes/day) scenarios depending on the transportation distance of the CCS site from the UCG-H₂ production plant. For SMR-CCS-based scenarios with a H₂ production of 607 tonnes/day, the costs varied from 87-158 \$C /tonne-CO₂-eq. When selling the CO₂ captured in the H₂ production plant (applicable in SMR-CCS and UCG-CCS) to an EOR operator was considered, it was found that not only were GHG abatement costs reduced but also an opportunity for revenue generation was realized in the UCG-CCS case.

5. There was no GHG abatement for implementing UCG without CCS for H₂ production; the life cycle GHG emissions are higher in UCG than in SMR with no CCS. However, CCS can play a significant role in reducing the GHG footprint of the bitumen upgrading industry; up to 22.6 Mt and 11.3 Mt of GHGs can be mitigated if H₂ were produced from UCG-CCS and SMR-CCS, respectively, for bitumen upgrading in 2022. The higher GHG mitigation potential of UCG-CCS was mainly because implementing a pre-combustion carbon capture scheme in UCG-based H₂ production led to higher carbon capture efficiency than in SMR-based H₂ production, ultimately leading to lower life cycle GHG emissions in the former case than the latter.

5.1.1. Research limitations

Following are some of the limitations of the research:

1. The life cycle assessment (LCA) model developed in this study evaluates only the global warming potential of the UCG-based H₂ production pathway. Other life cycle impact categories like land use, water use, human health, etc., are beyond the scope of this study.
2. The process model developed for the UCG process is based on the assumption that there is equilibrium between the constituent gases, surrounding rocks,

injection agents and ground water influx in the UCG cavity. The resolution of the dynamic nature of the UCG process is beyond the capacity of the model presented in this study. However, a sensitivity analysis of parameters like ground water influx, and syngas and heat losses in the UCG process is performed.

3. The life cycle GHG emissions associated with decommissioning of the UCG-syngas-based H₂ production plant equipment are not considered in the LCA. Furthermore, energy and material use associated with manufacturing of UCG injection and production wells are neglected due to lack of data.

5.2. Recommendations for future work

While the work carried out in this study is comprehensive in itself, further improvements in the current LCA model can be made. Moreover, the current model can be used to evaluate the environmental competitiveness of different products that can be produced from UCG-based syngas. The author recommends the following research work:

1. *UCG reservoir simulation*: The UCG process is highly dynamic with respect to syngas composition, pressure-temperature profiles in the cavity, cavity size and formation, etc. Moreover, the in situ coal seam life has a major role in the syngas quality. Therefore, it is imperative that the effect of these factors on the quality and quantity of syngas, which ultimately have an impact on the overall coal-to-H₂ conversion efficiency and life cycle GHG emissions, be determined. This can be

done through simulating the in situ coal reservoir in a computational fluid dynamics environment (like ANSYS, FLUENT) or in a thermal reservoir simulator (like Computer Modeling Group Ltd.'s STARS).

2. *LCA and techno-economic analysis of products (other than H₂) derived from UCG-based syngas:* The current scope of the study involved only H₂ as a product of the syngas produced from UCG. However, there are other useful products – electricity, liquid fuels, steam, etc. – that can be produced from the UCG-based syngas. An LCA and techno-economic study of these UCG-derived products along with consideration of CCS can be useful in evaluating their competitiveness with other conventional pathways. That being said, the existing Aspen Plus model can be used and modified depending upon the plant configuration and unit operations to produce these energy products.
3. *Improvements in the current simulation model:* The present Aspen Plus model can be improved by considering a detailed heat exchanger network for the waste heat recovered from different processes for steam and electricity co-production in the H₂ production pathway from UCG. This will be helpful in the overall energy management and optimization of the coal-to-H₂ conversion efficiency. Second, process equipment like air separation unit (ASU) for O₂ production, and Claus unit for sulphur removal, which are not modeled in the current simulation environment, can be modeled and integrated to increase the robustness of the current model.

4. *Development of a bottom-up Aspen Plus model for H₂ production from steam methane reforming:* The present results of life cycle GHG emissions in SMR-based H₂ production with carbon capture can be improved by developing a comprehensive and a bottom up simulation model in Aspen Plus. This will also allow flexibility to simulate different configurations of carbon capture – pre-combustion, post-combustion, etc. In addition, the developed model can also be integrated with bitumen upgrading process model as a retrofit option, which will help analyze scenarios for energy management and carbon capture.

5. *Consideration of different solvents and configurations in carbon capture:* In the present model, Selexol solvent is used for CO₂ capture before the combustion of the purge gas in the combined cycle plant. However, considerations of other amine- and alcohol-based solvents like MEA, MDEA, methanol, etc., and configurations like post-combustion CO₂ capture will enhance the scope of the study. This will help in analyzing the environmental and economic competitiveness of these additional schemes in H₂ production from SMR and UCG.

References

- [1] Murray R Gray. Tutorial on Upgrading of Oilsands Bitumen. Accessed: Aug 2014.
Available at:
<http://www.ualberta.ca/~gray/Links%20&%20Docs/Web%20Upgrading%20Tutorial.pdf>.
- [2] Gemayel JE, Macchi A, Hughes R, Anthony EJ. Simulation of the integration of a bitumen upgrading facility and an IGCC process with carbon capture. *Fuel*. 2014;117, Part B(0):1288-97.
- [3] Munteanu MC, Chen J. Optimizing Bitumen Upgrading Scheme –Modeling and Simulation Approach. CanmetENERGY. 2012 AIChE Spring Meeting. Available at:
<http://www.aiche-fpd.org/listing/125.pdf>. 2012.
- [4] Canadian Association of Petroleum Producers (CAPP). Crude oil: forecasts, markets and transportation. Available at:
<http://www.capp.ca/getdoc.aspx?DocId=247759&DT=NTV>. June 2014.
- [5] Energy Resources Conservation Board. ST98-2013. Alberta's Energy Reserves 2012 and Supply/Demand Outlook 2013–2022. May 2013. Available at:
<http://www.aer.ca/documents/sts/ST98/ST98-2013.pdf>.
- [6] Wang M. GREET, Model 4.02a; Argonne National Laboratory, U.S. Department of Energy. 2012.
- [7] Cetinkaya E, Dincer I, Naterer GF. Life cycle assessment of various hydrogen production methods. *International Journal of Hydrogen Energy*. 2012;37(3):2071-80.

- [8] Dufour J, Serrano DP, Gálvez JL, González A, Soria E, Fierro JLG. Life cycle assessment of alternatives for hydrogen production from renewable and fossil sources. *International Journal of Hydrogen Energy*. 2012;37(2):1173-83.
- [9] Granovskii M, Dincer I, Rosen MA. Exergetic life cycle assessment of hydrogen production from renewables. *Journal of Power Sources*. 2007;167(2):461-71.
- [10] Spath P, Mann M. Life Cycle Assessment of Hydrogen Production via Natural Gas Steam Reforming. NREL/TP-570-27637; 2005.
- [11] Olateju B, Kumar A. Techno-economic assessment of hydrogen production from underground coal gasification (UCG) in Western Canada with carbon capture and sequestration (CCS) for upgrading bitumen from oil sands. *Applied Energy*. 2013;111(0):428-40.
- [12] Cole S, Itani S. The Alberta Carbon Trunk Line and the Benefits of CO₂. *Energy Procedia*. 2013;37(0):6133-9.
- [13] Alberta Government. Alberta's Clean Energy Future. Climate Change. Available at: http://www.oilsands.alberta.ca/FactSheets/CCChange_FSht_Sep_2013_Online.pdf. 2013.
- [14] Government of Canada. Oil Sands: A strategic resource for Canada, North America and the global market. GHG Emissions. Available at: http://www.nrcan.gc.ca/sites/www.nrcan.gc.ca/files/energy/pdf/eneene/pubpub/pdf/12-0607-OS-GHG_Emissions_us-eng.pdf. Accessed: Aug 2014.
- [15] Beaton A, Langenberg W, Pană C. Coalbed methane resources and reservoir characteristics from the Alberta Plains, Canada. *International Journal of Coal Geology*. 2006;65(1-2):93-113.

- [16] Beaton A, Pana C, Chen D, Wynne D, Langenberg CW. Coalbed methane potential of Upper Cretaceous- Tertiary strata, Alberta Plains. Alberta Energy and Utilities Board, EUB/AGS Earth Sciences Report 2002-06. 2002.
- [17] Richardson RJ. Alberta's 2 Trillion Tonnes Of 'Unrecognized' Coal. Available at: eipa.alberta.ca/media/43006/alberta_2_trillion_tonnes_coal.pdf. 2010.
- [18] Energy Resources Conservation Board. Alberta's energy reserves 2008 and supply/demand outlook 2009–2017. Available at: <http://www.aer.ca/documents/sts/ST98/st98-2009.pdf>. 2009.
- [19] Pana C. Review of Underground Coal Gasification with Reference to Alberta's Potential. Energy Resources Conservation Board. Alberta Geological Survey. 2009.
- [20] Burton E, Friedmann J, Upadhye R. Best practices in underground coal gasification. Contract W-7405-Eng-48. Livermore, CA: Lawrence Livermore National Laboratory. 2006.
- [21] Gregg DW, Edgar TF. Underground coal gasification. *AIChE Journal*. 1978;24(5):753-81.
- [22] Bhutto AW, Bazmi AA, Zahedi G. Underground coal gasification: From fundamentals to applications. *Progress in Energy and Combustion Science*. 2013;39(1):189-214.
- [23] Khadse A, Qayyumi M, Mahajani S, Aghalayam P. Underground coal gasification: A new clean coal utilization technique for India. *Energy*. 2007;32(11):2061-71.
- [24] Friedmann SJ, Upadhye R, Kong F-M. Prospects for underground coal gasification in carbon-constrained world. *Energy Procedia*. 2009;1(1):4551-7.

- [25] Roddy DJ, Younger PL. Underground coal gasification with CCS: a pathway to decarbonising industry. *Energy & Environmental Science*. 2010;3(4):400-7.
- [26] Self S, Reddy B, Rosen M. Review of underground coal gasification technologies and carbon capture. *Int J Energy Environ Eng*. 2012;3(1):1-8.
- [27] Swan Hills SynFuels. Swan Hills In-Situ Coal Gasification Technology Development. Final Outcomes Report. Prepared for: Alberta Innovates – Energy and Environment Solutions. Available at: http://www.ai-ees.ca/media/6876/swan_hills.pdf 2012.
- [28] Khoo HH, Tan RBH. Life cycle investigation of CO₂ recovery and sequestration. *Environmental Science and Technology*. 2006;40(12):4016-24.
- [29] Natural Resources Canada, Government of Alberta. Accessed: August, 2014. Available at: <https://www.nrcan.gc.ca/energy/funding/current-funding-programs/4951>.
- [30] Alberta Carbon Capture and Storage Development Council. Accelerating Carbon Capture and Storage in Alberta, Final Report. March 2009. Available at: http://www.energy.alberta.ca/Org/pdfs/CCS_Implementation.pdf.
- [31] Mitrović M, Malone A. Carbon capture and storage (CCS) demonstration projects in Canada. *Energy Procedia*. 2011;4(0):5685-91.
- [32] Nakaten N, Schlüter R, Azzam R, Kempka T. Development of a techno-economic model for dynamic calculation of cost of electricity, energy demand and CO₂ emissions of an integrated UCG–CCS process. *Energy*. 2014;66(0):779-90.
- [33] Saygin D, van den Broek M, Ramírez A, Patel MK, Worrell E. Modelling the future CO₂ abatement potentials of energy efficiency and CCS: The case of the Dutch industry. *International Journal of Greenhouse Gas Control*. 2013;18(0):23-37.

- [34] Koroneos C, Dompros A, Roumbas G, Moussiopoulos N. Life cycle assessment of hydrogen fuel production processes. *International Journal of Hydrogen Energy*. 2004;29(14):1443-50.
- [35] Udo de Haes HA, Heijungs R. Life-cycle assessment for energy analysis and management. *Applied Energy*. 2007;84(7–8):817-27.
- [36] Wagner U, Geiger B, Schaefer H. Energy life cycle analysis of hydrogen systems. *International Journal of Hydrogen Energy*. 1998;23(1):1-6.
- [37] Ozbilen A, Dincer I, Rosen MA. Life cycle assessment of hydrogen production via thermochemical water splitting using multi-step Cu–Cl cycles. *Journal of Cleaner Production*. 2012;33(0):202-16.
- [38] International Organization for Standardization. ISO 14040:2006 and ISO 14044:2006: environmental management – life cycle assessment – principles and framework.
- [39] Brown MA. Market failures and barriers as a basis for clean energy policies. *Energy Policy*. 2001;29(14):1197-207.
- [40] Xiao H, Wei Q, Wang H. Marginal abatement cost and carbon reduction potential outlook of key energy efficiency technologies in China's building sector to 2030. *Energy Policy*. 2014;69(0):92-105.
- [41] Yang L, Zhang X, Liu S, Yu L, Zhang W. Field test of large-scale hydrogen manufacturing from underground coal gasification (UCG). *International Journal of Hydrogen Energy*. 2008;33(4):1275-85.
- [42] Rogut J, Steen M. Hydrogen oriented underground gasification of coal. 25th Annual International Pittsburgh Coal Conference, PCC - Proceedings. 2008;2:873-80

- [43] Prabu V, Jayanti S. Integration of underground coal gasification with a solid oxide fuel cell system for clean coal utilization. *International Journal of Hydrogen Energy*. 2012;37(2):1677-88.
- [44] Nourozieh H, Kariznovi M, Chen Z, Abedi J. Simulation Study of Underground Coal Gasification in Alberta Reservoirs: Geological Structure and Process Modeling. *Energy Fuels*. 2010;24:3540–50.
- [45] Chiesa P, Consonni S. Shift reactors and physical absorption for low-CO₂ emission IGCCs. *J Eng Gas Turb Power*. 1999;121:295-305.
- [46] Chiesa P, Consonni S, Kreutz T, Robert W. Co-production of hydrogen, electricity and CO₂ from coal with commercially ready technology. Part A: Performance and emissions. *International Journal of Hydrogen Energy*. 2005;30(7):747-67.
- [47] Cormos C-C. Integrated assessment of IGCC power generation technology with carbon capture and storage (CCS). *Energy*. 2012;42(1):434-45.
- [48] Damen K, Troost Mv, Faaij A, Turkenburg W. A comparison of electricity and hydrogen production systems with CO₂ capture and storage. Part A: Review and selection of promising conversion and capture technologies. *Progress in Energy and Combustion Science*. 2006;32(2):215-46.
- [49] Doctor RD, Molburg JC, Chess KL, Brockmeier NF, Thimmapuram PR. Hydrogen production and CO₂ recovery, transport and use from a KRW oxygen-blown gasification combined-cycle system. Argonne National Laboratory draft report, May 1999.
- [50] Doctor RD , Molburg JC , Thimmapuram PR KRW Oxygen-Blown Gasification Combined Cycle: Carbon Dioxide Recovery, Transport, and Disposal. Energy Systems Division, Argonne National Laboratory. ANL/ESD-34. 1996.

- [51] G.H.G. IEA. Decarbonisation of fossil fuels. International Energy Agency Greenhouse Gas R&D Programme, Cheltenham. 1996.
- [52] Klett MG, White JS, Schoff RL, Buchanan TL. Hydrogen production facilities. Plant performance and cost comparisons. Prepared for US DOE/NETL under subcontract 990700362, Task 50802 by Parsons Infrastructure and Technology Group Inc, 2002.
- [53] Li M, Rao AD, Scott Samuelsen G. Performance and costs of advanced sustainable central power plants with CCS and H₂ co-production. *Applied Energy*. 2012;91(1):43-50.
- [54] Mansouri Majoumerd M, De S, Assadi M, Breuhaus P. An EU initiative for future generation of IGCC power plants using hydrogen-rich syngas: Simulation results for the baseline configuration. *Applied Energy*. 2012;99(0):280-90.
- [55] National Research Council. The hydrogen economy. Opportunities, costs, barriers, and R&D needs. National Academic Press, Washington 2004.
- [56] Simbeck DR. Hydrogen costs with CO₂ capture. Seventh international conference on greenhouse gas control technologies, Vancouver, Canada. 2004.
- [57] Lee J-Y, Yu M-S, Cha K-H, Lee S-Y, Lim TW, Hur T. A study on the environmental aspects of hydrogen pathways in Korea. *International Journal of Hydrogen Energy*. 2009;34(20):8455-67.
- [58] Ozbilen A, Dincer I, Rosen MA. Comparative environmental impact and efficiency assessment of selected hydrogen production methods. *Environmental Impact Assessment Review*. 2013;42(0):1-9.
- [59] Ruether. J, Ramezan. M, Grol. E. Life-Cycle Analysis of Greenhouse Gas Emissions for Hydrogen Fuel Production in The United States from LNG and Coal. National Energy Technology Laboratory. DOE/NETL-2006/1227. 2005.

- [60] Pereira SR, Coelho MC. Life cycle analysis of hydrogen – A well-to-wheels analysis for Portugal. *International Journal of Hydrogen Energy*. 2013;38(5):2029-38.
- [61] Dufour J, Serrano DP, Gálvez JL, Moreno J, García C. Life cycle assessment of processes for hydrogen production. Environmental feasibility and reduction of greenhouse gases emissions. *International Journal of Hydrogen Energy*. 2009;34(3):1370-6.
- [62] Smitkova M, Janíček F, Riccardi J. Life cycle analysis of processes for hydrogen production. *International Journal of Hydrogen Energy*. 2011;36(13):7844-51.
- [63] O'Brien D, Shalloo L, Crosson P, Donnellan T, Farrelly N, Finnan J, et al. An evaluation of the effect of greenhouse gas accounting methods on a marginal abatement cost curve for Irish agricultural greenhouse gas emissions. *Environmental Science & Policy*. 2014;39(0):107-18.
- [64] Garg A, Shukla PR, Maheshwari J, Upadhyay J. An assessment of household electricity load curves and corresponding CO₂ marginal abatement cost curves for Gujarat state, India. *Energy Policy*. 2014;66(0):568-84.
- [65] Telsnig T, Tomaschek J, Özdemir ED, Bruchof D, Fahl U, Eltrop L. Assessment of selected CCS technologies in electricity and synthetic fuel production for CO₂ mitigation in South Africa. *Energy Policy*. 2013;63(0):168-80.
- [66] Molburg JC, Doctor RC. Hydrogen from steam-methane reforming with CO₂ capture. Argonne National Laboratory. Available at: <http://seca.doe.gov/technologies/ccbt/refs/argonne/papers/pgh/hydrogen%20from%20steam%20methane%20reforming%20for%20carbon%20dioxide%20cap.pdf>; June 2003.

- [67] Kariznovi M, Nourozieh H, Abedi J, Chen Z. Simulation study and kinetic parameter estimation of underground coal gasification in Alberta reservoirs. *Chemical Engineering Research and Design*. 2013;91(3):464-76.
- [68] Thorsness CB, Hill RW, Britten JA. Execution and performance of the CRIP process during the rocky mountain I UCG field test. Contract No.: UCRL-98641. Berkeley, CA: Lawrence Livermore National Laboratory (LLNL).1988.
- [69] Yang LH. A Review of the Factors Influencing the Physicochemical Characteristics of Underground Coal Gasification. *Energy Sources, Part A: Recovery, Utilization, and Environmental Effects*. 2008;30(11):1038-49.
- [70] Smith G, Cameron A, Bustin R. Coal resources of the western Canadian sedimentary Basin. *Geological Atlas of the Western Canada Sedimentary Basin*. Alberta Geological Survey. Available at:
http://www.ags.gov.ab.ca/publications/SPE/PDF/SPE_004/chapter_33.pdf.
- [71] Stańczyk K, Kapusta K, Wiatowski M, Świądrowski J, Smoliński A, Rogut J, et al. Experimental simulation of hard coal underground gasification for hydrogen production. *Fuel*. 2012;91(1):40-50.
- [72] Seifi M, Chen Z, Abedi J. Numerical simulation of underground coal gasification using the CRIP method. *The Canadian Journal of Chemical Engineering*. 2011;89(6):1528-35.
- [73] Merrick D. Mathematical models of the thermal decomposition of coal: 1. The evolution of volatile matter. *Fuel*. 1983;62(5):534-9.
- [74] Bucklin RW, Schendel RL. Comparison of Fluor Solvent and Selexol process. *Energy progress*. 1984;4(3):137-42.

- [75] Abella JP, Bergerson JA. Model to Investigate Energy and Greenhouse Gas Emissions Implications of Refining Petroleum: Impacts of Crude Quality and Refinery Configuration. *Environmental Science & Technology*. 2012;46(24):13037-47.
- [76] McCollum DL, Ogden JM. Techno-economic models for carbon dioxide compression, transport and storage & correlations for estimating carbon dioxide density and viscosity. Institute of Transportation Studies, University of California, Davis (2006).
- [77] Hertwich EG, Aaberg M, Singh B, Strømman AH. Life-cycle Assessment of Carbon Dioxide Capture for Enhanced Oil Recovery. *Chinese Journal of Chemical Engineering*. 2008;16(3):343-53.
- [78] Amos WA. Costs of Storing and Transporting Hydrogen. National Renewable Energy Laboratory. NREL/TP-570-25106. 1998.
- [79] Ogden JM. Conceptual Design of Optimized Fossil Energy Systems with Capture and Sequestration of Carbon Dioxide; DOE Award Number: DE-FC26-02NT41623. 2004.
- [80] Nakaten N, Kötting P, Azzam R, Kempka T. Underground Coal Gasification and CO₂ Storage Support Bulgaria's Low Carbon Energy Supply. *Energy Procedia*. 2013;40(0):212-21.
- [81] Brandt AR. Oil depletion and the energy efficiency of oil production: The case of California. *Sustainability*. 2011;3: 1833–54.
- [82] Heddle G, Herzog H, Klett M. The Economics of CO₂ Storage. Massachusetts Institute of Technology, Laboratory for Energy and the Environment; MIT LFEE 2003-003 RP; 2003.

[83] Serpa J, Morbee J, Tzimas E. Technical and Economic Characteristics of a CO₂ Transmission Pipeline Infrastructure; European Commission Joint Research Centre Institute for Energy;. 2011.

[84] Demofonti G, Spinelli CM. Technical challenges facing the transport of anthropogenic CO₂ by pipeline for carbon capture and storage purposes; PTC 6th Pipeline Technology Conference. 2011.

[85] Vermeer. T555 COMMANDER® 3 Tractor. Available at:
http://www2.vermeer.com/vermeer/NA/en/N/equipment/trenchers_pipeline/t555iii.
Accessed: December 2013.

[86] Gunter B, Longworth H. Overcoming the Barriers to Commercial CO₂-EOR in Alberta, Canada; Prepared for Alberta Innovates Energy and Environment Solutions. 2013.

[87] Hussain D, Dzombak DA, Jaramillo P, Lowry GV. Comparative lifecycle inventory (LCI) of greenhouse gas (GHG) emissions of enhanced oil recovery (EOR) methods using different CO₂ sources. International Journal of Greenhouse Gas Control. 2013;16(0):129-44.

[88] Encana. Life of the Well. Available at:
<http://www.encana.com/pdf/communities/usa/LifeOfTheWell2011.pdf>. Accessed:
December 2013. 2011.

[89] Remp LH. DOE Hydrogen Pipeline Working Group Workshop. Air Products. Available at:
https://www1.eere.energy.gov/hydrogenandfuelcells/pdfs/hpwgw_airprod_remp.pdf.
2005.

- [90] Savage B. Memorandum. Notice of Change for Emission Factor for Increased Grid Electricity Usage. Government of Alberta, Environment and Water Available at: <http://environmentgovabca/info/library/8429pdf>. 2011.
- [91] International Energy Agency (IEA). IEA Greenhouse Gas R&D Programme: decarbonisation of fossil fuels. Report PH2/2. 1996.
- [92] Carrara A, Perdichizzi A, Barigozzi G. Pd–Ag dense membrane application to improve the energetic efficiency of a hydrogen production industrial plant. *International Journal of Hydrogen Energy*. 2011;36(9):5311-20.
- [93] Kim TS. Comparative analysis on the part load performance of combined cycle plants considering design performance and power control strategy. *Energy*. 2004;29(1):71-85.

Appendix A

Aspen Plus Simulation Model

This appendix consists of screenshots of the Aspen Plus flow sheets developed for H₂ production from UCG with and without CCS. All the data (temperature, pressure, mass flow, heat flow, work flow, etc.) pertaining to material, heat and work streams in various flow sheets hold true for both scenarios – H₂ production with CCS and H₂ production without CCS.

The flow sheet is designed in such a way that the overall H₂ production pathway is subdivided into various hierarchy blocks. Each hierarchy block represents a unit operation in the H₂ production pathway. Figure A.1 shows the parent simulation flow sheet with eight hierarchy blocks representing different unit operations of the H₂ production pathway. The Table A.1 below enlists the features of the eight hierarchy blocks along with the property method used in simulating the unit operation. The specifications of key equipment and material stream flow rates (e.g. coal specification, efficiencies, flow rate of gasifying agents, steam-to-carbon ratio, H₂O-to-O₂ injection ratio, etc.) in these hierarchy blocks are input through MS Excel with the use of Aspen Simulation Workbook. Moreover, the results are extracted from the Aspen flow sheet environment to a MS Excel spreadsheet model for evaluating life cycle GHG emissions, H₂ compressor power requirement, CO₂ pipeline design, etc.

Table A.1: Hierarchy blocks of the Aspen Plus simulation model

S No.	Block Name	Property Method	Description
Hierarchy Block 1	INJECTIO	PENG- ROB	Consists of O ₂ compression and H ₂ O pumping, which are fed into the UCG cavity through the injection well
Hierarchy Block 2	UCG	PENG- ROB	Consists of injection of gasifying agents: H ₂ O and O ₂ , gasification of coal with the gasifying agents. Ground water influx and temperature decrease due to heat loss to the surrounding strata are also considered
Hierarchy Block 3	PIPE-EXP	PENG- ROB	Consists of syngas expansion and cooling
Hierarchy Block 4	AGR	PC-SAFT	Consists of H ₂ S removal using Selexol before syngas reforming
Hierarchy Block 5	SMR-WGSR	PENG- ROB	Consists of syngas reforming, water gas shift reactions
Hierarchy Block 6	CO2-CAP	PC-SAFT	Consists of capture of CO ₂ using Selexol, compression using five stages, PSA unit
Hierarchy	GT-PGBUR	PENG-	Consists of purge gas burner, along

Block 7		ROB	with electricity production by gas turbine
Hierarchy		PENG-	Consists of steam generation section
Block 8	HRSG-ST	ROB	along with electricity production by steam turbines

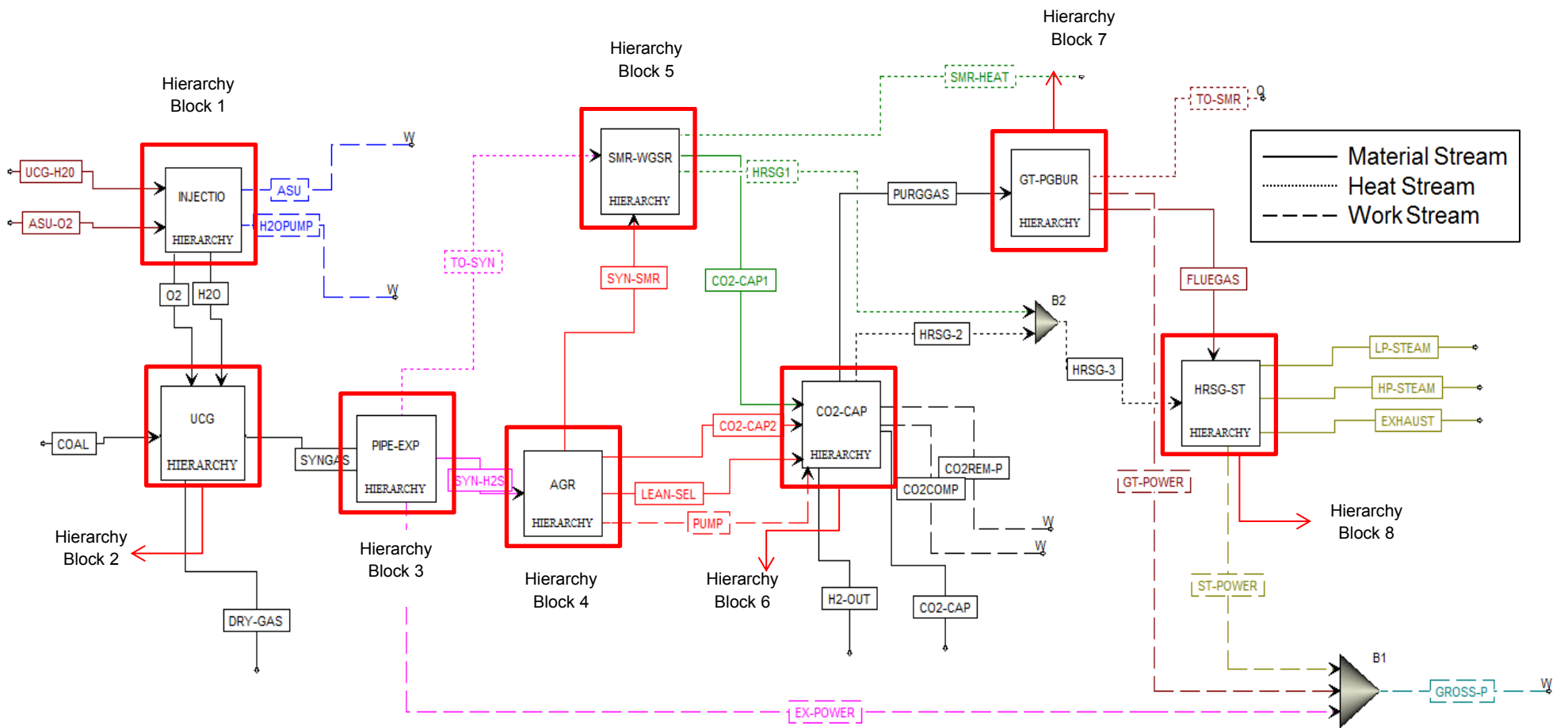


Figure A.1: Parent Aspen Plus simulation flow sheet for H₂ production from UCG. It consists of eight sub-simulation flow sheets called as hierarchy blocks, each of which is exploded in figures below.

Table A.2a: Material streams in parent simulation flow sheet

Stream Name	ASU-O2	UCG-H2O	H2O	O2	COAL¹	DRY-GAS	SYNGAS	SYN-H2S	SYN-SMR
Temperature, C	20.0	25.0	26.2	20.0	650.0	25.0	837.2	25.0	9.9
Pressure, bar	1.0	1.0	140.0	200.0	115.0	1.0	106.0	30.0	30.0
Total Mole Flow, kmol/hr	58.6	312.2	312.2	58.6	333.9	429.6	640.2	418.9	400.6
Total Mass Flow, kg/hr	1875.0	5625.0	5625.0	1875.0	4346.4	9926.6	13721.4	9734.4	8985.8
Mass Flow, kg/hr									
CH4	0.0	0.0	0.0	0.0	204.8	1141.7	1141.7	1141.7	1125.5
CO2	0.0	0.0	0.0	0.0	72.6	5959.0	5959.1	5958.1	5273.7
CO	0.0	0.0	0.0	0.0	149.6	2340.3	2340.3	2340.3	2328.8
H2	0.0	0.0	0.0	0.0	21.6	257.1	257.1	257.1	256.8
H2S	0.0	0.0	0.0	0.0	28.3	28.3	28.3	28.2	0.3
H2O	0.0	5625.0	5625.0	0.0	611.4	199.6	3994.4	8.5	0.3
C2H6	0.0	0.0	0.0	0.0	51.8	0.5	0.5	0.5	0.5
N2	0.0	0.0	0.0	0.0	0.0	0.0	0.0	0.0	0.0
DEPG	0.0	0.0	0.0	0.0	0.0	0.0	0.0	0.0	0.0
OXYGEN	1875.0	0.0	0.0	1875.0	0.0	0.0	0.0	0.0	0.0

Stream Name	ASU-O2	UCG-H2O	H2O	O2	COAL ¹	DRY-GAS	SYNGAS	SYN-H2S	SYN-SMR
ARGON	0.0	0.0	0.0	0.0	0.0	0.0	0.0	0.0	0.0
CARBON	0.0	0.0	0.0	0.0	3206.4	0.0	0.0	0.0	0.0

¹ Coal is characterized in the form of its constituents after its pyrolysis

Table A.2b: Material streams in parent simulation flow sheet

Stream Name	CO2-CAP1	CO2-CAP2	LEAN-SEL	CO2-CAP	H2-OUT	PURGGAS	FLUEGAS	HP-STEAM	LP-STEAM	EXHAUST
Temperature, C	25.0	12.8	25.0	25.0	25.0	-2.0	685.5	509.9	302.7	100.0
Pressure, bar	24.0	7.0	1.0	150.0	19.5	1.5	1.1	30.0	6.0	1.1
Total Mole Flow, kmol/hr	644.9	7.0	47.3	231.6	315.3	84.3	616.6	459.9	2.9	616.6
Total Mass Flow, kg/hr	11888.6	272.3	13234.4	9976.7	635.6	637.2	16888.5	8285.8	51.9	16888.5
Mass Flow, kg/hr										
CH4	458.2	13.5	0.0	98.3	0.0	373.2	0.0	0.0	0.0	0.0
CO2	10533.7	246.0	0.0	9869.8	0.0	0.0	1274.5	0.0	0.0	1274.5
CO	146.9	10.8	0.0	5.9	0.0	151.8	0.0	0.0	0.0	0.0
H2	749.4	0.3	0.0	2.0	635.6	112.2	0.0	0.0	0.0	0.0
H2S	0.3	1.3	0.0	0.5	0.0	0.0	0.0	0.0	0.0	0.0
H2O	0.0	0.4	0.0	0.1	0.0	0.0	2038.7	8285.8	51.9	2038.7

Stream Name	CO2-CAP1	CO2-CAP2	LEAN-SEL	CO2-CAP	H2-OUT	PURGGAS	FLUEGAS	HP-STEAM	LP-STEAM	EXHAUST
C2H6	0.0	0.0	0.0	0.0	0.0	0.0	0.0	0.0	0.0	0.0
N2	0.0	0.0	0.0	0.0	0.0	0.0	11678.4	0.0	0.0	11678.4
DEPG	0.0	0.0	13234.4	0.0	0.0	0.0	0.0	0.0	0.0	0.0
OXYGEN	0.0	0.0	0.0	0.0	0.0	0.0	1623.6	0.0	0.0	1623.6
ARGON	0.0	0.0	0.0	0.0	0.0	0.0	273.3	0.0	0.0	273.3
CARBON	0.0	0.0	0.0	0.0	0.0	0.0	0.0	0.0	0.0	0.0

Table A.3: Heat streams in parent simulation flow sheet

Stream Name	HRSG-2	HRSG-3	HRSG1	SMR-HEAT	TO-SMR	TO-SYN
QCALC ¹ , Gcal/hr	0.82	7.32	6.50	-3.07	3.07	3.59

¹ Negative value indicates heat input; positive value indicates heat output

Table A.4: Work streams in parent simulation flow sheet

Stream Name	ASU	CO2COM	CO2REM-	EX-	GROSS-	GT-	H2OPUM	PUM	ST-
		P	P	POWER	P	POWER	P	P	POWER

POWER¹,	550.4	929.9	1115.70	-1630.10	-4609.29	-1341.62	29.13	5.45	-1637.57
kW	5								

¹ Negative value indicates power output; positive value indicates power input

Table A.5: Block types in the parent Aspen Plus model

Block Name	Type
AGR, CO2-CAP, GT-PGBUR, HRSG-ST, INJECTIO, PIPE-EXP, SMR-WGSR, UCG	Hierarchy
B1, B2	Mixer

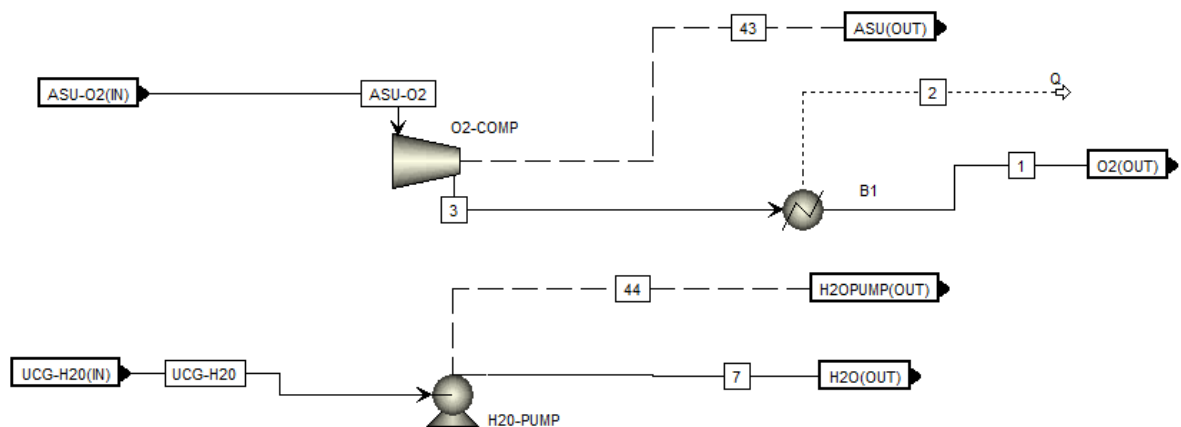


Figure A.2: Process flow diagram – Hierarchy Block 1: INJECTIO

Table A.6: Material streams in Hierarchy Block 1

Stream Name	1	3	7	ASU-O2	UCG-H2O
Temperature, C	20.0	1022.9	26.2	20.0	25.0
Pressure, bar	200.0	200.0	140.0	1.0	1.0
Total Mass Flow, kg/hr	1875.0	1875.0	5625.0	1875.0	5625.0
Mass Flow, kg/hr					
CH4	0.0	0.0	0.0	0.0	0.0
CO2	0.0	0.0	0.0	0.0	0.0
CO	0.0	0.0	0.0	0.0	0.0
H2	0.0	0.0	0.0	0.0	0.0
H2S	0.0	0.0	0.0	0.0	0.0
H2O	0.0	0.0	5625.0	0.0	5625.0
C2H6	0.0	0.0	0.0	0.0	0.0

Stream Name	1	3	7	ASU-O2	UCG-H2O
N2	0.0	0.0	0.0	0.0	0.0
DEPG	0.0	0.0	0.0	0.0	0.0
OXYGEN	1875.0	1875.0	0.0	1875.0	0.0
ARGON	0.0	0.0	0.0	0.0	0.0
CARBON	0.0	0.0	0.0	0.0	0.0

Table A.7: Work streams in Hierarchy Block 1

	43	44
POWER kW	550.4458	29.13168

Table A.8: Block types in Hierarchy Block 1

Block Name	Type
B1	Heater
H2O-PUMP	Pump
O2-COMP	Compr

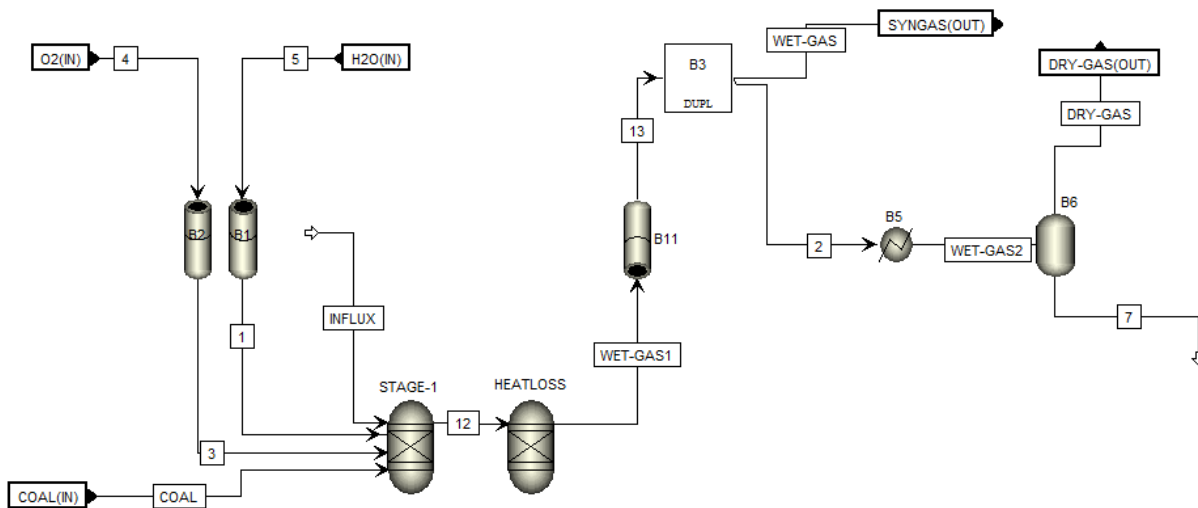


Figure A.3: Process flow diagram – Hierarchy Block 2: UCG

Table A.9: Material streams in Hierarchy Block 2

Stream Name	1	3	7	COAL	INFLUX	WET-GAS1	WET-GAS	DRY-GAS
Temperature, C	26.4	36.0	25.0	650.0	60.0	837.2	837.2	25.0
Pressure, bar	276.3	241.5	1.0	115.0	115.0	115.0	106.0	1.0
Mass Flow, kg/hr	5625.0	1875.0	3794.8	4346.4	1875.0	13721.4	13721.4	9926.6
Mass Flow, kg/hr								
CH4	0.0	0.0	0.0	204.8	0.0	1141.7	1141.7	1141.7
CO2	0.0	0.0	0.0	72.6	0.0	5959.1	5959.1	5959.0
CO	0.0	0.0	0.0	149.6	0.0	2340.3	2340.3	2340.3
H2	0.0	0.0	0.0	21.6	0.0	257.1	257.1	257.1
H2S	0.0	0.0	0.0	28.3	0.0	28.3	28.3	28.3
H2O	5625.0	0.0	3794.8	611.4	1875.0	3994.4	3994.4	199.6
C2H6	0.0	0.0	0.0	51.8	0.0	0.5	0.5	0.5
N2	0.0	0.0	0.0	0.0	0.0	0.0	0.0	0.0

Stream Name	1	3	7	COAL	INFLUX	WET-GAS1	WET-GAS	DRY-GAS
DEPG	0.0	0.0	0.0	0.0	0.0	0.0	0.0	0.0
OXYGEN	0.0	1875.0	0.0	0.0	0.0	0.0	0.0	0.0
ARGON	0.0	0.0	0.0	0.0	0.0	0.0	0.0	0.0
CARBON	0.0	0.0	0.0	3206.4	0.0	0.0	0.0	0.0

Table A.10: Block types in Hierarchy Block 2

Block Name	Type
B1, B2, B11	Pipe
B3	Dupl
B5	Heater
B6	Flash2
HEATLOSS, STAGE-1	RGibbs

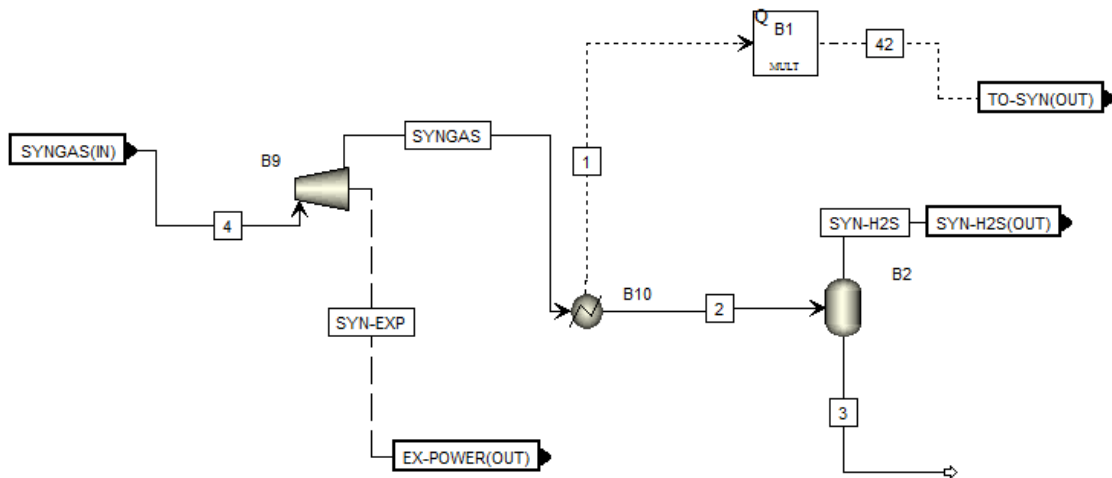


Figure A.4: Process flow diagram – Hierarchy Block 3: PIPE-EXP

Table A.11: Material streams in Hierarchy Block 3

Stream Name	SYNGAS	2	3	SYN-H2S
Temperature, C	629.4	25.0	25.0	25.0
Pressure, bar	30.0	30.0	30.0	30.0
Vapor Fraction	1.0	0.7	0.0	1.0
Total Flow, kg/hr	13721.4	13721.4	3987.1	9734.4
Mass Flow, kg/hr				
CH4	1141.7	1141.7	0.0	1141.7
CO2	5959.1	5959.1	1.0	5958.1
CO	2340.3	2340.3	0.0	2340.3
H2	257.1	257.1	0.0	257.1
H2S	28.3	28.3	0.2	28.2
H2O	3994.4	3994.4	3985.9	8.5
C2H6	0.5	0.5	0.0	0.5
N2	0.0	0.0	0.0	0.0
DEPG	0.0	0.0	0.0	0.0
OXYGEN	0.0	0.0	0.0	0.0
ARGON	0.0	0.0	0.0	0.0
CARBON	0.0	0.0	0.0	0.0

Table A.12: Heat streams in Hierarchy Block 3

Stream Name	1	42
QCALC,	6.0	3.6
Gcal/hr		

Table A.13: Work streams in Hierarchy Block 3

Stream Name	SYN-EXP
POWER kW	-1630.1

Table A.14. Block types in Hierarchy Block 3

Block Name	Type
B1	Mult
B2	Flash2
B9	Compr
B10	Heater

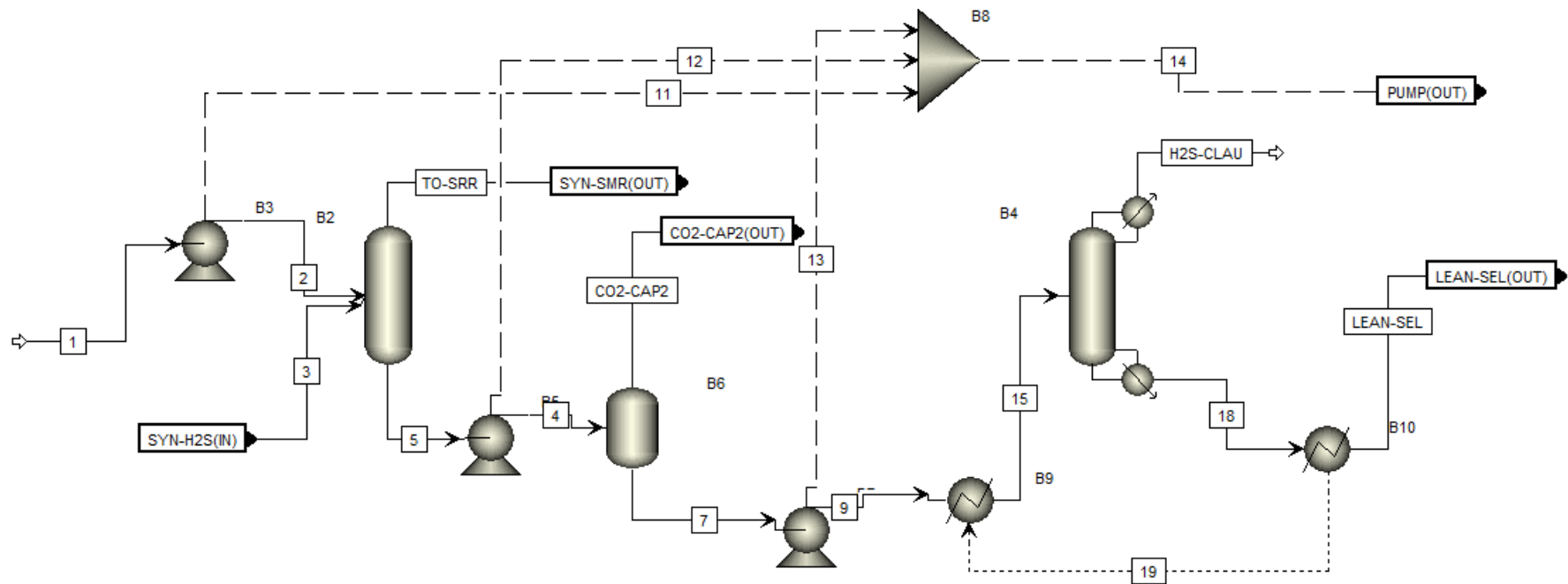


Figure A.5: Process flow diagram – Hierarchy Block 4: AGR

Table A.15: Material streams in Hierarchy Block 4

Stream Name	1	2	4	5	7	9	15	18	CO2-CAP2	H2S-CLAU	LEAN-SEL	TO-SRR
Temperature, C	0.0	0.7	15.6	15.7	12.8	12.8	273.8	316.4	12.8	269.9	25.0	9.9

Stream Name	1	2	4	5	7	9	15	18	CO2-CAP2	H2S-CLAU	LEAN-SEL	TO-SRR
Pressure, bar	1.0	30.0	7.0	30.0	7.0	1.0	1.0	1.0	7.0	1.0	1.0	30.0
Vapor Fraction	0.0	0.0	0.0	0.0	0.0	0.0	0.3	0.0	1.0	1.0	0.0	1.0
Total Flow, kg/hr	14461.9	14461.9	15210.5	15210.5	14938.2	14938.2	14938.2	13234.4	272.3	1703.8	13234.4	8985.8
Mass Flow, kg/hr												
CH4	0.0	0.0	16.2	16.2	2.7	2.7	2.7	0.0	13.5	2.7	0.0	1125.5
CO2	0.0	0.0	684.4	684.4	438.4	438.4	438.4	0.0	246.0	438.4	0.0	5273.7
CO	0.0	0.0	11.5	11.5	0.7	0.7	0.7	0.0	10.8	0.7	0.0	2328.8
H2	0.0	0.0	0.3	0.3	0.0	0.0	0.0	0.0	0.3	0.0	0.0	256.8
H2S	0.0	0.0	27.9	27.9	26.6	26.6	26.6	0.0	1.3	26.6	0.0	0.3
H2O	0.0	0.0	8.2	8.2	7.8	7.8	7.8	0.0	0.4	7.8	0.0	0.3
C2H6	0.0	0.0	0.1	0.1	0.0	0.0	0.0	0.0	0.0	0.0	0.0	0.5
N2	0.0	0.0	0.0	0.0	0.0	0.0	0.0	0.0	0.0	0.0	0.0	0.0
DEPG	14461.9	14461.9	14461.9	14461.9	14461.9	14461.9	14461.9	13234.4	0.0	1227.5	13234.4	0.0
OXYGEN	0.0	0.0	0.0	0.0	0.0	0.0	0.0	0.0	0.0	0.0	0.0	0.0
ARGON	0.0	0.0	0.0	0.0	0.0	0.0	0.0	0.0	0.0	0.0	0.0	0.0
CARBON	0.0	0.0	0.0	0.0	0.0	0.0	0.0	0.0	0.0	0.0	0.0	0.0

Table A.16: Work streams in Hierarchy Block 4

Stream	11	12	13	14
Name				
POWER,	13.7	-6.6	-1.7	5.4
kW				

Table A.17: Block types in Hierarchy Block 4

Block Name	Type
B6	Flash2
B9, B10	Heater
B8	Mixer
B3, B5, B7	Pump
B2, B4	RadFrac

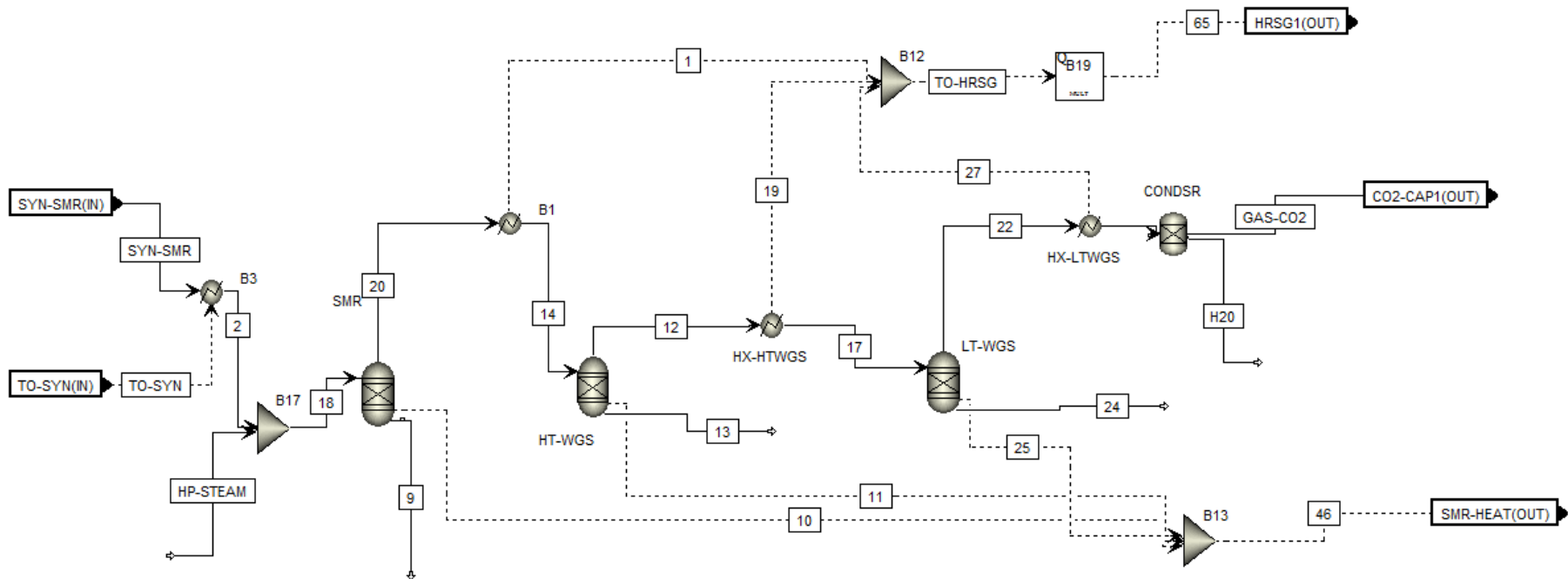


Figure A.6: Process flow diagram – Hierarchy Block 5: SMR-WGSR

Table A.18: Material streams in Hierarchy Block 5

Stream Name	2	20	14	12	17	22	26	GAS-CO2	H2O	HP-STEAM
Temperature, C	916.0	800.0	350.0	450.0	250.0	275.0	25.0	25.0	25.0	510.0
Pressure, bar	29.4	27.7	27.1	26.0	25.5	24.5	24.0	24.0	24.0	30.0
Vapor Fraction	1.0	1.0	1.0	1.0	1.0	1.0	0.7	1.0	0.0	1.0
Total Flow, kg/hr	8985.8	17271.6	17271.6	17271.6	17271.6	17271.6	17271.6	11888.6	5383.1	8285.8
Mass Flow, kg/hr										
CH4	1125.5	458.2	458.2	458.2	458.2	458.2	458.2	458.2	0.0	0.0
CO2	5273.7	6473.9	6473.9	9422.9	9422.9	10533.7	10533.7	10533.7	0.0	0.0
CO	2328.8	2730.8	2730.8	853.9	853.9	146.9	146.9	146.9	0.0	0.0
H2	256.8	563.5	563.5	698.5	698.5	749.4	749.4	749.4	0.0	0.0
H2S	0.3	0.3	0.3	0.3	0.3	0.3	0.3	0.3	0.0	0.0
H2O	0.3	7045.0	7045.0	5837.8	5837.8	5383.1	5383.1	0.0	5383.1	8285.8
C2H6	0.5	0.0	0.0	0.0	0.0	0.0	0.0	0.0	0.0	0.0
N2	0.0	0.0	0.0	0.0	0.0	0.0	0.0	0.0	0.0	0.0

Stream Name	2	20	14	12	17	22	26	GAS-CO2	H2O	HP-STEAM
DEPG	0.0	0.0	0.0	0.0	0.0	0.0	0.0	0.0	0.0	0.0
OXYGEN	0.0	0.0	0.0	0.0	0.0	0.0	0.0	0.0	0.0	0.0
ARGON	0.0	0.0	0.0	0.0	0.0	0.0	0.0	0.0	0.0	0.0
CARBON	0.0	0.0	0.0	0.0	0.0	0.0	0.0	0.0	0.0	0.0

Table A.19: Work streams in Hierarchy Block 5

Stream Name	1	10	11	19	25	27	46	65	TO-HRSG	TO-SYN
QCALC, Gcal/hr	3.9	-2.8	-0.2	1.7	0.0	5.2	-3.1	6.5	10.8	3.6

Table A.20: Block types in Hierarchy Block 5

Block Name	Type
B1, B3, HX-HTWGS, HX-LTWGS	Heater
B12, B13, B17	Mixer

Block Name	Type
B19	Mult
HT-WGS, LT-WGS, SMR	
CONDSR	Sep

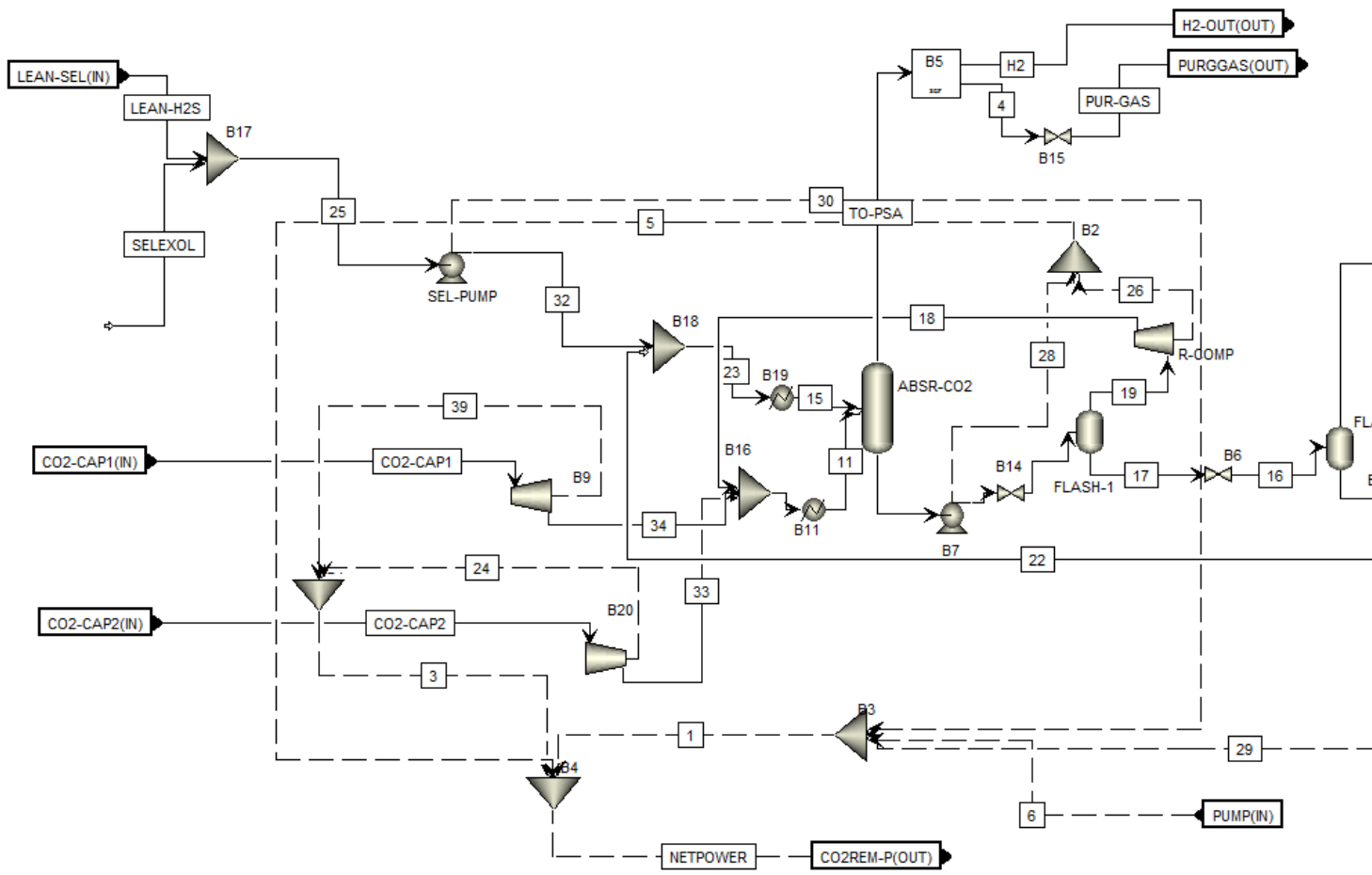


Figure A.7a: Process flow diagram – Hierarchy Block 6: CO₂-CAP (consists of CO₂ capture using Selexol, portion of Selexol flash)

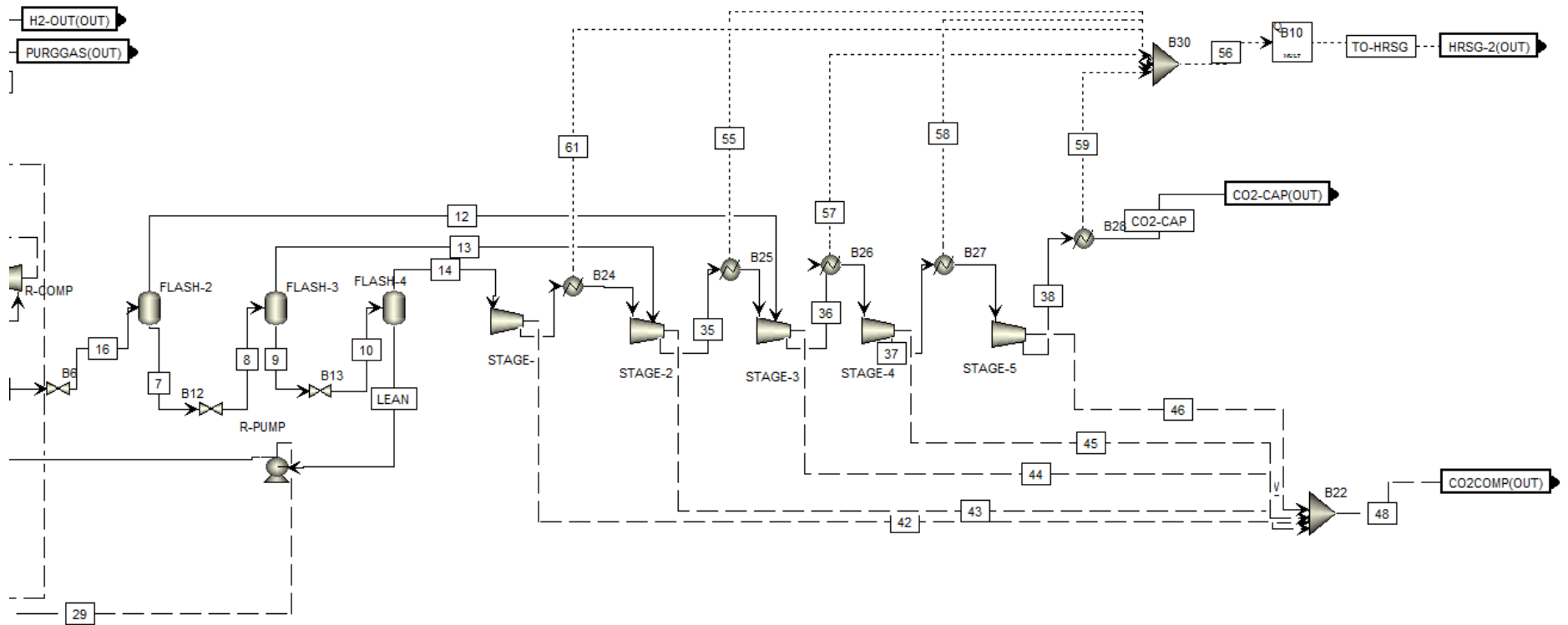


Figure A.7b: Process flow diagram – Hierarchy Block 6: CO₂-CAP (consists of Selexol flash and CO₂ compression)

Table A.21a: Material streams in Hierarchy Block 6

Stream Name	2	7	8	9	10	11	12	13	14	15	16	17
Temperature, C	9.9	25.0	21.5	25.0	23.7	25.0	25.0	25.0	25.0	0.0	23.6	25.0
Pressure, bar	17.0	9.5	3.2	3.2	1.1	50.0	9.5	3.2	1.1	50.0	9.5	17.0
Vapor Fraction	0.0	0.0	0.1	0.0	0.0	1.0	1.0	1.0	1.0	0.0	0.1	0.0
Total Flow, kg/hr	242625.7	238755.5	238755.5	233311.1	233311.1	13355.3	2676.7	5444.4	1855.6	230543.2	241432.2	241432.2
Mass Flow, kg/hr												
CH4	164.9	31.5	31.5	2.2	2.2	538.2	67.0	29.3	2.0	0.0	98.5	98.5
CO2	11881.2	8178.0	8178.0	2764.0	2764.0	11881.2	2602.6	5413.9	1853.3	0.0	10780.5	10780.5
CO	17.2	0.8	0.8	0.0	0.0	169.0	5.1	0.8	0.0	0.0	5.9	5.9
H2	17.2	0.1	0.1	0.0	0.0	764.9	1.9	0.1	0.0	0.0	2.0	2.0
H2S	1.6	1.5	1.5	1.3	1.3	1.6	0.0	0.2	0.2	0.0	1.5	1.5
H2O	0.4	0.4	0.4	0.4	0.4	0.4	0.0	0.1	0.1	0.0	0.4	0.4
C2H6	0.1	0.0	0.0	0.0	0.0	0.1	0.0	0.0	0.0	0.0	0.1	0.1
N2	0.0	0.0	0.0	0.0	0.0	0.0	0.0	0.0	0.0	0.0	0.0	0.0
DEPG	230543.2	230543.2	230543.2	230543.2	230543.2	0.0	0.0	0.0	0.0	230543.2	230543.2	230543.2
OXYGEN	0.0	0.0	0.0	0.0	0.0	0.0	0.0	0.0	0.0	0.0	0.0	0.0
ARGON	0.0	0.0	0.0	0.0	0.0	0.0	0.0	0.0	0.0	0.0	0.0	0.0

Stream Name	2	7	8	9	10	11	12	13	14	15	16	17
CARBON	0.0	0.0	0.0	0.0	0.0	0.0	0.0	0.0	0.0	0.0	0.0	0.0

Table A.21b: Material streams in Hierarchy Block 6

Stream Name	19	20	21	27	31	32	18	33	34	35	36	37
Temperature, C	25.0	97.4	10.0	9.9	101.8	26.2	124.4	192.	94.6	105.1	109.4	110.4
								8				
Pressure, bar	17.0	50.0	50.0	23.0	2.4	50.0	50.0	50.0	50.0	5.6	13.2	30.2
Vapor Fraction	1.0	1.0	0.0	0.0	1.0	0.0	1.0	1.0	1.0	1.0	1.0	1.0
Total Flow,	1193.	13354.	242625.	242625.	1855.	230543.	1193.	272.	11888.	7300.	9976.	9976.
kg/hr	5	4	7	7	6	2	5	3	6	0	7	7
Mass Flow,												
kg/hr												
CH4	66.5	538.2	164.9	164.9	2.0	0.0	66.5	13.5	458.2	31.3	98.3	98.3
CO2	1100.	11880.	11881.2	11881.2	1853.	0.0	1100.	246.	10533.	7267.	9869.	9869.

Stream Name	19	20	21	27	31	32	18	33	34	35	36	37
	6	3			3		6	0	7	2	8	8
CO	11.2	169.0	17.2	17.2	0.0	0.0	11.2	10.8	146.9	0.8	5.9	5.9
H2	15.2	764.9	17.2	17.2	0.0	0.0	15.2	0.3	749.4	0.1	2.0	2.0
H2S	0.0	1.6	1.6	1.6	0.2	0.0	0.0	1.3	0.3	0.4	0.5	0.5
H2O	0.0	0.4	0.4	0.4	0.1	0.0	0.0	0.4	0.0	0.1	0.1	0.1
C2H6	0.0	0.1	0.1	0.1	0.0	0.0	0.0	0.0	0.0	0.0	0.0	0.0
N2	0.0	0.0	0.0	0.0	0.0	0.0	0.0	0.0	0.0	0.0	0.0	0.0
DEPG	0.0	0.0	230543.	230543.	0.0	230543.	0.0	0.0	0.0	0.0	0.0	0.0
			2	2		2						
OXYGEN	0.0	0.0	0.0	0.0	0.0	0.0	0.0	0.0	0.0	0.0	0.0	0.0
ARGON	0.0	0.0	0.0	0.0	0.0	0.0	0.0	0.0	0.0	0.0	0.0	0.0
CARBON	0.0	0.0	0.0	0.0	0.0	0.0	0.0	0.0	0.0	0.0	0.0	0.0

Table A.21c: Material streams in Hierarchy Block 6

Stream Name	38	49	50	51	52	CO2-CAP	H2	22	LEAN	23	PUR-GAS	SELEXOL	TO-PSA
Temperature,	196.7	31.1	31.1	31.1	31.1	25.0	25	26.2	25.0	26.2	-2.0	25.0	-0.1
C													
Pressure, bar	150.0	2.4	5.6	13.2	30.2	150.0	19.5	50.0	1.1	50.0	1.5	1.0	50.0
Vapor	1.0	1.0	1.0	1.0	1.0	0.0	1.0	0.0	0.0	0.0	1.0	0.0	1.0
Fraction													
Total Flow,	9976.7	1855.6	7300.0	9976.7	9976.7	9976.7	635.6	231455.5	231455.5	230543.2	637.2	217308.8	1272.8
kg/hr													
Mass Flow,													
kg/hr													
CH4	98.3	2.0	31.3	98.3	98.3	98.3	0.0	0.1	0.1	0.0	373.2	0.0	373.2
CO2	9869.8	1853.3	7267.2	9869.8	9869.8	9869.8	0.0	910.7	910.7	0.0	0.0	0.0	0.0
CO	5.9	0.0	0.8	5.9	5.9	5.9	0.0	0.0	0.0	0.0	151.8	0.0	151.8
H2	2.0	0.0	0.1	2.0	2.0	2.0	635.6	0.0	0.0	0.0	112.2	0.0	747.8
H2S	0.5	0.2	0.4	0.5	0.5	0.5	0.0	1.1	1.1	0.0	0.0	0.0	0.0
H2O	0.1	0.1	0.1	0.1	0.1	0.1	0.0	0.3	0.3	0.0	0.0	0.0	0.0
C2H6	0.0	0.0	0.0	0.0	0.0	0.0	0.0	0.0	0.0	0.0	0.0	0.0	0.0

Stream Name	38	49	50	51	52	CO2-CAP	H2	22	LEAN	23	PUR-GAS	SELEXOL	TO-PSA
N2	0.0	0.0	0.0	0.0	0.0	0.0	0.0	0.0	0.0	0.0	0.0	0.0	0.0
DEPG	0.0	0.0	0.0	0.0	0.0	0.0	0.0	230543.3	230543.3	230543.2	0.0	217308.8	0.0
OXYGEN	0.0	0.0	0.0	0.0	0.0	0.0	0.0	0.0	0.0	0.0	0.0	0.0	0.0
ARGON	0.0	0.0	0.0	0.0	0.0	0.0	0.0	0.0	0.0	0.0	0.0	0.0	0.0
CARBON	0.0	0.0	0.0	0.0	0.0	0.0	0.0	0.0	0.0	0.0	0.0	0.0	0.0

Table A.22: Heat streams in Hierarchy Block 6

Stream Name	55	56	57	58	59	61	TO-HRSG
QCALC, Gcal/hr	0.1	1.4	0.2	0.2	0.8	0.0	0.8

Table A.23: Work streams in Hierarchy Block 6

Stream Name	1	3	5	6	24	26	28	29	30	39	42	43	44	45	46	48	NETPOWER
POWER, kW	761.8	439.6	-85.7	5.4	13.2	36.0	-121.7	378.8	377.5	426.4	35.6	144.3	200.9	187.5	361.6	929.9	1115.7

Table A.24: Block types in Hierarchy Block 6

Block Name	Type
B9, B20, R-COMP, STAGE-1, STAGE-2, STAGE-3, STAGE-4, STAGE-5	Compr
FLASH-1, FLASH-2, FLASH-3, FLASH-4	Flash 2
B11, B19, B24, B25, B26, B27, B28	Heater
B16, B17, B18, B1, B2, B3, B4, B22, B30	Mixer
B10	Mult
R-PUMP, SEL-PUMP, B7	Pump
B5	Sep
B14, B15, B6, B12	Valve

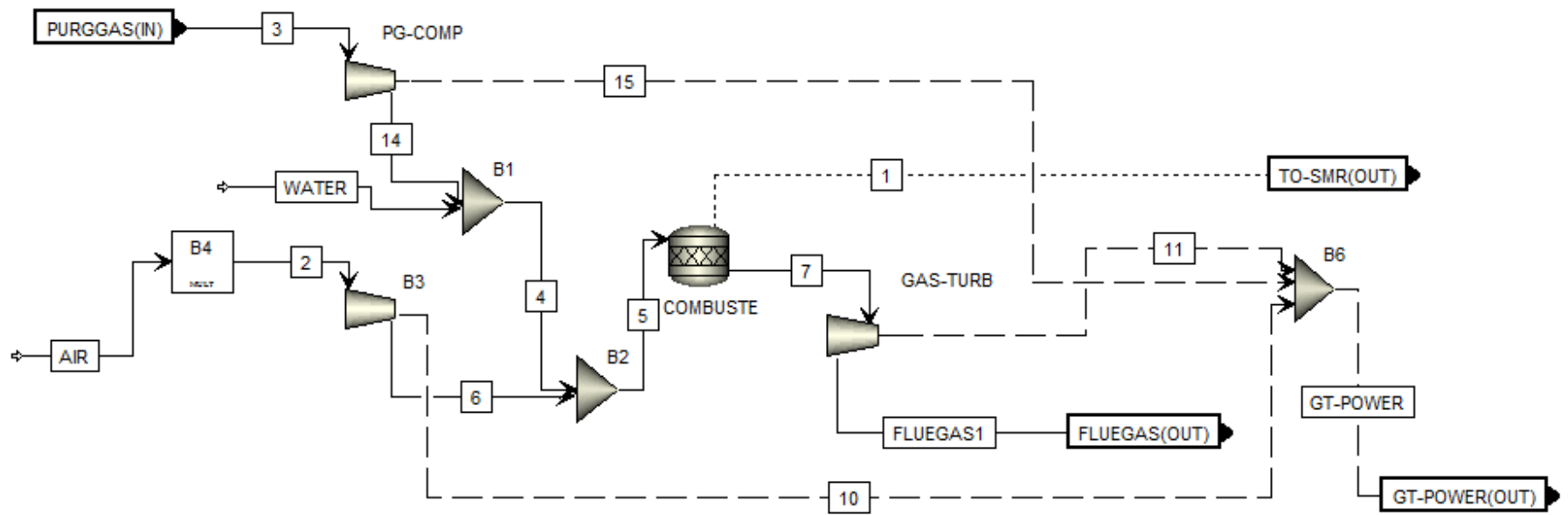


Figure A.8: Process flow diagram – Hierarchy Block 7: GT-PGBUR

Table A.25: Material streams in Hierarchy Block 7

Stream Name	2	3	4	5	6	7	14	AIR	FLUEGAS1	WATER
Temperature, C	15.0	-2.0	115.1	351.6	397.7	1299.9	256.2	15.0	685.5	164.3

Stream Name	2	3	4	5	6	7	14	AIR	FLUEGAS1	WATER
Pressure, bar	1.0	1.5	14.8	14.8	15.0	14.8	14.8	1.0	1.1	14.8
Vapor Fraction	1.0	1.0	1.0	1.0	1.0	1.0	1.0	1.0	1.0	0.0
Total Flow, kg/hr	16053.2	637.2	835.4	16888.5	16053.2	16888.5	637.2	9679.5	16888.5	198.2
Mass Flow, kg/hr										
CH4	0.0	373.2	373.2	373.2	0.0	0.0	373.2	0.0	0.0	0.0
CO2	12.1	0.0	0.0	12.2	12.1	1274.5	0.0	7.3	1274.5	0.0
CO	0.0	151.8	151.8	151.8	0.0	0.0	151.8	0.0	0.0	0.0
H2	0.0	112.2	112.2	112.2	0.0	0.0	112.2	0.0	0.0	0.0
H2S	0.0	0.0	0.0	0.0	0.0	0.0	0.0	0.0	0.0	0.0
H2O	0.0	0.0	198.2	198.2	0.0	2038.7	0.0	0.0	2038.7	198.2
C2H6	0.0	0.0	0.0	0.0	0.0	0.0	0.0	0.0	0.0	0.0
N2	11678.4	0.0	0.0	11678.4	11678.4	11678.4	0.0	7041.6	11678.4	0.0
DEPG	0.0	0.0	0.0	0.0	0.0	0.0	0.0	0.0	0.0	0.0
OXYGEN	4089.3	0.0	0.0	4089.3	4089.3	1623.6	0.0	2465.7	1623.6	0.0
ARGON	273.3	0.0	0.0	273.3	273.3	273.3	0.0	164.8	273.3	0.0
CARBON	0.0	0.0	0.0	0.0	0.0	0.0	0.0	0.0	0.0	0.0

Table A.26: Heat streams in Hierarchy Block 7

	1
QCALC, Gcal/hr	3.1

Table A.27: Work streams in Hierarchy Block 7

	10	11	15	GT- POWER
POWER, kW	2333.5	-3872.2	197.1	-1341.6

Table A.28. Block types in Hierarchy Block 7

Block Name	Type
B1, B2, B6	Mixer
B4	Mult
COMBUSTE	RStoich
B3, GAS-TURB, PG-COMP	Compr

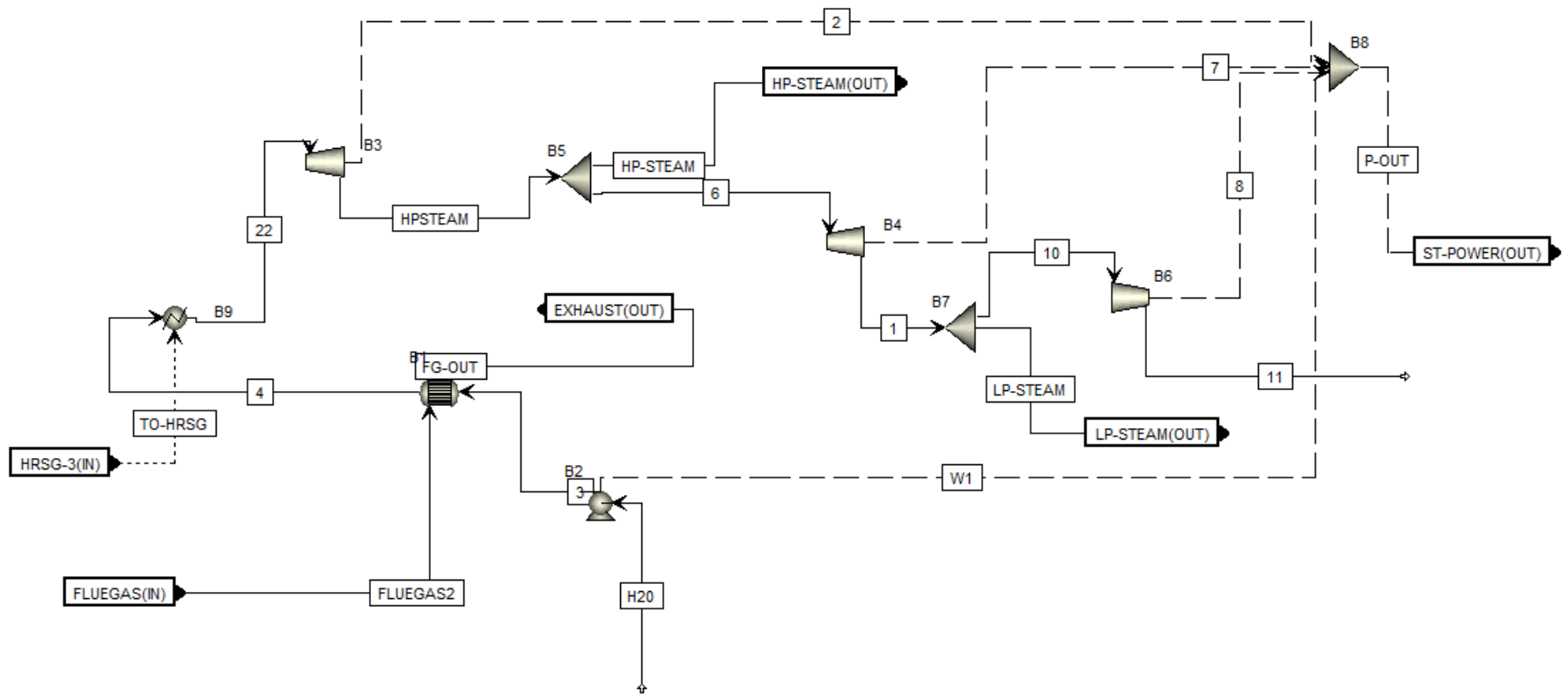


Figure A.9: Process flow diagram – Hierarchy Block 8: HRSG-ST

Table A.29: Material streams in Hierarchy Block 8

Stream Name	1	3	4	6	10	11	22	FG-OUT	FLUEGAS2	H2O	HP-STEAM	LP-STEAM
Temperature, C	302.7	25.9	248.7	509.9	302.7	164.3	702.0	100.0	685.5	25.0	509.9	302.7
Pressure, bar	6.0	100.0	100.0	30.0	6.0	1.5	97.5	1.1	1.1	1.0	30.0	6.0
Vapor Fraction	1.0	0.0	0.0	1.0	1.0	1.0	1.0	1.0	1.0	0.0	1.0	1.0
Total Flow, kg/hr	2752.4	11038.3	11038.3	2752.4	2700.5	2700.5	11038.3	16888.5	16888.5	11038.3	8285.8	51.9
Mass Flow, kg/hr												
CH4	0.0	0.0	0.0	0.0	0.0	0.0	0.0	0.0	0.0	0.0	0.0	0.0
CO2	0.0	0.0	0.0	0.0	0.0	0.0	0.0	1274.5	1274.5	0.0	0.0	0.0
CO	0.0	0.0	0.0	0.0	0.0	0.0	0.0	0.0	0.0	0.0	0.0	0.0
H2	0.0	0.0	0.0	0.0	0.0	0.0	0.0	0.0	0.0	0.0	0.0	0.0
H2S	0.0	0.0	0.0	0.0	0.0	0.0	0.0	0.0	0.0	0.0	0.0	0.0
H2O	2752.4	11038.3	11038.3	2752.4	2700.5	2700.5	11038.3	2038.7	2038.7	11038.3	8285.8	51.9
C2H6	0.0	0.0	0.0	0.0	0.0	0.0	0.0	0.0	0.0	0.0	0.0	0.0
N2	0.0	0.0	0.0	0.0	0.0	0.0	0.0	11678.4	11678.4	0.0	0.0	0.0
DEPG	0.0	0.0	0.0	0.0	0.0	0.0	0.0	0.0	0.0	0.0	0.0	0.0
OXYGEN	0.0	0.0	0.0	0.0	0.0	0.0	0.0	1623.6	1623.6	0.0	0.0	0.0
ARGON	0.0	0.0	0.0	0.0	0.0	0.0	0.0	273.3	273.3	0.0	0.0	0.0
CARBON	0.0	0.0	0.0	0.0	0.0	0.0	0.0	0.0	0.0	0.0	0.0	0.0

Table A.30: Work streams in Hierarchy Block 8

Stream Name	2	7	8	P-OUT	W1
POWER, kW	-1173.9	-307.7	-196.7	-1637.6	40.7

Table A.31: Block types in Hierarchy Block 8

Block Name	Type
B1	HeatX
B2	Pump
B3, B4, B6	Compr
B5, B7	FSplit
B8	Mixer
B9	Heater